

**Rock mechanics for construction of the gravimeter vault at the Matjiesfontein
Space Geodesy and Earth Observation Observatory**

by
Peter Ryan van Wyk

Thesis presented in fulfilment of the requirements for the degree of Master of Engineering at
Stellenbosch University



Supervisor: Mr Leon Croukamp

Faculty of Civil Engineering

December 2013

Declaration

By submitting this thesis electronically, I declare that the entirety of the work contained therein is my own, original work, that I am the sole author thereof (unless to the extent explicitly otherwise stated), that reproduction and publication thereof by Stellenbosch University will not infringe any third party rights and that I have not previously in its entirety or in part submitted it for obtaining any qualification.

December 2013

Abstract

The suitability of local construction materials for construction purposes is governed by several rock mechanical properties. Strength, durability, performance and petrography of aggregates all influence the decisions engineers make in deciding if the aggregate is suitable and sustainable throughout the lifetime of a structure. This thesis investigates these properties by combining engineering, chemistry and geological disciplines to make informed decisions.

The pertaining project for which the research was conducted is the construction of the gravimeter vault at the Matjiesfontein Geodesy and Earth Observation Observatory (MGO) although the research acquired can be used for other projects of a similar nature and other outbuildings at the MGO. Material at and around the site were tested for strength and durability according to certain South African National Standards (SANS). Slake durability was tested as certain rock types tend to slake when exposed to the atmosphere such as tillite of the Dwyka formation and shale of the Karoo Supergroup. Concrete cube strength was determined on cubes containing crushed rock from Matjiesfontein as well as river sand. Cube strength was conducted to analyse performance and to establish a mix design that would be sustainable throughout the lifetime of the project. Petrographic examination using Powder X-ray diffraction (PXRD), X-ray fluorescence (XRF), Scanning Electron Microscopy (SEM) and inspection under a petrographic microscope were conducted. These methods were used to determine if a risk exists for alkali-silica reactivity (ASR) in concrete when the rock types are used as aggregate, particularly if high quartz-bearing rock types such as quartzite of the Table Mountain group were to be used as coarse aggregate. Inspection of thin sections for strained quartz under a petrographic microscope and SEM imaging were important in determining if ASR may occur. The gravimeter vault was constructed using materials sourced mainly from Laingsburg.

Tillite satisfied all tests and analyses conducted during the research, making it more suitable for construction than the other materials from Matjiesfontein. The slake durability test indicates that tillite is nearly as durable as quartzite, which is considered the most durable rock type at Matjiesfontein. This is due to atmospheric conditions in the Karoo being very dry with low humidity in comparison to the coast where slaking is known to occur. Slaking properties were most prominent for shale at Matjiesfontein and if excavated, it is recommended to cover the exposed shale with a layer of asphalt or cement to prevent slaking. The 10% fines aggregate crushing test (10%FACT) value for tillite was over the 210 kN prerequisite and the wet-to-dry ratio over 75% making it suitable for road construction according to the 10%FACT. All cube tests reached the desired 40 MPa prerequisite although the mixtures containing local river sand were unworkable. Unlike quartzite and quartzitic sandstone from Matjiesfontein, tillite is low in quartz and has minimal strained quartz. Therefore, no risk exists for ASR if tillite were to be used as aggregate in concrete.

Opsomming

Die geskiktheid van plaaslike konstruksiemateriale vir konstruksiedoeleindes word deur sekere rots meganiese eienskappe beïnvloed. Sterkte, duursaamheid, volhoubaarheid en petrografie van aggregraat beïnvloed die besluite wat ingenieurs moet neem sodat die aggregraat aan standarde voldoen en gedurende die leeftyd van 'n struktuur volhoubaar is. Hierdie tesis ondersoek die genoemde eienskappe deur ingenieurs-, chemiese- en geologiese dissiplines te kombineer.

Die voorgenome projek, waarvoor die navorsing ter sprake is, is vir die konstruksie van die gravimeterkluis by die “Matjiesfontein Geodesy and Earth Observation Observatory (MGO)”, alhoewel die navorsing ook gebruik kan word vir soortgelyke projekte, sowel as die konstruksie van die res van die geboue by die MGO. Materiale van die terrein en die omgewing is volgens sekere Suid-Afrikaanse kodes vir sterkte en duursaamheid getoets. Die blusbaarheid van materiale is getoets omdat sekere materiale, soos tilliet van die Dwyka-formasie en skalie van die Karoo Supergroep blus wanneer dit aan die atmosfeer blootgestel word. Die betonsterkte van kubusse, waarin plaaslike gesteentes en riviersand van Matjiesfontein vir aggregraat gebruik is, is bepaal. Die kubusse is getoets om die sterkte daarvan te analiseer en om 'n betonmengsel, wat tydens die leeftyd van die projek volhoubaar is, daar te stel. Petrografiese eksaminering deur X-straal difraksie (XRD), X-straal fluoressensie (XRF), Skandeerelektronmikroskopie (SEM) en inspeksie onder 'n petrografiese mikroskoop is gedoen. Met die doel om die petrografiese samestelling van materiale van Matjiesfontein te bepaal, is hierdie metodes gevolg om te uit te vind of daar 'n risiko vir alkalie-silikaat reaksies (ASR) bestaan, as die gesteentes in beton gebruik word. Veral gesteentes met 'n hoë hoeveelheid kwarts, soos kwartsiet van die Tafelberg-groep, is hier ter sprake. Inspeksie van dunsnitte vir gespanne kwarts onder 'n petrografiese mikroskoop en SEM was belangrik om die risiko vir ASR te bepaal. Die gravimeterkluis is hoofsaaklik met materiale afkomstig van Laingsburg gebou.

In vergelyking met die ander gesteentes by Matjiesfontein is tilliet, volgens alle toetsparameters, die mees geskikte gesteente vir konstruksiedoeleindes. Die blusbaarheid van tilliet vergelyk goed met kwartsiet, wat as die sterkste en duursaamste gesteente by Matjiesfontein, beskou word. Die rede hiervoor is die atmosferiese toestande wat baie droër is, asook die laer humiditeit in die Karoo, in vergelyking met gebiede nader aan die kus waar blusting meer algemeen voorkom. Die blusbaarheid van skalie by Matjiesfontein kom algemeen voor. As daar dus uitgraving in hierdie gebied plaasvind, word dit aanbeveel dat 'n laag sement of asfalt oorgegooi word om die blusting te verhoed. Die 10%FACT waarde vir tilliet was bo die vereiste 210 kN, asook bo die 75% nat-teenoor-droog-verhouding en daarom is dit volgens die 10%FACT-toets as padboumateriaal geskik. Alhoewel mengsels, wat plaaslike riviersand bevat het, onwerkbaar was, het alle toetsmonsters (kubusse) die vereiste 40 MPa- sterkte bereik. In vergelyking met kwartsiet en kwarsitiese sandsteen, bevat tilliet min kwarts en ook minimale gespanne kwarts. Daar bestaan dus geen risiko vir ASR indien tilliet van Matjiesfontein in die beton gebruik word nie.

Acknowledgements

I would like to thank my supervisor, Mr Leon Croukamp for his guidance throughout the thesis and for the opportunity to take part in the MGO project. I would also like to thank everyone involved with the Inkaba ye’Afrika programme and Inkaba ye’Afrika for financing my postgraduate studies. I am also especially thankful towards my family for their support and encouragement throughout my studies.

Table of Contents

Abstract	i
Opsomming	ii
Acknowledgements	iii
Table of Contents	iv
List of Figures	vii
List of Tables.....	ix
List of Abbreviations.....	x
Chapter 1. Introduction	1
1.1. Background	1
1.2. Problem statement	1
1.3. Motivation for research	2
1.4. Research objective.....	2
1.5. Definitions.....	2
1.6. Report layout.....	3
Chapter 2. Literature Review	4
2.1. Introduction	4
2.2. History of Matjiesfontein	4
2.3. Location.....	5
2.4. Gravimetric surveys	5
2.5. Concrete aggregate	6
2.5.1. Standard Concrete tests	7
2.5.2. Aggregates from natural resources.....	9
2.6. Alkali-silica reaction (ASR).....	9
2.6.1. ASR in South Africa.....	10
2.6.2. Minimizing ASR	10
2.6.3. Criteria and analysing ASR	10
2.6.4. Petrography	11
2.7. Rock Characterization	14
2.7.1. Rock Mass Classification	14
2.7.2. Core Logging.....	19
2.7.3. Soil Profiling	20
2.7.4. Chip Logging.....	21
2.8. Properties of construction materials	21
2.8.1. Sandstone.....	21
2.8.2. Quartzite	22
2.8.3. Shale	23
2.8.4. Tillite	24

2.9.	Other work completed at Matjiesfontein.....	25
2.9.1.	Joint survey.....	25
2.9.2.	Rock mass description.....	26
2.9.3.	UCS test.....	28
2.9.4.	RMR.....	28
2.9.5.	ACV test.....	28
2.9.5.	Petrography.....	29
Chapter 3.	Method.....	30
3.1.	Tests.....	30
3.1.1.	Slake Durability.....	30
3.1.2.	10%FACT.....	31
3.1.3.	UCS test.....	32
3.1.4.	Grading Analysis.....	32
3.1.5.	RD – Pycnometer method.....	34
3.2.	Design.....	35
3.2.1.	Concrete mix design.....	35
3.2.2.	Vault design.....	38
3.3.	Petrographic analysis.....	44
3.3.1.	PXRD analysis.....	44
3.3.2.	XRF analysis.....	45
3.3.3.	SEM analysis.....	46
3.3.4.	Petrographic microscope – strained quartz.....	47
Chapter 4.	Results.....	49
4.1.	Test results and interpretation.....	49
4.1.1.	Slake durability results.....	49
4.1.2.	10%FACT results.....	50
4.1.3.	UCS results.....	51
4.1.4.	Grading analysis.....	52
4.1.5.	RD results.....	55
4.2.	Cube strength.....	55
4.3.	Vault Construction.....	56
4.3.1.	Difficulties experienced during construction.....	56
4.3.2.	Costs.....	57
4.4.	Petrography.....	58
4.4.1.	PXRD results.....	58
4.4.2.	XRF results.....	59
4.4.3.	SEM results.....	61
4.4.4.	Petrographic microscope examination – strained quartz.....	64

Chapter 5. Conclusions and recommendations	65
5.1. Slake durability.....	65
5.2. 10%FACT	65
5.3. Rock strength.....	66
5.4. Mix design.....	66
5.5. Vault construction	67
5.6. Cost comparison to using local materials for construction.....	67
5.7. Final remarks.....	68
References	70
Appendix A	75
Appendix B	80
Appendix C	82
Appendix D	89

List of Figures

Figure 2.1: Map of the Western Cape (Republic of South Africa) showing Matjiesfontein's location roughly in the centre of the Western Cape (Map of the Region, 2008).....	5
Figure 2.2: Grading limits for sand used in concrete (Addis, 1998:88).....	7
Figure 2.3: Thin-section of a concrete sample containing cracks formed from reactive chert and strained quartz (Hime & Erlin, 2013).....	9
Figure 2.4: Typical petrographic microscope (McHone, 2013).....	11
Figure 2.5: Schematic illustration of Bragg's Law (Sanchez-Garrido, 2013).....	13
Figure 2.6: Illustration of XRF principle (Sanchez-Garrido, 2013).....	14
Figure 2.7: Example of the procedure in order to calculate RQD of a core sample (Deere, 1989 cited in Hoek, 2007).....	16
Figure 2.8: Photo of a typical drilled core stored in a core box (Davis, 2012).....	19
Figure 2.9: Simple point load testing apparatus used in the field (Davis, 2012).....	20
Figure 2.10: Photo showing the different components of a soil profile (photo from Wikimedia Commons, 2012).....	20
Figure 2.11: Looking from the bottom of the depression towards the mountain one can see white/grey quartzite rocks protruding from the mountain side (Cilliers & Opperman, 2009).....	22
Figure 2.12: ASR in a bridge showing map cracks affecting the aesthetic value of the structure (Reactive Solutions, 2012).....	23
Figure 2.13: Typical soil profile of shale (Geology of KwaZulu-Natal, 2007) of the Ecca Group, which is similar to that found in the Karoo and Matjiesfontein.....	23
Figure 2.14: Illustration of how tillite is formed (Geology of KwaZulu-Natal, 2007).....	24
Figure 2.15: Typical picture of tillite (Geology of KwaZulu-Natal, 2007).....	25
Figure 2.16: Left - Stereoplot (upper hemisphere) showing great circles, which represents the joint direction. Right - Stereoplot with the poles plotted as points (Croukamp et al., 2011).....	26
Figure 2.17: Side-on view of a more exposed part of the ridge along which the gravimeter vault is located. One can see the vertical bedding planes.....	26
Figure 2.18: Rock face into which vault was to be constructed, with a 5 m imaginary core (Croukamp et al., 2011).....	27
Figure 3.1: Apparatus used for the slake durability test. From left to right in consecutive containers: quartzite, tillite, sandstone and shale.....	30
Figure 3.2: Left: tamping the aggregate lightly with tamping rod (a), plunger (b), base plate (c), steel cylinder (d) and measure (e). Right: assembly in compression testing machine.....	31
Figure 3.3: Core specimens of 100 mm depth and diameter in the compression testing machine. Left: quartzite core sample. Right: tillite core sample.....	32
Figure 3.4: Pycnometer consisting of a glass jar with a sealed spun top used to determine relative density of material (Pycnometer Top and Jar, 2013).....	35

Figure 3.5: Original mix design 3. The design was unworkable because of the dust within the river sand.....	36
Figure 3.6: Images of mix design 4. The slump (right) was about 40 mm.....	38
Figure 3.7: Plinth/beam design with reinforcement. Note that the drawing is not to scale.....	39
Figure 3.8: Gravimeter vault design with bending schedule for steel reinforcement for the floor slab and the plinth, on which gravimetric instrumentation are to be installed.....	40
Figure 3.9: Gravimeter vault design. Floor and roof level view.	41
Figure 3.10: Gravimeter vault design. Front and left hand side view.	42
Figure 3.11: Gravimeter vault design. Rear and right hand side view.	43
Figure 3.12: Left: Tungsten-carbide Zibb mill use to mill material into a fine powder. Right: Milling bowl, in which material is placed to be milled into a fine powder.....	44
Figure 3.13: PANalytical X'Pert Pro machine used for XRD analysis.	45
Figure 3.14: Melting of the samples, which are then cooled to make fusion discs.	46
Figure 3.15: SEM machine and computer used in the SEM analysis.....	47
Figure 4.1: Slake durability test results of the percentage, which the different rock types degraded and the percentage of the initial mass remained in the bins after test completion.	49
Figure 4.2: Images of the different rock types prior to the slake durability test and after.	50
Figure 4.3: 10%FACT results showing the 10%FACT value for each rock type in the wet and dry condition.....	51
Figure 4.4: Test specimens after testing. Left to right: quartzite, tillite 2 and tillite 1.	52
Figure 4.5: First natural sieve analysis curve of river sand (without sieving out the larger material > 4.75 mm) as found in a river at Matjiesfontein close to the MGO site.	53
Figure 4.6: Grading of natural river sand from Matjiesfontein showing the fine/coarse limits according to Addis (1998: 88).	54
Figure 4.7: Sieve analysis of crushed tillite and quartzite from the MGO site for the use of coarse aggregate.	54
Figure 4.8: Cube strength testing of mix design 1.....	56
Figure 4.9: MGO gravimeter vault at completion.	56
Figure 4.10: XRF results.	60
Figure 4.11: SEM images indicating what may be strained quartz in a quartzite sample.	61
Figure 4.12: Zircon mineral in quartzite sample.	62
Figure 4.13: Elemental mapping indicating some prominent elements (silicon, aluminium, potassium and titanium) by the brighter shades in quartzite sample.	63
Figure 4.14: Strained quartz in the quartzitic sandstone identified by undulatory extinction in the quartz grains.	64
Figure 4.15: Quartz crystal in tillite sample.	64
Figure 5.1: Hierarchy of rock types in terms of strength.....	66
Figure 5.2: Red Rhino Series 5000 mini crusher.	68

List of Tables

Table 2.1: Description of Rock Quality according to RQD percentage (Deere and Deere, 1988 cited in Milne <i>et al.</i> , 1998).....	16
Table 2.2: RMR system according to Bieniawski (1989 cited in Hoek, 2007).....	18
Table 2.3: UCS results from samples from Sutherland and Matjiesfontein (data adopted from Rossouw, 2010).....	28
Table 2.4: Summary of ACV results according to Janse van Rensburg (2012).....	29
Table 2.5: Summary of petrography from analysis under a polarizing microscope. Sample V1 from the original intended location for the gravimeter vault and Lun1 from the site where the LLR station is to be built.....	29
Table 3.1: Mix design 1.....	35
Table 3.2: Mix design 2.....	36
Table 3.3: Mix design 3 (original).....	36
Table 3.4: Newly proposed mix design 3.....	37
Table 3.5: Mix design 4.....	37
Table 4.1: Wet-to-dry 10%FACT ratio results.....	51
Table 4.2: UCS test results.....	52
Table 4.3: Average 28-day compression cube strength of mix designs.....	55
Table 4.4: Costs involved with building the gravimeter vault at the MGO.....	57
Table 4.5: Average relative phase amounts (weight %) of materials from Matjiesfontein.....	59

List of Abbreviations

10%FACT – 10% fines aggregate crushing test
ACV – aggregate crushing value
ASTM – American Society for Testing and Materials
ASR – alkali-silica reaction
BSE – backscattered electron
CAF – Central Analytical Facility
CBD – compacted (or consolidated) bulk density
CSF – condensed silica fume
EDX – Energy-dispersive X-ray spectroscopy
FA – fly ash
FM – fineness modulus
GGBS – ground granulated blastfurnace slag
HartRAO – Hartebeesthoek Radio Astronomy Observatory
ISRM - International Society of Rock Mechanics
KZN – KwaZulu-Natal
LBD – loose bulk density
LLR – Lunar Laser Ranger
LOI – Loss on Ignition
MCCSSO – moisture condition, colour, consistency, structure, soil type and origin
MGO – Matjiesfontein Space Geodesy and Earth Observation Observatory
OPC – Ordinary Portland Cement
PXRD – Powder X-ray Diffraction
PVC – Polyvinyl Chloride
RD – relative density
RMR – Rock Mass Rating
ROI – return on investment
RQD – Rock Quality Designation
SAAO – South African Astronomical Observatory
SABS – South African Bureau of Standards
SANS – South African National Standard
SEM – Scanning Electron Microscopy
SPT – Standard Penetration Test
TMH1 – Technical Methods for Highways number 1
UCS – Unconfined Compressive Strength
XRD – X-ray Diffraction
XRF – X-ray Fluorescence
XRFS – X-ray Fluorescence Spectrometry

Chapter 1. Introduction

1.1. Background

About five kilometers south of Matjiesfontein, in a small depression in the northern foothills of the Witteberge, an observatory is to be built. It is known as the Matjiesfontein Space Geodesy and Earth Observation Observatory (MGO). Of the various outbuildings, a vault or strong room known as the gravimeter vault will house a permanent gravimeter, seismometer, accelerometer and other highly sensitive equipment that detect movements in the Earth's crust.

The location of the gravimeter vault is such that minimal on-site interferences, such as the movement of vehicles and machinery, can be detected by the instruments and that the platforms on which the instruments stand are connected onto solid bedrock. Therefore, to avoid these interferences, the vault is built a safe distance away from the main access road and sheltered just within the depression up against a foothill; also shielding it from possible microwaves and radio signals from Matjiesfontein village and the N1 national road. The gravimeter vault will also serve as a relay communication station for other outbuildings situated within the depression as all operations are to be done electronically from a control center in Matjiesfontein village.

The main building on-site is the Lunar Laser Ranger (LLR) building. The LLR is a large telescope that emits a laser beam one meter in diameter to the moon, from where the beam is reflected back to Earth by 1 m² retro-reflectors that were placed on the moon during the Apollo program.

1.2. Problem statement

The gravimeter vault is the first of the outbuildings constructed as data collection of Earth movements needs to commence prior to Lunar Laser Ranging. This is in order to accurately calibrate instrumentation and measurements. Prior to the gravimeter vault, the only construction thus far is a simple dirt road to the site, which over the years has eroded severely causing large gullies in parts of the road and making it difficult for delivery of necessary construction equipment and materials. Therefore, possible options of using local materials are investigated in this thesis; i.e., investing in or hiring a small-scale crusher to crush on-site excavated rock and then screen out aggregate of sizes specified in accordance to concrete mix design.

The gravimeter vault's location is on a slope consisting mostly of sandstone and quartzitic sandstone. This rock type is generally high in silica, which can potentially react with the highly alkaline cement solution. This is known as alkali-silica reaction (ASR) and sometimes occurs in concrete engineering if certain atmospheric circumstances allow the reaction to take place such as moisture and temperature.

Other rock types in the area include shale, tillite and quartzite. Each rock type has its own properties in terms of durability and composition, which often, during design may seem unweathered and adequate for construction purposes but could pose problems in the future. Shale and tillite, for instance, slake when exposed to the atmosphere, often without any mechanical action such as wind and water.

1.3. Motivation for research

Usually in construction in remote locations, use of local materials is overlooked as time constraints are more important than reducing transportation and procurement costs. With better planning and research such as in this thesis, this can be overcome. Although this thesis focuses on the construction of the gravimeter vault, if local materials are proven adequate, they can be used for the construction of the other buildings on site as well as the access roads and projects of a similar nature in remote areas. By using local construction materials, not only would it reduce procurement and transportation costs but also indirectly preserve the natural environment through sustainable construction, which the local community proudly upholds. This can be done through utilizing excavated material instead of disposing it, which alone has costs involved.

1.4. Research objective

The research objective is to study the rock mechanics of local materials at Matjiesfontein and bring to light the use of local materials for construction in the Karoo and other isolated locations. The study of rock mechanics looks into the strength, durability and petrography of the aforementioned rock types. It also investigates the risk of ASR in concrete when quartzite, quartzitic sandstone or sandstone is used as concrete aggregate. Another research objective is to determine whether it is economically justifiable to use local materials for construction at Matjiesfontein and other projects in remote areas.

1.5. Definitions

When mentioning the rock types in this thesis, unless otherwise stated, tillite is of the Dwyka formation, quartzite/quartzitic sandstone/sandstone are of the Table Mountain group and shale is a mud rock of the Karoo Supergroup. Quartzitic sandstone in this thesis refers to sandstone that is very hard and may exhibit properties close to that of a quartzite and has been subjected to partial metamorphism during the development of the rock. Slaking is a phenomenon that some fine grained rock types (especially shale) exhibit when exposed to the atmosphere (air or moisture). The rocks crumble and break along bedding planes that exist within the rock causing rock to disintegrate at a rapid pace.

Geodesy, geodic measurements or geodic roaming all relate to the scientific method, derived from applied mathematics and Earth sciences, for measuring distances. Among other purposes, these measurements are done to create models for reference frameworks such as the celestial framework and African Reference Framework.

1.6. Report layout

The thesis is reported in six main chapters including introduction, literature review, method, results, discussion, followed by conclusions and recommendations.

The literature review introduces the Matjiesfontein project, history and location of Matjiesfontein and the site. Gravimetric surveying is explained briefly and other aspects concerning the project including aggregate for concrete, alkali-silicate reactivity, rock characterization, properties of local rock materials and other work completed for the MGO project.

In the method chapter, the tests conducted are explained in chronological order that they were conducted. The design for concrete and the gravimeter vault as it was constructed is described. Petrographic analyses are explained according to the different techniques used.

The cube strength and other results from the tests conducted are in the results chapter as well as vault construction in terms of difficulties experienced and costs involved. The findings of the petrographic analyses are then discussed for the risk of ASR and the general petrography of materials at Matjiesfontein relevant to the project.

The findings are then discussed in chapter 5 such as the construction potential of certain rock types according to the results of the rock mechanics studies and costing when using local materials for construction.

The appendices include all test results in tabular form as well as calculations used during design, images taken during construction of the gravimeter vault and petrographic imaging.

Chapter 2. Literature Review

2.1. Introduction

The MGO is to be an extension of the Hartebeesthoek Radio Astronomy Observatory (HartRAO). As the name suggests, the Earth and its characteristics can be studied through geodetic measurements. These measurements will contribute to a worldwide network of similar geodetic stations that study geographical phenomena on Earth such as Earth tides, polar motion and crustal motion. Amongst other collocated instruments a gravimeter at Matjiesfontein will measure local gravity and Earth tides.

The gravimeter vault is to house a permanent micro-gravimeter, seismometer and accelerometer and is located in a sandstone/quartzitic sandstone rock face. The purpose of the gravimeter, amongst others, is to determine tidal crust movement of the Earth, which is needed in calculations involving the distance to the moon and gravitational pull of the Moon (Combrinck, pers. comm., 2012). The seismometer is to be used to determine seismic movement in the Earth and records the amplitude of the movement where acceleration of the seismic movement is recorded by the accelerometer (Fourie, pers. comm., 2012).

Care must be exercised in preserving the natural environment, also with regard to its aesthetic character. Often in projects, local materials for construction purposes are overlooked. The use of local materials could minimise costs and improve procurement and transport economy. The use of local materials would also minimise the introduction of foreign materials, thereby minimising environmental impacts. Therefore, an analysis of the local building materials is conducted.

The literature review provides a comprehensive theoretical background and analysis through gaining knowledge from related work previously conducted. Although very little work on the subject has been conducted at the specific site; i.e., at Matjiesfontein, the literature review synthesises the possibilities through academic research.

2.2. History of Matjiesfontein

Matjiesfontein's history dates back to the late 1800's when a young Scottish immigrant, James Douglas Logan, recognized a potential business opportunity of providing necessities to travellers whom were making their way inland from the Cape. The location was at a seemingly unimportant railway station. He purchased land on which his personal English colonial homestead was built (Tweedside Lodge) as well as the Milner Hotel, which is still a popular stopover for motorists. During the Anglo-Boer War the hotel was used as headquarters to the British forces for the western region of South Africa as well as a hospital for injured soldiers.

2.3. Location

Matjiesfontein is a small village in the Western Cape situated next to the N1 between Touws River and Laingsburg as shown in figure 2.1 below. Roughly 120 km due north of Matjiesfontein is Sutherland where the South African Astronomical Observatory (SAAO) is situated.



Figure 2.1: Map of the Western Cape (Republic of South Africa) showing Matjiesfontein's location roughly in the centre of the Western Cape (Map of the Region, 2008).

The site for the MGO is roughly five kilometres south of Matjiesfontein and lies in a depression just below the Witteberg Mountains and marks the boundary between the Cape and Karoo Supergroups. The depression protects the highly sensitive equipment from radio signals and possible micro waves produced by the Matjiesfontein village. Africa and Southern Africa in particular is generally stable in terms of seismic activity, which is conducive to geodic surveying. The location for the vault, under discussion with Croukamp, pers. comm. (2013), was decided upon to be at the following location:

- Latitude: 33° 15' 51.003''
- Longitude: 20° 34' 52.56''

2.4. Gravimetric surveys

“The gravitational attraction of a body of non-homogeneous density will vary from point to point, in response to the distribution of density within the body. For this reason, measurements of the variation, with location, of the gravitational attraction of the Earth can provide valuable information about the

subsurface geology.” The preceding statement from Seigel (1995) is the basis for the science of gravimetric measurements and applies to a range of applications including: regional geological mapping, petroleum exploration, mineral exploration, geotechnical and archaeological studies, groundwater and environmental studies, tectonic studies, volcanology and geothermal studies.

Like the ocean, the Earth and air also experience tidal movement. Although not visibly noticeable like the ocean, the Earth’s crust also has a high and low tide ranging on average between eight and twelve inches (roughly between twenty and thirty centimetres) (Earth and air tides, n.d.). This movement was discovered using highly sensitive instruments such as the gravimeter where discrepancies were noticed in data indicating fluctuations in the gravitational pull to the moon, which could only mean that the Earth had tidally moved.

Although the average value $g = 9.80 \text{ m/s}^2$ is often used in scientific and mathematical calculations, projects such as the MGO need more accurate readings as many factors influence gravitational attraction. Some of these factors are variations in latitude, elevation, terrain, time and the density of different rock types and minerals (Seigel, 1995). Part of the LLR’s purpose is to determine the distance to the moon and if the Earth is experiencing tidal movement, the distance to the moon will vary over time and; therefore, need to be taken into account.

2.5. Concrete aggregate

Aggregates for concrete provide the bulk of a concrete mixture in terms of volume and mass. Typically fine and coarse aggregates occupy 60-75% of the concrete volume and 70-85% by mass (Kosmatka, Kerkhoff, & Panarese, 2003:79). According to the South African National Standard (SANS) 201 (2008), aggregates are divided according to size where sand smaller than 4.75 mm is considered as fine aggregate and stone larger than 4.75 mm in size is coarse aggregate.

Rock types in the area at Matjiesfontein exhibit characteristics of both the Cape and Karoo Supergroups including shale, tillite, sandstone, quartzitic sandstone and quartzite. For the construction of the gravimeter vault, the use of local construction materials as concrete aggregate with minimal impact on the environment is preferable. This will reduce procurement and transportation costs but will require a crusher on-site to crush the rock and a screening process to acquire the necessary size aggregate. The predominant rock type at the proposed site for the gravimeter vault is sandstone and quartzitic sandstone. According to Cole (2011) sandstone forms a good quality concrete aggregate especially quartzitic sandstones of the Peninsula and Skurweberg formations. These aggregates are extensively used in the Knysna, George and Bredasdorp regions. By excavating the site where the gravimeter vault is to be built and then using the excavated material for construction would be ideal. Minimal impacts on the surrounding area would occur because none of the material would have to be quarried and no extra transport expenses would be necessary.

2.5.1. Standard Concrete tests

To ensure the concrete is workable in a fresh state as well as dimensionally stable, strong and durable in a hardened state, certain characteristics are essential to determine the aggregate suitability. These, according to Addis (1998:80) include:

- Grading
- Bulk density
- Particle relative density
- Particle shape
- Surface texture
- Strength
- Shrinkage
- Geological type

Grading

The standard South African Bureau of Standards (SABS) sieve sizes for analysis of sand are: 4.75; 2.36; 1.18; 0.6; 0.3; 0.15 and 0.075 mm; and for stone: 75; 37.5; 19; 9.5 and 4.75 mm; and although not always necessary intermediate sizes 26.5; 13.2 and 6.7 mm can also be used (Addis, 1998:80). From the grading of a particular sample the fineness modulus (FM) and dust content can be determined, which expresses how fine or coarse (usually sand) the aggregate is (SANS 201, 2008).

With sands, a grading within the limits shown in figure 2.2 below is generally adequate for concrete mixtures. If the grading is outside the limits one can still have a satisfactory mix through proper mix design by using certain admixtures such as superplasticizers.

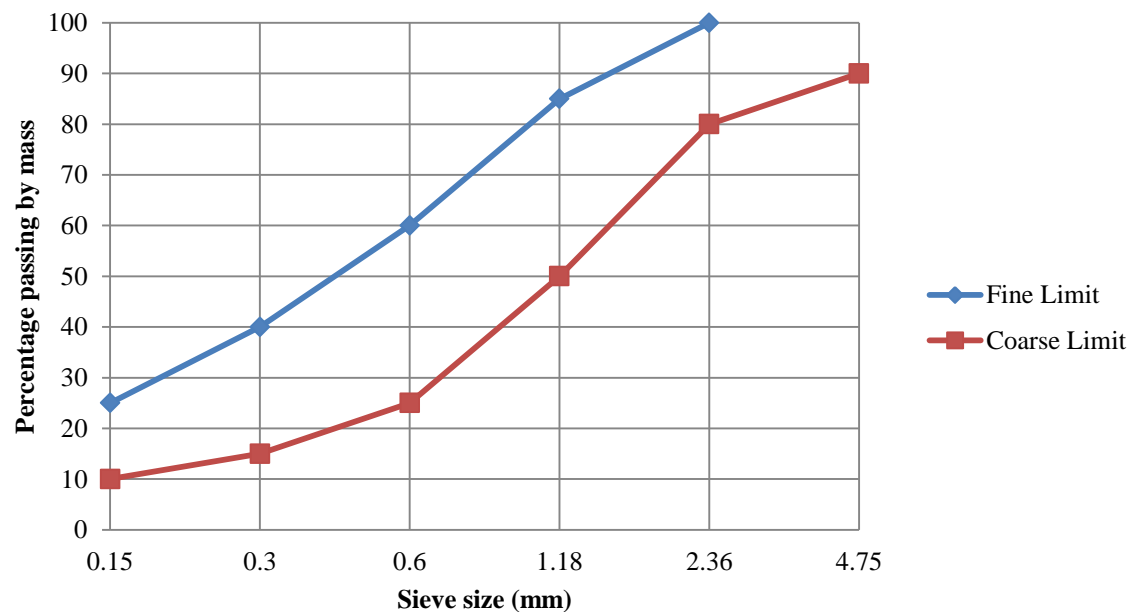


Figure 2.2: Grading limits for sand used in concrete (Addis, 1998:88).

Sands from a natural source such as the sands found in the non-perennial rivers at Matjiesfontein need to be relatively clean (free of clay particles and organic matter) and not have a predominant particle size; i.e., good grading, to be used in construction (A'Bear, pers. comm., 2012).

Bulk density

Bulk density is defined as the aggregate mass needed to fill a 1 m³ container at a specific temperature and in a specific condition; i.e., dry, saturated surfacedry or “as received” (SANS 5845, 2006). When the aggregate is being placed into the container without compaction it is referred to as loose bulk density (LBD) or uncompacted bulk density and with compaction, compacted (or consolidated) bulk density (CBD) (Addis, 1998:83).

Particle relative density

Relative density (RD) is defined as the relation of the density of a particle compared to that of water and is used in mix design, batching and helps to determine yields (Addis, 1998:83). Water density usually depends on temperature but by convention is generally defined as 1000 kg/m³ (1 g/cm³) (Properties of water, 2012). Siliceous materials have a RD of about 2.65; and most natural sands and stones vary from 2.6 to 2.95 (Addis, 1998:83).

Particle shape

Particle shape is done through visual inspection and varies from spherical (rounded), cubical, flat, angular and elongated. The rounder or more spherical the particles in an aggregate are, the less water is needed in a mix design and the mix is also more workable (Addis, 1998:89).

Strength

Two methods are used to determine the strength (crushing resistance) of coarse concrete aggregate. These are the aggregate crushing value (ACV) (SANS 5841, 2008) and the 10% fines aggregate crushing test (10%FACT) value (SANS 5842, 2006).

Shrinkage

Aggregate shrinkage refers to the ability of an aggregate to absorb water and shrink when dried. Addis (1998: 85) states that the purpose of aggregate is to dimensionally stabilize concrete. In order to do this, aggregate shrinkage needs to be lower than that of the hardened cement paste.

Geological type

As mentioned before, the rock types at and around the MGO site are quartzite, sandstone, tillite and shale. According to Addis (1998:86), quartzite aggregate sources of the Table Mountain Group are from areas along the southern and eastern seaboard. Sandstone (and quartzitic sandstone) of the Karoo Supergroup are also used from the interior of South Africa and tillite of the Dwyka formation (of the Karoo Supergroup) are also sourced from regions in KwaZulu-Natal (KZN).

Natural river sands are usually clean without any clay particles and consist mostly of rounded particles conducive to a low water requirement in a mixture but normally have particles more or less the same size; therefore, often lacking in particles small enough to pass through the 0.15 mm sieve (Addis, 1998:86). In order to have a mixture that is workable, a good grading is needed; i.e., rather than having one size particle predominating, a good distribution in particle size is needed.

2.5.2. Aggregates from natural resources

Often when considering building material from a particular area where little information exists about the construction materials; further testing is needed to determine if the material is suitable or not.

According to SANS 1083 (2006) the requirements stipulate that the aggregate is classified into three classes namely: a) naturally disintegrated aggregate; b) aggregate formed from crushing of rock; or c) a mixture of aggregate derived from blending aggregate (a) and (b). In order to determine the best performance parameters, aggregates of each class need to be tested using the natural rock/sand from the Matjiesfontein site and its surroundings.

2.6. Alkali-silica reaction (ASR)

ASR is a phenomenon that sometimes occurs in concrete resulting in the expansion and cracking of concrete (figure 2.3). The occurrence is due to highly alkaline pore solutions in concrete reacting with metastable forms of silica (Oberholster, 2001) in aggregate producing an alkali-silica gel forming cracks within the concrete. The rock types at Matjiesfontein, which could be susceptible to ASR, are quartzite/quartzitic sandstone/sandstone of the Table Mountain formation bearing strained quartz.

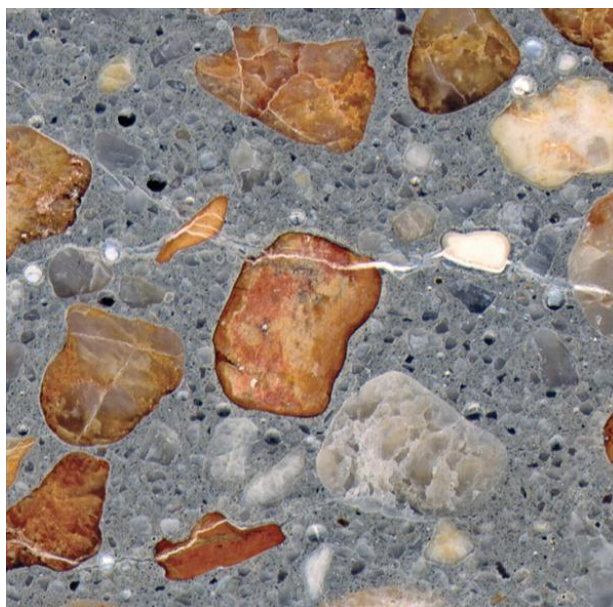


Figure 2.3: Thin-section of a concrete sample containing cracks formed from reactive chert and strained quartz (Hime & Erlin, 2013).

Strained quartz occurs when quartz grains in the aggregate are stressed causing plastic deformation of the grains resulting in a bending/deformation of the crystal lattice. Under a petrographic microscope,

this is observed as undulatory extinction across a quartz grain. Undulatory extinction is when the grain does not darken uniformly as the rotating stage is turned (West, 1996). Quartz exhibiting undulatory extinction; i.e., strained quartz, is prone to ASR (Concrete Society, 1987 cited in West, 1996) because the internal strain energy arising from the deformed lattice increases the solubility and hence the reactivity.

2.6.1. ASR in South Africa

The most occurrences associated with ASR in South Africa are in the Cape Peninsula where aggregates are sourced from areas of the Malmesbury group. Concrete structures containing quartzite of the Table Mountain Group where ASR has taken place are in the Eastern Cape and to a much smaller scale than occurrences in the Cape Peninsula (Oberholster, 2001). Other aggregates in the Eastern Cape involving ASR are quartzite pebbles of the Enon Formation and Quaternary gravels. In the Transvaal (Pretoria-Johannesburg-Heidelberg-Welkom), quartzite and shale of the Witwatersrand Supergroup (Oberholster, 2001) are associated with ASR.

2.6.2. Minimizing ASR

In addition to the concrete pore solution having a high alkaline content and the aggregate being alkali reactive; the internal relative humidity needs to be more than 75%; i.e., sufficiently moist, in order for ASR's to take place (Oberholster, 2001:166). Unfortunately, there are no clear indications of when an aggregate is alkali-reactive or non-reactive, or when the pore solution contains unsafe alkali concentrations, or when environmental conditions are conducive to ASR as environmental circumstances fluctuate. However, there are methods one may use in order to reduce the risk of ASR. These according to Oberholster (2001:167-169) include:

- Using cement having less than 0.6% Na₂O
- Use of cement extenders such as ground granulated blastfurnace slag (GGBS), fly ash (FA) and condensed silica fume (CSF)
- Use of chemical admixtures containing lithium compounds such as lithium nitrate (LiNO₃) and lithium monohydrate (LiOH.H₂O)
- Using clinker containing lithium

2.6.3. Criteria and analysing ASR

There are several ways in which ASR can be examined, tested and evaluated such as (Oberholster, 2001):

- Petrographic examination of the aggregate
- The gel-pat test
- American Society for Testing and Materials (ASTM) C289: Potential reactivity of aggregate (Chemical method)

- ASTM C227: Potential alkali reactivity of cement aggregate combinations (mortar-bar method)
- Accelerated mortar-prism (bar) tests
- Concrete prism method
- Ultra-accelerated concrete performance tests
- ASTM C586: Potential alkali reactivity of carbonate rocks for concrete aggregates (rock cylinder method)

2.6.4. Petrography

Petrography is known as the description and classification of rocks (Moorhouse, 1959). The ASTM C295 (1998) provides a standard for petrographic examination. ASR in concrete can be identified by examining a concrete thin-section with the use of a petrographic microscope. X-ray Diffraction (XRD)/Powder X-ray Diffraction (PXRD) analysis, X-ray Fluorescence (XRF) testing and Scanning Electron Microscopy (SEM) are additional procedures that can be used in petrographic examinations when investigating particular problems such as ASR in concrete. According to ASTM C295 (1998), alkali-silica reactive constituents found in aggregates include: “opal, cristobalite, tridymite, siliceous and intermediate volcanic glass, chert, glassy to cryptocrystalline acid volcanic rocks, synthetic siliceous glasses, some argillites, phyllites, metamorphic graywackes, rocks containing highly metamorphic quartz such as graywackes, phyllites, schists, gneisses, gneissic granites, vein quartz, quartzite, and sandstone”.

Petrographic microscope

Analysis under a petrographic microscope, also known as a polarizing microscope, is the most commonly used instrument in observing and classifying minerals in rock material. Rock, representative of the material under study, is thinly cut and polished into a thin section, which is then observed under a petrographic microscope.

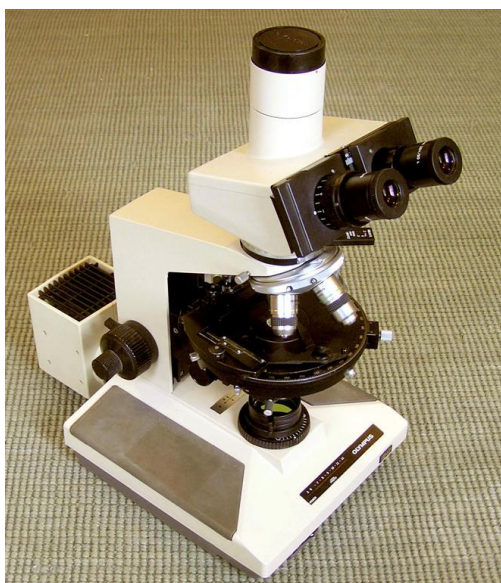


Figure 2.4: Typical petrographic microscope (McHone, 2013).

The general sequence in identifying minerals according to Moorhouse (1959) is as follows:

- a) Form and crystallographic properties
 - Crystal form if developed
 - Cleavage, parting, or fracture: number of cleavages and angular relationships to one another, perfection of cleavage, characteristics of parting and fracture
 - Shape of grain, if distinctive (fibrous, acicular, bladed, radiating, reticulate, tabular, platy)
 - Inclusions, intergrowths, alteration, association with other minerals
 - twinning
- b) Optical Properties
 - Opaque minerals: colour by reflected light
 - Transparent and translucent minerals
 - Colour and pleochroism
 - Relative index and relief
- c) Examination under crossed nicols
 - Isotropic or anisotropic
 - In anisotropic minerals, interference colours and identification of birefringence
 - Extinction angle

PXRD

In geological studies, PXRD is a commonly applied method used in the qualitative and/or quantitative analysis of mineral phases in rock samples. During analysis (PXRD) the rock samples are crushed and milled into a fine powder with a particle size of between 1 and 50 μm (Smith, 2013). It is a common occurrence for these samples to consist of multiple phases. The diffraction method used in determining the petrography of a rock sample is a non-destructive means of analysis. This means that the samples do not have to be melted or dissociated in any way.

When X-rays are emitted onto a powdered sample, atoms (electron density) in the sample interact with the X-rays resulting in XRD (Will, 2006). Bragg's law is fundamental to XRD theory, which shows that at certain wavelengths and angles, x-rays are diffracted producing intense peaks of reflected (diffracted) radiation (Bragg's law, 2013). The diffraction pattern obtained from the diffraction experiment is characteristic of the mineral(s) present in the sample and can; therefore, be used to identify the mineral phase.

According to Sanchez-Garrido (2013) and schematically illustrated in figure 2.5, Bragg's law is as follows:

$$\lambda_0 = 2d(\sin \theta)$$

Where, λ_0 is the characteristic x-ray wave length indicative of atom/element
 d is the interplanar spacing of the crystal
 θ is the incidence angle of the x-ray (Bragg's angle)

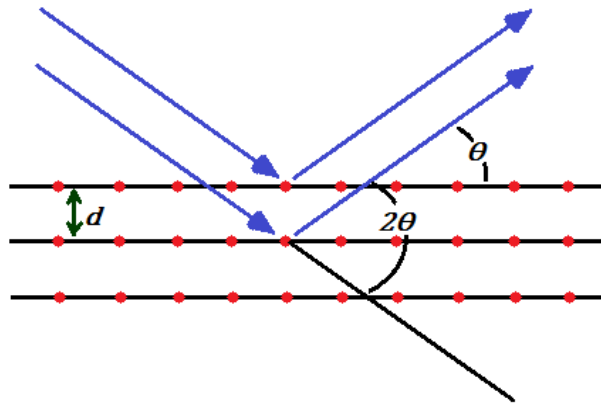


Figure 2.5: Schematic illustration of Bragg's Law (Sanchez-Garrido, 2013).

According to Smith (2013), engineers can use PXRD analysis for:

- Particle size and shape analysis
- Phase characterization in determining mineral identification and content
- Core samples
- Coal analysis
- Damage assessment
- Concrete analysis (e.g., alkali/silica content in ASR)

XRF

XRF, or also known as X-ray Fluorescence Spectrometry (XRFS), is useful in determining the chemical composition of wide range of materials albeit solids, powders or liquids. XRF theory is illustrated in figure 2.6 below. As a sample is bombarded with x-rays, the x-rays hit an atom's electron, with enough energy to knock it out of the inner-most shell, releasing it from its orbital. This creates a vacancy in the atom's inner shell, which is then filled with an electron from an outer shell. The transition of electron emits an x-ray photon, which is detected through instrumentation. Each x-ray photon emitted has a characteristic wavelength and energy corresponding to a certain atom/element; therefore, making it possible to classify and quantify. Bragg's law also applies to XRF on which programs analyzing such data are based.

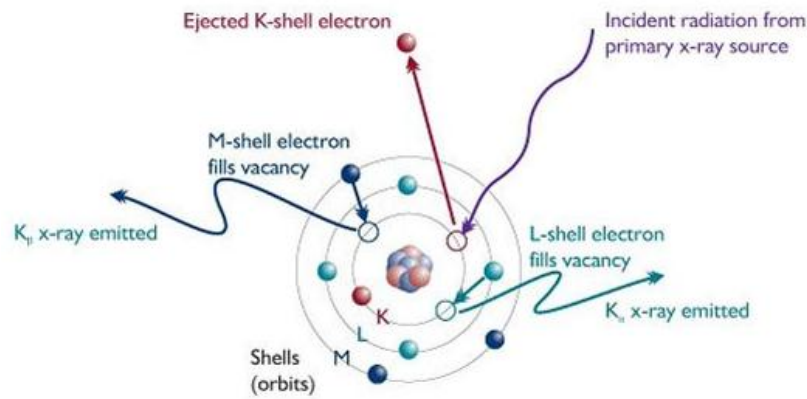


Figure 2.6: Illustration of XRF principle (Sanchez-Garrido, 2013).

Like PXRD, XRF is non-destructive and can be used for qualitative and quantitative analyses. Fusion discs or pressed pellets can be prepared and used in XRF analysis. Fusion discs are prepared by melting a milled sample of rock (dried) in a flux¹ followed by cooling to form a disc. Pressed pellets are just milled material that is pressed into a pellet. The difference in analysis of these two types is that major elements are determined using fusion discs whereas in pressed pellets, trace elements are determined (Sanchez-Garrido, pers. comm., 2013).

SEM

SEM makes use of a highly technical microscope that produces a high resolution image of a sample's surface by scanning it with a beam of high-energy electrons. Information such as surface texture, chemical composition, crystalline structure and orientation of crystals making up the sample are obtained (Swapp, 2013).

SEM is useful in determining a sample's composition because the user does not need a thorough knowledge of geology compared to when using a petrographic microscope (Frazenburg, pers. comm., 2013). This is because the SEM detects the composition electronically, producing a peak list diagram, whereas with a petrographic microscope the user visually characterizes the elements in the sample. Therefore, petrographic microscopy requires a good understanding of mineralogy.

2.7. Rock Characterization

2.7.1. Rock Mass Classification

Milne, Hadjigeorgiou, & Pakalnis (1998) encapsulates the purpose of rock mass classification in the following statement: "The primary objective of all classification systems is to quantify the intrinsic properties of the rock mass based on past experience." Rock mass classification is an important part of the geotechnical investigation of projects involving the excavation into a rock structure. Projects involving mining, tunnelling and foundations are typical projects where rock mass classification is

¹ Flux is a substance usually made up of lithium borates, which allows the sample to melt by lowering the fusion temperature

used for stability analysis and engineering design. The traditional approach is to use rock mass classification systems to provide stability performance guidelines, to group areas of similar geomechanical features and to design/select the appropriate support structure needed for stabilisation (Milne *et al.*, 1998). One such traditional method, and the first reference to rock mass classification used to describe tunnel support, is that of Terzaghi (1946 cited in Hoek, 2007). Terzaghi's descriptive classification is as follows (quoted directly from Hoek, 2007):

- **Intact rock** contains neither joints nor hair cracks. Hence, if it breaks, it breaks across sound rock. On account of the damage to the rock due to blasting, spalls may drop off the roof several hours or days after blasting. This is known as a *spalling* condition. Hard, intact rock may also be encountered in the *popping* condition involving the spontaneous and violent detachment of rock slabs from the sides of the rock.
- **Stratified** rock consists of individual strata with little or no resistance against separation along the boundaries between the strata. The strata may or may not be weakened by transverse joints. In such rock the spalling condition is quite common.
- **Moderately jointed** rock contains joints and hair cracks, but the blocks between joints are locally grown together or so intimately interlocked that vertical walls do not require lateral support. In rocks of this type, both spalling and popping conditions may be encountered.
- **Blocky and seamy** rock consists of chemically intact or almost intact rock fragments, which are entirely separated from each other and imperfectly interlocked. In such rock, vertical walls may require lateral support.
- **Crushed** but chemically intact rock has the character of crusher run. If most or all of the fragments are as small as fine sand grains and no recementation has taken place, crushed rock below the water table exhibits the properties of a water-bearing sand.
- **Squeezing** rock slowly advances into the tunnel without perceptible volume increase. A prerequisite for squeeze is a high percentage of microscopic and sub-microscopic particles of micaceous minerals or clay minerals with a low swelling capacity.
- **Swelling** rock advances into the tunnel chiefly on account of expansion. The capacity to swell seems to be limited to those rocks that contain clay minerals such as montmorillonite, with a high swelling capacity.

More modern practises utilising analytical and numerical methods in combination with the traditional approaches have since been used. Although there are many methods in classifying rock, two methods are described below. Namely Rock Quality Designation (RQD) and Rock Mass Rating (RMR).

RQD

A core sample from a core logging can be used to determine the RQD by expressing the length of intact core pieces longer than 100 mm (10 cm) as a percentage of the total length (Deere, 1989 cited in Hoek, 2007) as shown in figure 2.7.

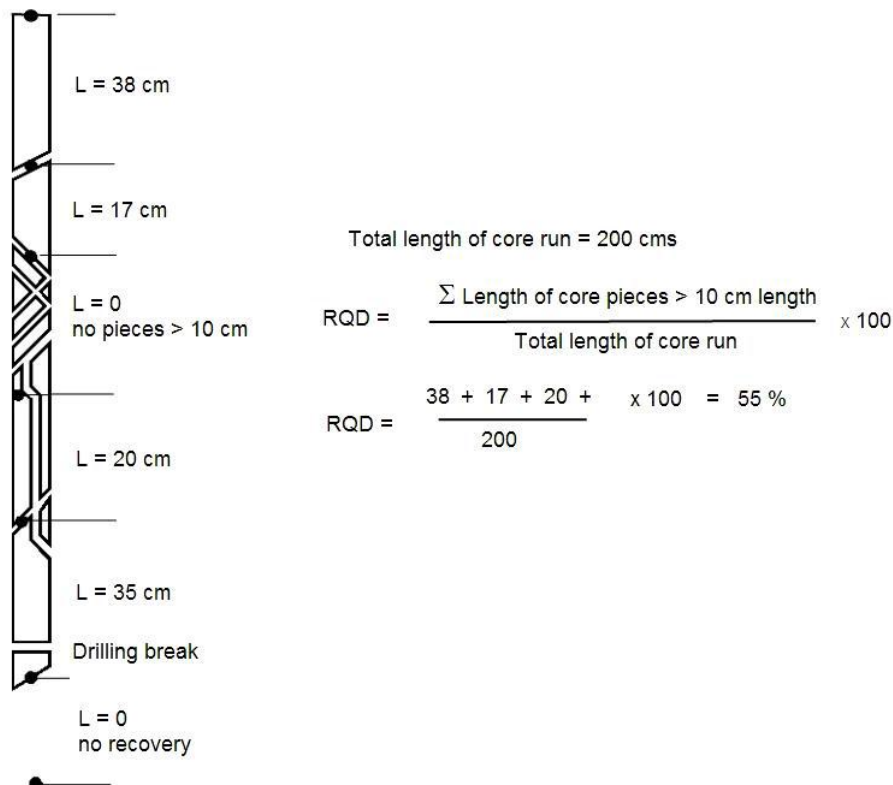


Figure 2.7: Example of the procedure in order to calculate RQD of a core sample (Deere, 1989 cited in Hoek, 2007).

During the drilling process and handling, the core is often broken or fractured, which can easily be seen due to colour distortions and driller’s breaks. These human-induced discontinuities need to be ignored when calculating the RQD and only natural fractures considered.

Other definitions associated with RQD and core loggings are material recovery and core recovery. Material recovery is the length of all material recovered in a core run, expressed as a percentage of the total length of the core run where core recovery is the length of the rock pieces expressed as a percentage of the total core run length (Davis, 2012). The core pieces include the pieces that could be conceivably re-assembled in core.

The RQD system follows a simple way of classifying the rock quality as shown in table 2.1. The higher the RQD percentage is, the greater the quality of the rock.

Table 2.1: Description of Rock Quality according to RQD percentage (Deere and Deere, 1988 cited in Milne *et al.*, 1998).

RQD (Rock Quality Designation) (%)	Description of Rock Quality
0 – 25	Very Poor
25 – 50	Poor
50 – 75	Fair
75 – 90	Good
90 – 100	Excellent

RMR

According to Bieniawski (1989 cited in Hoek, 2007) the RMR system classifies rock mass according to six parameters as follows:

1. Uniaxial compressive strength of rock material
2. RQD
3. Spacing of discontinuities
4. Condition of discontinuities
5. Groundwater conditions
6. Orientation of discontinuities

These parameters, depending on the circumstances under consideration, are given a rating according to table 2.2. Consider if a tunnel (assuming damp tunneling conditions) is driven through highly weathered rock with a dominant joint set at 45° in the direction of the drive. From core logging data and in-situ point load testing average point-load strength was found to be 5 MPa as well as an average RQD of 60%. The slightly rough and highly weathered joints show <1 mm separation spaced at roughly 700 mm. From the rating system in table 2.2 the following shows how to calculate the RMR.

<i>Table</i>	<i>Item</i>	<i>Value</i>	<i>Rating</i>
2.2: A.1	Point load index	5 MPa	12
2.2: A.2	RQD	60%	13
2.2: A.3	Spacing of discontinuities	700 mm	15
2.2: E	Condition of discontinuities	Note 1	16
2.2: A.5	Groundwater	Wet	10
2.2: B	Adjustment for joint orientation	Note 2	-2
		Total	64

Note 1) For slightly rough walls, separation < 1mm and highly weathered walls the rating is 20 according to table 2.2: A.4. However, under closer examination, table 2.2: E can give a more refined rating. In this instance: (3-10 m discontinuity length) + (0.1-1.0 mm separation) + (slightly rough walls) + (no infilling) + (highly weathered) = 2 + 4 + 3 + 6 + 1 = 16

Note 2) According to table 2.2: E, the drive with a dip of between 20° and 45° is considered favourable. By contrast, in table 2.2: B, the same conditions are given a rating of -2 for tunnels and mines.

Altogether the RMR = 64, which, according to table 2.2: C, classifies the rock as good rock with class number II. Class number II, according to table 2.2: D, has an average stand-up time of 1 year for a 10 meter span, 200-300 kPa cohesion strength of rock mass and a friction angle of between 35° and 45°. This information is helpful in making engineering decisions.

Table 2.2: RMR system according to Bieniawski (1989 cited in Hoek, 2007).

A: CLASSIFICATION PARAMETERS AND THEIR RATINGS									
Parameter			Range of values						
1	Strength of intact rock material	Point-load strength index	> 10 MPa	4-10 MPa	2-4 MPa	1-2 MPa	For this low range – uniaxial compressive test is preferred		
		Uniaxial comp. strength	> 250 MPa	100-250 MPa	50-100 MPa	25-50 MPa	5-25 MPa	1-5 MPa	< 1 MPa
	Rating	15	12	7	4	2	1	0	
2	Drill core Quality RQD		90-100 %	75-100 %	50-75 %	25-50 %	< 25%		
	Rating		20	17	13	8	3		
3	Spacing of discontinuities		> 2 m	0.6-2 m	200-600 mm	60-200 mm	< 60 mm		
	Rating		20	15	10	8	5		
4	Condition of discontinuities (See E)		Very rough surfaces. Not continuous. No separation. Unweathered wall rock.	Slightly rough surfaces. Separation < 1 mm. Slightly weathered walls.	Slightly rough surfaces. Separation < 1 mm. Highly weathered walls.	Slickensided surfaces or Gouge < 5 mm thick or Separation 1-5 mm. Continuous.	Soft gouge > 5 mm thick or Separation > 5 mm. Continuous		
	Rating		30	25	20	10	0		
5	Groundwater	Inflow per 10 m tunnel length (l/m)	None	< 10	10-25	25-125	> 125		
		(Joint water press) / (Major principal σ)	0	< 0.1	0.1-0.2	0.2-0.5	> 0.5		
		General conditions	Completely dry	Damp	Wet	Dripping	Flowing		
	Rating		15	10	7	4	0		
B: RATING ADJUSTMENT FOR DISCONTINUITY ORIENTATIONS (SEE F)									
Strike and dip orientations			Very favourable	Favourable	Fair	Unfavourable	Very unfavourable		
Ratings	Tunnels & mines		0	-2	-5	-10	-12		
	Foundations		0	-2	-7	-15	-25		
	Slopes		0	-5	-25	-50			
C: ROCK MASS CLASSES DETERMINED FROM TOTAL RATINGS									
Rating			100 ← 81	80 ← 61	60 ← 41	40 ← 21	< 21		
Class number			I	II	III	IV	V		
Description			Very good rock	Good rock	Fair rock	Poor rock	Very poor rock		
D: MEANING OF ROCK CLASSES									
Class number			I	II	III	IV	V		
Average stand-up time			20 yrs for 15 m span	1 yr for 10 m span	1 week for 5 m span	10 hrs for 2.5 m span	30 min for 1 m span		
Cohesion of rock mass (kPa)			> 400	300-400	200-300	100-200	< 100		
Friction angle of rock mass (deg)			> 45	35-45	25-35	15-25	< 15		
E: GUIDELINES FOR CLASSIFICATION OF DISCONTINUITY CONDITIONS									
Discontinuity length (persistence)			< 1 m	1-3 m	3-10 m	10-20 m	> 20 m		
Rating			6	4	2	1	0		
Separation (aperture)			None	< 0.1 mm	0.1-1 mm	1-5 mm	> 5 mm		
Rating			6	5	4	1	0		
Roughness			Very rough	Rough	Slightly rough	Smooth	Slickensided		
Rating			6	5	3	1	0		
Infilling (gouge)			None	Hard filling < 5 mm	Hard filling > 5 mm	Soft filling < 5 mm	Soft filling > 5mm		
Rating			6	4	2	2	0		
Weathering			Unweathered	Slightly weathered	Moderately weathered	Highly weathered	Decomposed		
Rating			6	5	3	1	0		
F: EFFECT OF DISCONTINUITY STRIKE AND DIP ORIENTATION IN TUNNELLING									
Strike perpendicular to tunnel axis					Strike parallel to tunnel axis				
Drive with dip – Dip 45-90°			Drive with dip – Dip 20-45°		Dip 45-90°		Dip 20-45°		
Very favourable			Favourable		Very unfavourable		Fair		
Drive against dip – Dip 45-90°			Drive against dip – Dip 20-45°		Dip 0-20° - Irrespective of strike				
Fair			Unfavourable		Fair				

2.7.2. Core Logging

Core logging is a means to record the observations of an experienced geologist studying an obtained core sample. From a core log one can specifically distinguish between different horizons under the surface of the Earth and calculate important rock mass parameters in rock engineering. These parameters can include qualitative descriptions through visual inspection and simple field tests (Association of Engineering Geologists, 1976). Although the borehole core represents what is under the surface of the Earth, it is disturbed by the drilling process and also the effects of atmospheric interferences on the core sample (Davis, 2012). By logging/inspecting a core, the experienced person can extrapolate possible behaviour of the rock mass. Although cores are commonly associated with rock material, many boreholes pass through or start with a soil horizon. This is an important part of a borehole log and must be considered when logging a core sample. In addition to the description of the rock material, discontinuities along the rock surface need to be recorded as well as the material filling the fractures (Association of Engineering Geologists, 1976).



Figure 2.8: Photo of a typical drilled core stored in a core box (Davis, 2012).

Field tests on core samples include tests for strength and deformation such as point load testing, whereas borehole testing involves testing for water pressure/levels (Lugeon).



Figure 2.9: Simple point load testing apparatus used in the field (Davis, 2012).

2.7.3. Soil Profiling

According to A’Bear (2012B) a soil profile is separated into four different components. These are, from top to bottom: transported soil, pebble marker, reworked residual soil and residual soil as shown in figure 2.10 below.

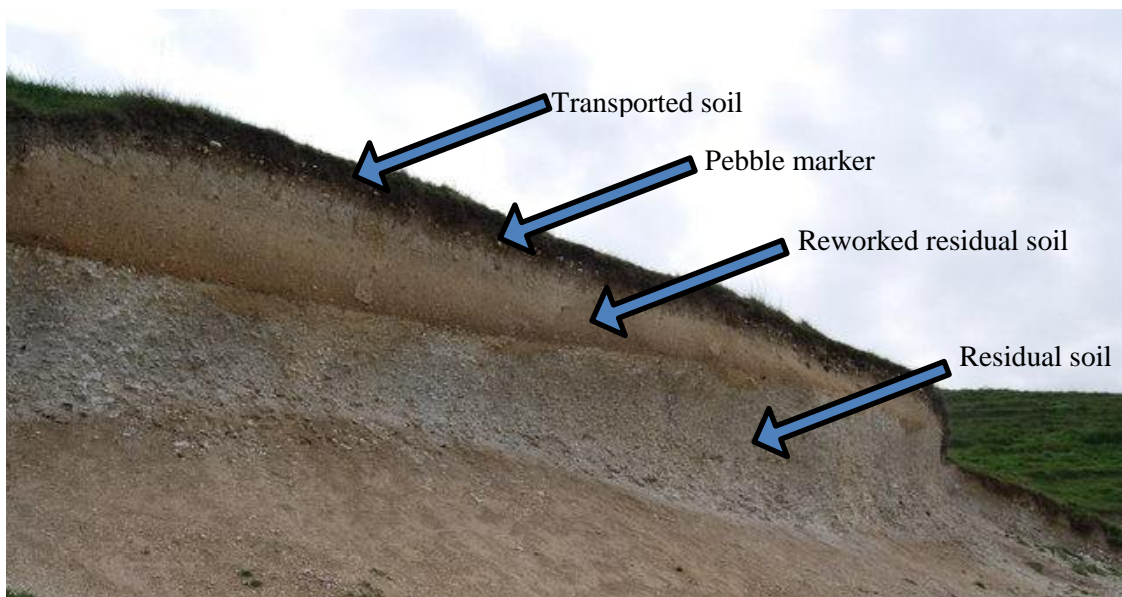


Figure 2.10: Photo showing the different components of a soil profile (photo from Wikimedia Commons, 2012).

The most recognisable feature in Southern African soils is the ‘pebble marker’, which is known as a band of gravel demarking the transition of transported soils (top) and residual soils (below).

Soil profiling describes each layer from top (surface) to bottom (bedrock). It is the first assessment in an engineering project and describes each layer according to key descriptors, which include moisture condition, colour, consistency, structure, soil type and origin (MCCSSO) (Jennings, Brink, & Williams, 1973).

2.7.4. Chip Logging

Chip logging involves the recording of material coming out of a drilled hole where a percussion drill was used for the drilling process. Percussion drilling is a destructive process where soil and rock is broken up into gravel (chip) sizes or smaller. The material is then collected at certain depth intervals by blowing it out of the hole using compressed air. Percussion drilling is quick and costs less but a lot of detail is lost in the samples and certain geotechnical parameters cannot be determined, such as strength of the material recovered (A'Bear, 2012A).

When describing the samples on the logging sheet the following parameters are recorded (A'Bear, 2012A):

- Soil
 - Colour
 - Described when wet (using Munsell or Burland chart)
 - Soil texture
 - Using same descriptors as for soil profiling (MCCSSO)
- Rock
 - Colour
 - Weathering
 - Using same descriptors as for core logging (e.g., highly weathered)
 - Rock type
- Origin

2.8. Properties of construction materials

Apart from quartzite, which is metamorphic in nature, the construction materials at the MGO are all sedimentary rocks.

2.8.1. Sandstone

As mentioned in Table Mountain Sandstone (Geological Formation) (2011), sandstone of the Table Mountain formation forms part of the Cape Supergroup and developed from marine sand deposition and natural cementation, resulting in an extremely weather-resistant sedimentary rock. This rock is the reason why Table Mountain, in Cape Town, has steep grey crags, since softer rock has been eroded away, leaving the harder sandstone.

Sandstone contains minerals such as quartz, mica and feldspar and undergoes chemical weathering and wind erosion (to an extent) but it is generally known to be more weather-resistant than tillite and shale. One may find varying degrees of weathered sandstone; some, which are perhaps less weather resistant than tillite.

Quartzitic sandstone is often a term used when referring to a sandstone rock mass that has been subjected to partial metamorphism resulting in a harder rock.

2.8.2. Quartzite

Quartzite is a metaphoric rock that originated from sandstone. The sandstone undergoes immense tectonic compression and is heated to form hard rock. At the MGO site and in many other parts of the Karoo, quartzite is recognised as a white or grey rock, with a clearly visible sparkling complexion in the sun, which looks like “streaky” lines or large boulders on mountain ranges (figure 2.11). Weathered quartzite can be found further down in the valley in the form of smaller rocks. Quartzite is a very hard, dense rock and is extremely durable. It is often used in the home industry for table tops and flooring. Because quartzite is hard and dense, the main weathering process it undergoes is chemical weathering.



Figure 2.11: Looking from the bottom of the depression towards the mountain one can see white/grey quartzite rocks protruding from the mountain side (Cilliers & Opperman, 2009).

Problems associated with quartzite as a construction material

Along with sandstone and quartzitic sandstone, quartzite has a high content of silica minerals (quartz in particular). As mentioned earlier in the thesis, strained quartz could result in ASR in concrete affecting the aesthetic value of the structure, exposing steel reinforcement (which can result in rust forming on the steel) and in severe cases structural failure. The most extensively used aggregates in South Africa do not contain any quartz and are made up mostly of basalts and dolerites; therefore, are not at risk of developing ASR.



Figure 2.12: ASR in a bridge showing map cracks affecting the aesthetic value of the structure (Reactive Solutions, 2012).

2.8.3. Shale

Shale is the most abundant sedimentary rock worldwide and this is also the case at the MGO. Shale (in the form of fresh rock) is dense, meaning that due to a very low content of voids, it is relatively impermeable to water and transforms back into clay when weathering takes place. Shale is almost always found as layers of fine particles. This creates a bedding structure and readily shears along the planes/layers, a process called slaking; making it unsuitable for engineering purposes (Handy & Spangler, 2007).

Shale is a much softer rock than sandstone and quartzite. Shale weathers faster, due to shearing planes and the fact that it is made up of clay deposits. Therefore, durability of shale is minimal.



Figure 2.13: Typical soil profile of shale (Geology of KwaZulu-Natal, 2007) of the Ecca Group, which is similar to that found in the Karoo and Matjiesfontein.

Problems associated with shale in construction

When shale is excavated, pressure is removed from the soil causing the shale to rebound and expand. Expansion is aggravated if water (moisture) is available to weaken the electrostatic bonds that exist in the clay. A solution to this, apart from avoiding exposure of an excavated area to the atmosphere for extended periods of time, is to cover the area with a thin layer of cement/concrete or asphalt (Handy & Spangler, 2007). This ‘covering’ layer will need to be done as soon as possible after excavation in order to avoid the expansion and the infiltration of moisture/water.

Weathered shale used as fill on site, despite its hardness in the form of fresh rock, can easily absorb moisture and soften into clay. The moisture content can increase from as low as 2/3% in the form of hard rock to between 25% and 50% in the form of clay and can cause slope failures many years after completion of a project (Handy & Spangler, 2007).

2.8.4. Tillite

Approximately 300 million years ago South Africa was part of the super continent Gondwana and was very close to the South Pole. It was completely covered with ice and massive glaciers moved over the landscape in which rocks were collected and imbedded in the ice as illustrated in figure 2.14. Matjiesfontein forms part of the Karoo Supergroup basin in which the Dwyka Group is the oldest deposition from the glacial movement (Geology of KwaZulu-Natal, 2007).

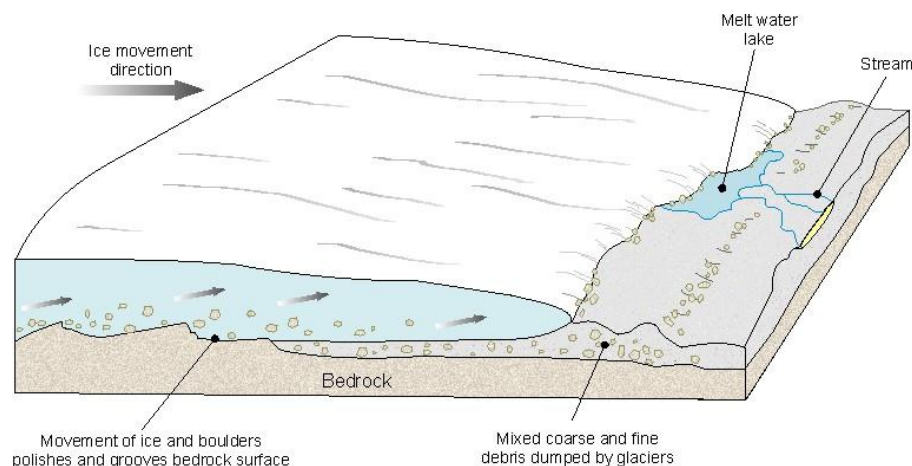


Figure 2.14: Illustration of how tillite is formed (Geology of KwaZulu-Natal, 2007).

Tillite rock is easily recognised as a finely grained, clay matrix with pieces of rock or small pebbles/boulders within the clay, which were picked up by the glaciers as they grinded over the landscape. In KZN, tillite typically disintegrates in a yellowish colour (Geology of KwaZulu-Natal, 2007). The glacial movement in the Matjiesfontein area was from north to south and often striations of rock surfaces can be seen making them look like they have been cut through by a chain saw leaving distinct lines indicating the direction of movement (Croukamp, pers. comm., 2011).



Figure 2.15: Typical picture of tillite (Geology of KwaZulu-Natal, 2007).

Problems associated with tillite as a construction material

Clay in tillite makes it a “soft” construction material, which steadily erodes to a more stable form (smaller fragments and small flaked off material). Tillite is generally used as an aggregate in concrete and asphalt but when on its own it breaks up and weathers, which can pose difficulties for the Matjiesfontein project.

In some regions, one of the major engineering problems with tillite is that it can disintegrate from solid, blue rock into relatively small cubical size blocks. This occurs when tillite is exposed to the atmosphere and does not undergo any chemical alteration but rather a physical breakdown (slaking); most likely because of the expansion and contraction of clay minerals within the rock when exposed to continual wetting and drying (Paige-Green, 1980 cited in Brink, 1983:37).

2.9. Other work completed at Matjiesfontein

Most work done regarding the rock mechanics for construction of the gravimeter vault, prior to this thesis, is that of Croukamp, Rossouw, Fourie, & Combrinck (2011). This included a site investigation through a joint survey, a rock mass description of the rockface (quartzitic sandstone) of the original location of the gravimeter vault, Unconfined Compressive Strength (UCS) test, RMR, and petrography. Other important work relevant to this thesis was the ACV test according to Janse van Rensburg (2012).

2.9.1. Joint survey

The joint survey was conducted to ascertain structural features that could potentially pose problems during construction in terms of rock stability and design accordingly. Slope direction, strata orientation and joint set largely affect the stability of a rock face or slope. Originally, the idea was to tunnel into the rock face in which to build the gravimeter vault. Two hundred joint readings over a span of approximately 200 m were taken and plotted on a stereoplot as shown in figure 2.16.

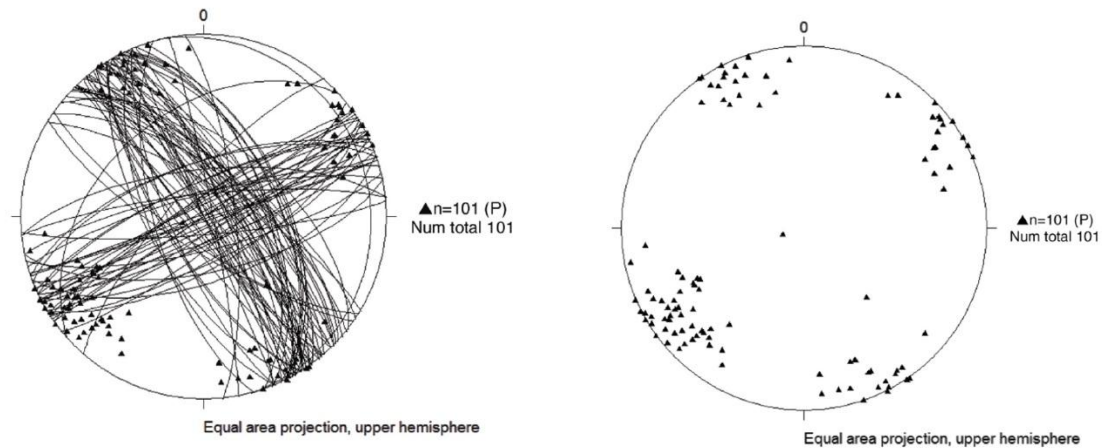


Figure 2.16: Left - Stereoplot (upper hemisphere) showing great circles, which represents the joint direction. Right - Stereoplot with the poles plotted as points (Croukamp et al., 2011).

The ridge is from east-to-west in the form of a trending fold axis with two distinct joint directions as can be seen in the stereoplot and figure 2.17 below. Croukamp *et al.* (2011) says, “The joints range from surface cracks to very deep joints. Major joint directions are perpendicular to the fold axial plane, simplifying the excavation procedure. However because of the high density of joints, roof stability inside the vault, during and after construction, might pose challenges for local stability.”



Figure 2.17: Side-on view of a more exposed part of the ridge along which the gravimeter vault is located. One can see the vertical bedding planes.

2.9.2. Rock mass description

RQD

Usually the RQD is calculated from drilled core samples as described earlier but because no core was available from the site, a simulation of a RQD was done over the rock face at the original location for the gravimeter vault (figure 2.18).

The RQD was found to be 69%, which is classified as ‘fair’ rock according to table 2.1. It is to be expected that pieces of rock will break off along the joints as the rock is disturbed, because the joint set is so discontinuous, with distances between joints varying between 2 and 50 cm. The RQD; therefore, is more a representation of the degree of fracturing and does not include an assessment of rock strength. The RQD should be used in conjunction with the RMR system to more accurately determine geometrical properties.



Figure 2.18: Rock face into which vault was to be constructed, with a 5 m imaginary core (Croukamp *et al.*, 2011).

Point Load Testing

The Brazilian Test Method was used to determine the Point Load Strength Index (I_s) and done according to the International Society for Rock Mechanics Commission on Testing Methods (1985 cited in Croukamp *et al.*, 2011). As the core samples tested were 40 mm in diameter, a correction factor (F) was used to determine the size-corrected Point Load Strength Index ($I_{st(50)}$) (Croukamp *et al.*, 2011).

The average $I_{st(50)}$ was found to be 6.39 MPa and most samples broke irregularly (Rossouw, 2010).

Lump Tests

Instead of using core samples, lumps of rock of relatively the same size (10 cm × 10 cm roughly) were subjected to Point Load Testing as done with the core samples. The sizes of the lumps were converted to an equivalent diameter of core (D_e) as the relative areas of the lumps were known (10 cm × 10 cm = 100 cm²). As done above in the Brazilian Test Method, F and $I_{st(50)}$ were calculated but instead of D, D_e was used (Croukamp *et al.*, 2011).

The average $I_{st(50)}$ was found to be 8.17 MPa and most of the breaks were irregular along bedding planes that exist within the rock (Rossouw, 2010).

2.9.3. UCS test

Three samples were tested for UCS, two of which were dolerite samples from the SAAO near Sutherland and the other from the previously proposed site for the gravimeter vault at the MGO. The reason for the comparison with Sutherland is that at the SAAO a similar vault has been built housing a superconducting gravimeter, which has been in operation for a few years.

The dolerite samples from Sutherland shattered sending splinters in different directions whereas the quartzitic sandstone from MGO crumbled as the pressure was increased. This is characteristic of the two rock types. The results from the UCS tests on the three samples can be seen in table 2.3 below.

Table 2.3: UCS results from samples from Sutherland and Matjiesfontein (data adopted from Rossouw, 2010).

Sample	Cross-sectional area (m ²)	Volume (m ³)	Unit Weight (kg/m ³)	Stress (MPa)
1 (SAAO)	0.01	0.001	3116.4	113.36
2 (SAAO)	0.01	0.001	3112.9	84.48
3 (MGO)	0.01	0.001	2630.1	54.6

2.9.4. RMR

The RMR was done as explained in 2.7.1 and table 2.2. According to Croukamp *et al.* (2011) the RMR was found to be 68, which classifies the rock as class number II (“good rock”). This means that for the purposes of tunneling, an unsupported, 10 m span has a stand-up time of 1 year and the cohesion in the rock is 300-400 kPa with a friction angle of 35-45°.

2.9.5. ACV test

According to Janse van Rensburg (2012), ACV tests were conducted on quartzitic sandstone, shale and tillite from the MGO site. The tests were conducted according to Technical Methods for Highways number 1 (TMH1) (1986), method B1, and the results are summarized in table 2.4. Although the test method suggests conducting three tests, only two ACV tests on each rock type were conducted. The results were generally close to each other for each different material; therefore, it was assumed that the results accurately revealed the ACV value.

The ACV is known as the percentage of material passing the 2.36 mm sieve, when material passing the 13.2 mm sieve and retained on the 9.5 mm sieve is crushed to an applied load of 400 kN (TMH1, 1986).

$$ACV = \frac{M_{2.36}}{M} \times 100$$

Where, $M_{2.36}$ is the mass (g) fraction passing the 2.36 mm sieve
 M is the mass (g) of the sample

Table 2.4: Summary of ACV results according to Janse van Rensburg (2012).

Material type	Sample number	Mass of sample (g)	Material mass passing 2.36 mm (g)	ACV (%)	Average ACV (%)
Quartzitic sandstone	1	1229.0	411.4	33.40	31.72
	2	1043.3	312.6	29.96	
Shale	1	1065.2	175.3	16.46	16.27
	2	1156.5	186.1	16.09	
Tillite	1	1079.3	133.2	12.34	13.32
	2	1147.1	164.0	14.30	

2.9.5. Petrography

According to Rossouw (2010), petrographic analyses (petrographic microscope) of two polished thin-sections were conducted on samples from the MGO site. These samples were both from along the same ridge at the location of the gravimeter vault. Both samples were classified as medium to coarse grained (0.5–1.0 mm) orthosandstone. Table 2.5 below summarizes the properties of the two samples. V1 is the sample taken from the original intended location for the gravimeter vault and Lun 1 is from the location of the LLR.

Table 2.5: Summary of petrography from analysis under a polarizing microscope. Sample V1 from the original intended location for the gravimeter vault and Lun1 from the site where the LLR station is to be built.

V1	Lun1
<ul style="list-style-type: none"> • No quartz veins observed • Sedimentary bedding well developed • Petrography <ul style="list-style-type: none"> ➢ Predominantly quartz ➢ Accessory potassium feldspar ➢ Traces of white mica ➢ Potassium feldspar not altered to sericite ➢ Some quartz-rich aggregates of earlier well cemented quartzite present ➢ Iron staining common particularly in vugs, which are rimmed by goethite-limonite ➢ Clay content negligible in pristine rock ➢ Where weathering advanced → thin rims of sericite/clay may expose grains and combine with iron ➢ Mineral phase unidentifiable ➢ Quartz grains closely packed and subrounded ➢ Grain size distribution slightly bimodal → high maturity sediment (monomineralic composition) ➢ On fresh surface, break is through grains rather than around → quartzite name applicable ➢ Cementing agent is secondary silica → not advanced to significant extent because the clastic grain outline is clearly visible 	<ul style="list-style-type: none"> • Less vuggy than V1 → harder than V1 • At least two generations of thin (1-2 mm) quartz veins → may contribute to silicification of rock matrix • Sedimentary bedding not well displayed • Petrography <ul style="list-style-type: none"> ➢ Predominantly quartz ➢ Scattered potassium feldspar grains ➢ Very similar to V1 ➢ Traces of chlorite and rutile ➢ Quartzitic aggregates observed ➢ Grained tightly packed ➢ Clear evidence of cementation by secondary silica → explains greater hardness than V1 ➢ Sedimentology features such as packing, grain size, roundness and sorting similar to V1 ➢ Although sedimentary bedding not visible macroscopically → well displayed microscopically by beds showing vertical grain size variations ➢ Less weathered than V1 → secondary clay fraction insignificant ➢ On fresh surface, break is through grains rather than around → quartzite name applicable ➢ Cementing agent is secondary silica → not advanced to significant extent because the clastic grain outline is clearly visible

Chapter 3. Method

3.1. Tests

3.1.1. Slake Durability

In the slake durability test, seven lumps of rock, for each of the four different rock types (quartzite, tillite, sandstone and shale), were placed in four respective bins/drums. The assembly was rotated on an axle for five wet/dry cycles (1 cycle – wet for 12 hours during the day and dry for 12 hours during the night). During the wet period of a cycle, the bins were partially submerged in water in order for all the lumps of rock to be submerged when not rotating and then for the dry period of a cycle, the water was completely drained.

After the five wet/dry cycles were complete, the mass of rocks left over in each respective bin was compared to that of the total original mass that was put in the respective bins prior to the test. This data was then used to calculate the percentage of deterioration that each rock type underwent during the rotation cycles.

Photos before and after were also taken for visual comparisons in degradation.

Test Apparatus

Four bins with a width of 100 mm and diameter of 250 mm were constructed. The circumference of each bin consisted of Polyvinyl Chloride (PVC) pipe (250 mm in diameter) with a matrix of 20 mm diameter holes and closed on the sides with 13 mm mesh. Each bin was positioned on an axle and rotated at five rotations per minute.



Figure 3.1: Apparatus used for the slake durability test. From left to right in consecutive containers: quartzite, tillite, sandstone and shale.

Assumptions and limitations

According to Brink (1983:89-90), the standard International Society of Rock Mechanics (ISRM) slake durability test is suitable for the breakdown of samples into particle sizes. However, for disintegrating rocks the most suitable test was to qualitatively evaluate the behaviour of six lumps of rock (36.5-26.5

mm in particle size) in wire-mesh baskets during five wet-dry cycles in water. The cycles were conducted by Venter (1980, cited in Brink, 1983:90).

Because the slaking of disintegrating rocks into different shapes and sizes were to be tested, the test conducted by Venter (1980, mentioned in Brink, 1983:90) was adapted and an apparatus was constructed that would release ≤ 20 mm particle/lump sizes. Along with a qualitative evaluation, quantitative results were also recorded for comparison with future analysis.

3.1.2. 10%FACT

During the 10%FACT two samples of each rock type were tested for their 10%FACT value. One sample for each rock type was tested under dry conditions and the other under wet conditions (soaked for 24 hours).

The purpose of the 10%FACT test was to determine the force required that would yield 10% fines (10% of the original specimen mass) in a dry and wet condition and was conducted in accordance with SANS 5842 (2006). The present 10%FACT specification for the wet-to-dry ratio for road aggregates is a minimum of 75%, and the minimum 10%FACT value in the dry condition is 210 kN (Thothela, Robertson, & Jenkins, 2011).



Figure 3.2: Left: tamping the aggregate lightly with tamping rod (a), plunger (b), base plate (c), steel cylinder (d) and measure (e). Right: assembly in compression testing machine.

Assumptions and limitations

An assumption was made that the aggregate would yield a percentage fines in the region of 7.5% to 12.5% with the estimated forces, which can be found in Appendix A (table A.2 and A.3) and if not the force was adjusted to yield between 7.5% and 12.5% fines. The equation below from SANS 5842 (2006) was used to determine the 10%FACT value for each rock type.

$$F = \frac{14 \times x}{y + 4}$$

Where, F is the force necessary to produce 10% fines (kN)
 x is the force necessary to produce a percentage fine between 7.5% and 12.5% (kN)
 y is the percentage fines that correlate with force x

3.1.3. UCS test

The main purpose of the UCS test is to determine the UCS value of quartzite and tillite (the two strongest rocks from the MGO site). Rock cores (100 mm in diameter) were drilled from quartzite and tillite samples from the MGO site, cut, measured and tested as described in Method for Determining the Unconfined Compressive Strength of Intact Rock Specimens (n.d.).

Even though the UCS test was conducted on three samples from the original location for the gravimeter vault and the SAAO prior to this thesis as mentioned in the literature study; in this thesis other rocks from around the site/area were tested in order to see how they compared to that tested in Rossouw (2010).



Figure 3.3: Core specimens of 100 mm depth and diameter in the compression testing machine. Left: quartzite core sample. Right: tillite core sample.

3.1.4. Grading Analysis

A grading analysis was conducted for fine and coarse aggregate of local materials from Matjiesfontein. The analysed fine aggregate was local river sand from a non-perennial river at Matjiesfontein whereas for coarse aggregate, quartzite (Table Mountain Group) and tillite (Dwyka formation) were analysed. The method that was followed was according to SANS 201 (2008).

Two grading analyses were done on the natural river sand (fine aggregate). The first was of a large sample of roughly 3 kg. The sand was washed, dried and sieved in order to determine if at least 90%

of the material passes the 4.75 mm sieve and is retained on the 0.075 mm sieve as well as have a general natural grading. This would classify it as ‘sand’ (SANS 1083, 2006). The mass recorded in the ‘receiver’ (table A.1 in Appendix A) is the mass of the material left over in the pan plus that of the material washed out prior to the sieving and drying process. The second sieve analysis was conducted more accurately in accordance with SANS 201 (2008) only on fine aggregate (≤ 4.75 mm sieve aperture size); i.e., the larger material was sieved out.

In both the coarse and fine aggregate sieve analyses, large samples of aggregate were divided using a riffler. This was done to get the correct mass needed for the relevant tests and, as far as possible, keep an accurate representation of the sample as a whole.

Fine aggregate

From the grading analysis of the fine aggregate (river sand ≤ 4.75 mm), the dust content and FM were calculated as follows (SANS 201, 2008):

$$\text{Dust content} = \frac{(a - b) + c}{M_{Ff}} \times 100$$

Where,

- a is the original sample mass (g)
- b is the sample mass (g) after wet sieving
- c is mass of the material (g) that passes the 0.075 mm (75 μm) sieve
- M_{Ff} is the total sample mass (g) of the test sample after sieving, plus (a – b)

$$FM = \frac{\text{sum of percentages of material retained on each sieve (except 0.075 mm sieve)}}{100}$$

Fineness modulus gives the degree of coarseness of the fine aggregate through a numerical value. Lower values indicate a finer sand and higher values, a coarser sand.

Coarse aggregate

For coarse aggregate the dust content is the percentage of material passing the 0.075 mm sieve. From the grading analysis of the coarse aggregate (quartzite and tillite); the dust content was calculated as follows (SANS 201, 2008):

$$\text{Dust content} = \frac{d - g}{M_{Fc}} \times 100$$

Where,

- d is the original test sample mass (g)
- g is the material mass (g) after wet sieving
- M_{Fc} is the total test sample mass (g) after sieving

From the grading analysis the coefficient of uniformity for quartzite and tillite coarse aggregate was calculated as follows (SANS 1083, 2006):

$$U_a = \frac{D_{60}}{D_{30}}$$

Where, U_a is the uniformity coefficient
 D_{60} is the hypothetical aperture size through which 60% of the material passed by mass, which can be calculated from the grading graph or from tabular results
 D_{30} is the hypothetical aperture size through which 30% of the material passed by mass, which can be calculated from the grading graph or from tabular results

Assumptions and limitations

In SANS 201 (2008) the sieve apertures may differ slightly from the analyses conducted. For instance, a sieve with a sieve aperture size of 5 mm was used instead of 4.75 mm as the 4.75 mm sieve was unavailable. It was assumed that these sizes are very close and that material passing through a 5 mm sieve aperture would be 4.75 mm in size. The sieves used and their relevant aperture sizes are as shown in Appendix A.

For the coarse aggregate analysis, the nominal particle size of the aggregate was not known because the crusher used to crush the stone is not calibrated to deliver a specific stone size and no screening process had been done to deliver a specific nominal aggregate size. Therefore, a mass of roughly 3 kg, as crushed, was analyzed.

In SANS 1083 (2006), table 2, there is no reference to a lower limit for fines in coarse aggregate; therefore, it was assumed that only the dust content needs to be determined to satisfy the prerequisite.

3.1.5. RD – Pycnometer method

The RD test was conducted according to the pycnometer method in SANS 5844 (2006). The pycnometer with aggregate and water was subjected to a vacuum in order to remove trapped air. The RD was calculated as follows:

$$RD = \frac{M_w}{M_w + M_s - M_T}$$

Where, M_w is the mass (g) of the water used to fill the pycnometer excluding the aggregate in the pycnometer
 M_s is the mass (g) of the stone or sand aggregate used to fill a third of the pycnometer
 M_T is the mass (g) of the stone or sand aggregate and plus water to fill the pycnometer

Three different RD tests were conducted on each of the respective materials from Matjiesfontein to be used in the concrete mix design; i.e., quartzite, tillite and river sand. Then an average of the three RD's

was calculated, which was then used to determine the relevant mix designs, which is discussed in 3.2.1.



Figure 3.4: Pycnometer consisting of a glass jar with a sealed spun top used to determine relative density of material (Pycnometer Top and Jar, 2013).

3.2. Design

3.2.1. Concrete mix design

Four mix designs were considered during testing. In all the designs local rocks (quartzite and tillite) were crushed and screened for 19 mm coarse aggregate, which was used. In the first two designs Malmesbury sand was used as fine aggregate, which is a common fine aggregate used in construction in the Western Cape, and local river sand was used as fine aggregate in the final two mix designs. Ordinary Portland Cement (OPC), category CEM II/B-M (L-S) 42.5 N, was used in all the mixtures. The desired 28 day strength prescribed for the concrete was 40 MPa with a water-cement (W:C) ratio of 0.55. The mix designs were conducted as described in Addis (1998:106-111) with minor changes as advised by Ramat, pers. comm. (2012). Concrete cubes were made and the cube strength was determined for the different concrete mix designs.

Table 3.1: Mix design 1.

W:C = 0.55	On 1000L						On 10 L
	Mass (kg)		Relative density (RD)		Mass (kg)		Mass (kg)
Water	180	÷	1	=	180	(Σ = 648)	1.80
CEM II/B-M (L-S) 42.5 N	327	÷	3.14	=	104		3.27
Stone (quartzitic sandstone)	950	÷	2.61	=	364		9.50
Sand (Malmesbury)	922	=	2.62	×	352	(1000 – Σ)	9.22

Table 3.2: Mix design 2.

W:C = 0.55	On 1000L						On 10 L
	Mass (kg)		Relative density (RD)		Mass (kg)		Mass (kg)
Water	180	÷	1	=	180	(Σ = 641)	1.80
CEM II/B-M (L-S) 42.5 N	327	÷	3.14	=	104		3.27
Stone (Tillite)	950	÷	2.66	=	357		9.50
Sand (Malmesbury)	941	=	2.62	×	359	(1000 – Σ)	9.41

In mix design 3 (table 3.3), the mixture was found to be unworkable, as can be seen in figure 3.5, probably due to the sand containing a predominating particle size and being too coarse. In order to counteract this, a new mixture (table 3.4) was mixed, in which the water content was increased; increasing the cement content. This is not ideal, because of the higher cement content, which is more expensive.

Table 3.3: Mix design 3 (original).

W:C = 0.55	On 1000L						On 10 L
	Mass (kg)		Relative density (RD)		Mass (kg)		Mass (kg)
Water	180	÷	1	=	180	(Σ = 648)	1.80
CEM II/B-M (L-S) 42.5 N	327	÷	3.14	=	104		3.27
Stone (Quartzitic sandstone)	950	÷	2.61	=	364		9.50
Sand (River sand)	936	=	2.66	×	352	(1000 – Σ)	9.36



Figure 3.5: Original mix design 3. The design was unworkable because of the dust within the river sand.

Table 3.4: Newly proposed mix design 3.

W:C = 0.55	On 1000L						On 10 L
	Mass (kg)		Relative density (RD)		Mass (kg)		Mass (kg)
Water	215	÷	1	=	215	(Σ = 704)	2.15
CEM II /B-M (L-S) 42.5 N	391	÷	3.14	=	125		3.91
Stone (sandstone)	950	÷	2.61	=	364		9.50
Sand (River sand)	787	=	2.66	×	296	(1000 – Σ)	7.87

Although the new design showed improvement, the slump achieved was in the region of 10 mm. This, according to Ramat, pers. comm. (2012) is too low as the desirable slump should be approximately 75 mm. A slump of 75 mm is commonly used in construction and is conducive to workability with minimal segregation (Ramat, pers. comm., 2012). The low slump that was achieved was possibly also because the aggregate was a lot more weathered than that of mix design 1 (quartzitic sandstone) classifying it more as a weathered sandstone. During the tamping process, the sandstone aggregate would disintegrate further into sand particles, thus increasing the amount of fines that would ultimately make the mixture less workable. Even though the above statement may be true, it does not fully explain the low slump; therefore, it was concluded that if a less weathered sandstone (or quartzitic sandstone) was used, the slump would still not achieve the desired 75 mm.

Table 3.5: Mix design 4.

W:C = 0.55	On 1000L						On 10 L
	Mass (kg)		Relative density (RD)		Mass (kg)		Mass (kg)
Water	215	÷	1	=	215	(Σ = 697)	2.15
CEM II /B-M (L-S) 42.5 N	391	÷	3.14	=	125		3.91
Stone (Tillite)	950	÷	2.66	=	357		9.50
Sand (River sand)	806	=	2.66	×	303	(1000 – Σ)	8.06

Similarly, the slump of mix design 4 (table 3.5), did not achieve the desired slump of 75 mm. The slump of mix design 4 was about 40 mm.



Figure 3.6: Images of mix design 4. The slump (right) was about 40 mm.

3.2.2. Vault design

The vault design was made as simple as possible and robust to ensure that the building will experience minimal movement; either from crustal movement, vibrations caused by the movement of vehicles/machinery or wind. This is because the instruments used for gravimetric surveying are very sensitive and can detect very small movements. The whole building was built on solid bedrock and the plinth, on which the instruments are to be installed is independent of the rest of the vault. The plinth is also sunken deeper than the bottom level of the floor slab as to ensure it is solidly connected to the Earth's crust. Building foam fills the gap around the plinth in order to absorb any human induced shock movements or another non-seismic activity. According to Combrinck, pers. comm. (2012), small movements do occur and are accepted as background noise but minimising it as much as possible is preferred and where possible the movements will be filtered out during analyses.

The calculations for the plinth/beam and floor slab design, in terms of steel reinforcement, can be found in Appendix C. As can be seen in figures 3.7 and 3.8, the steel rebar is made up of high yielding steel of 9 and 16 mm in diameter. Mesh reinforcement (ref: 500) in the floor slab is sufficient as minimal loads are to be applied on the floor surface. The diameter of the bars of the mesh reinforcement is 9 mm and procured in standard mesh sheets of 6×2.4 meters. Figure 3.8 through to 3.11 shows the design of vault.

The walls for the gravimeter vault were built using bricks (220×105×73 mm) procured locally from a community project in Laingsburg. Damp course plastic was used to prevent moisture to penetrate through into the walls and roof. On every third layer of bricks, 'brick force' was placed to strengthen the wall. Stone cladding using local rock was placed and tied on the outside of the walls in order to blend in with the rest of the environment. Lintels (150×75×3000 mm) were stacked next to each other to make up the roof, on which a 100 mm slab was cast.

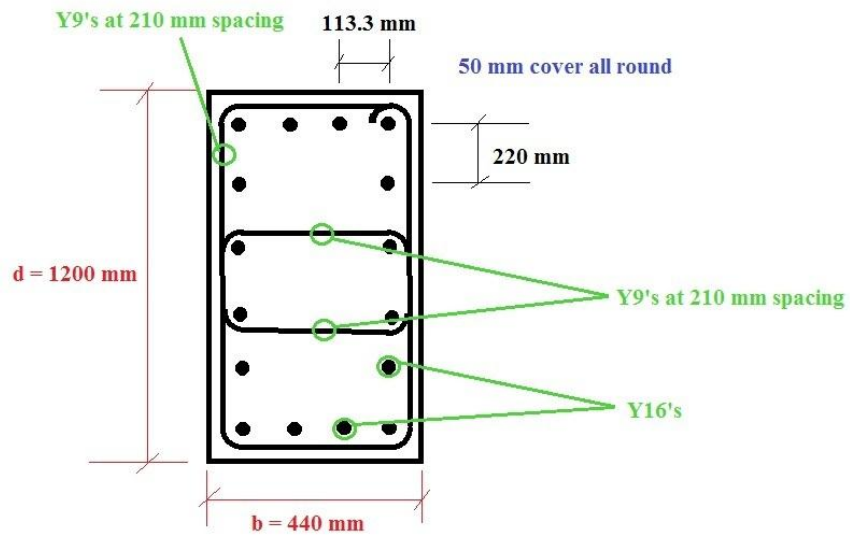
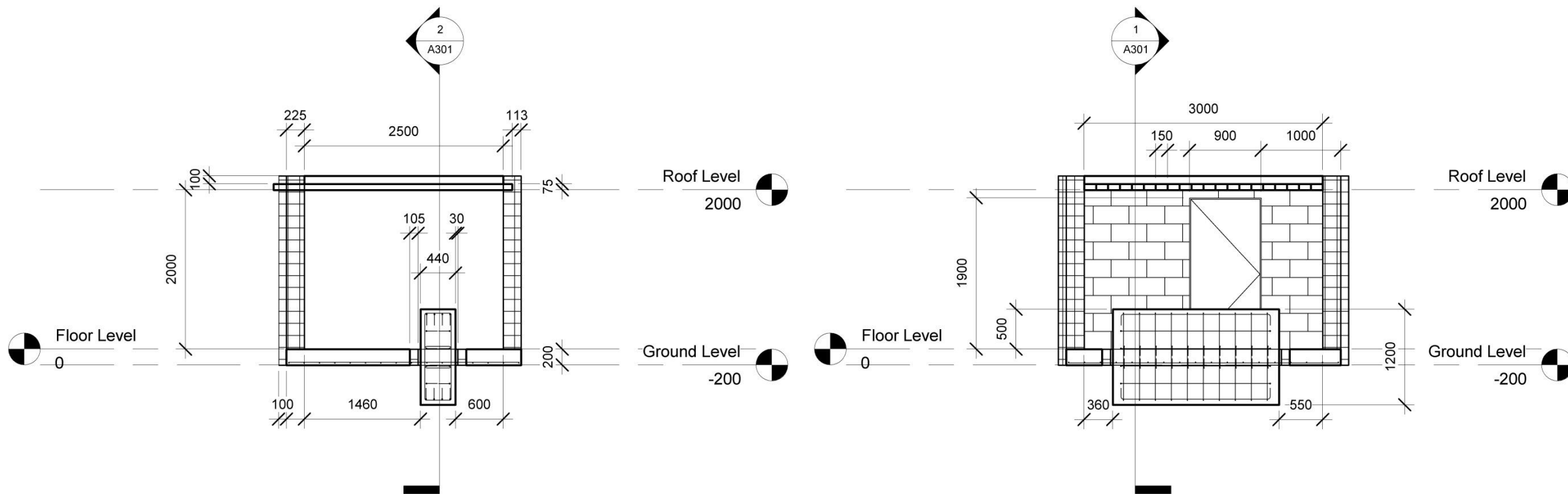


Figure 3.7: Plinth/beam design with reinforcement. Note that the drawing is not to scale.



1 Section 1
1 : 50

Rebar Schedule							
Bar Diameter	Spacing	Quantity	Bar Length	Shape	A	B	Description
9	200	8	3400	Rebar Shape 1			Ref. 500 Mesh
9	200	4	400	Rebar Shape 1			Ref. 500 Mesh
9	200	4	590	Rebar Shape 1			Ref. 500 Mesh
9	200	4	3400	Rebar Shape 1			Ref. 500 Mesh
9	200	2	2900	Rebar Shape 1			Ref. 500 Mesh
9	200	13	1500	Rebar Shape 1			Ref. 500 Mesh
9	200	13	640	Rebar Shape 1			Ref. 500 Mesh
9	200	3	2900	Rebar Shape 1			Ref. 500 Mesh

2 Section 2
1 : 50

Rebar Schedule							
Bar Diameter	Spacing	Quantity	Bar Length	Shape	A	B	Description
9		10	3300	74	1100	340	Plinth Reinforcement
9		10	540	35	340	0	Plinth Reinforcement
9		10	540	35	340	0	Plinth Reinforcement
16		4	2130	35	1890	0	Plinth Reinforcement
16		4	2130	35	1890	0	Plinth Reinforcement
16		4	2130	35	1890	0	Plinth Reinforcement
16		4	2130	35	1890	0	Plinth Reinforcement



No.	Description	Date

Leon Croukamp
Matjiesfontein Geodesy Observatory

Sectioned Views		
Project number	A301	
Date	18/07/2013	
Drawn by	R.G. Strydom	
Checked by	P.R. Van Wyk	Scale 1 : 50

2013/08/02 12:55:51 PM

Figure 3.8: Gravimeter vault design with bending schedule for steel reinforcement for the floor slab and the plinth, on which gravimetric instrumentation are to be installed.

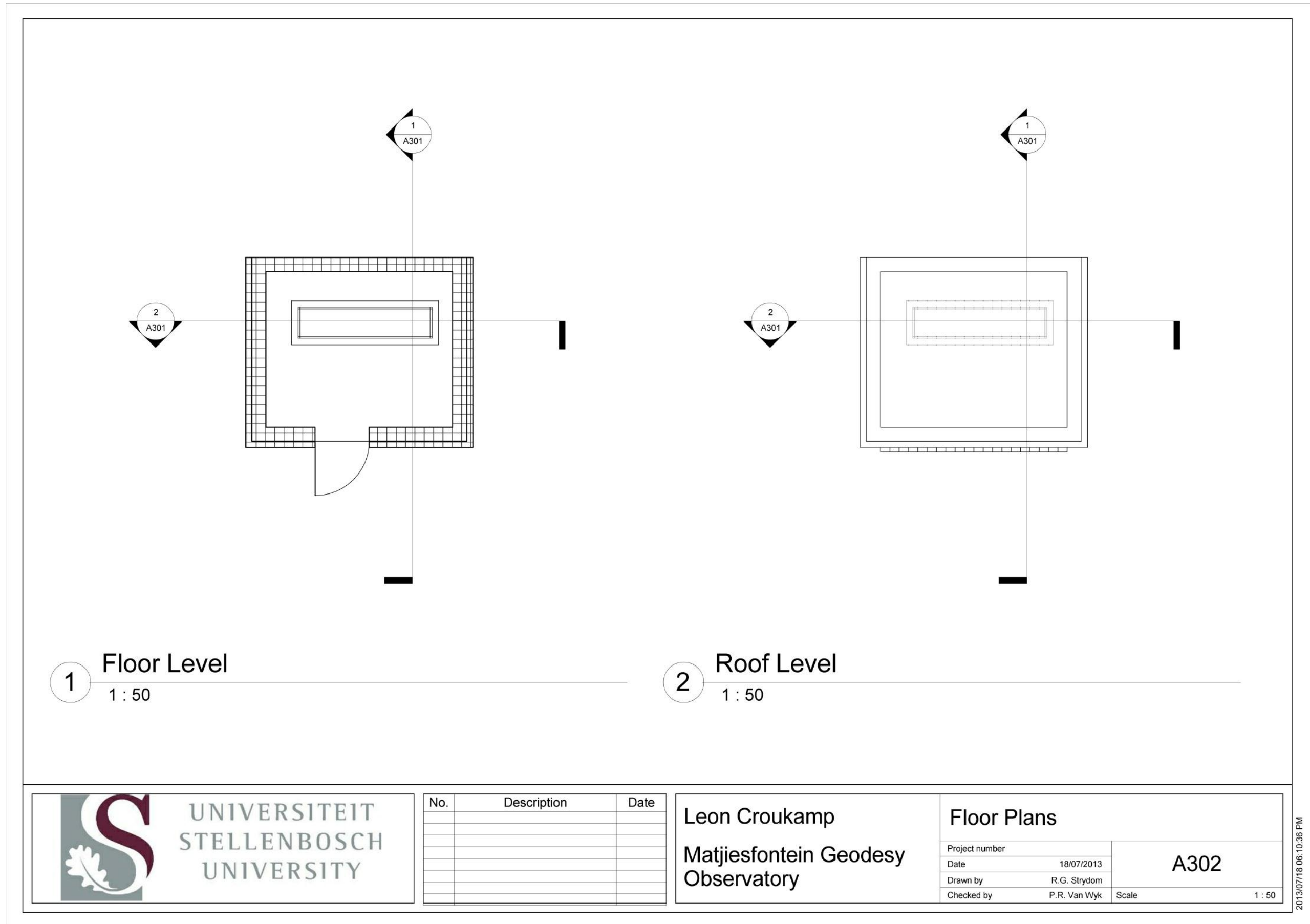


Figure 3.9: Gravimeter vault design. Floor and roof level view.

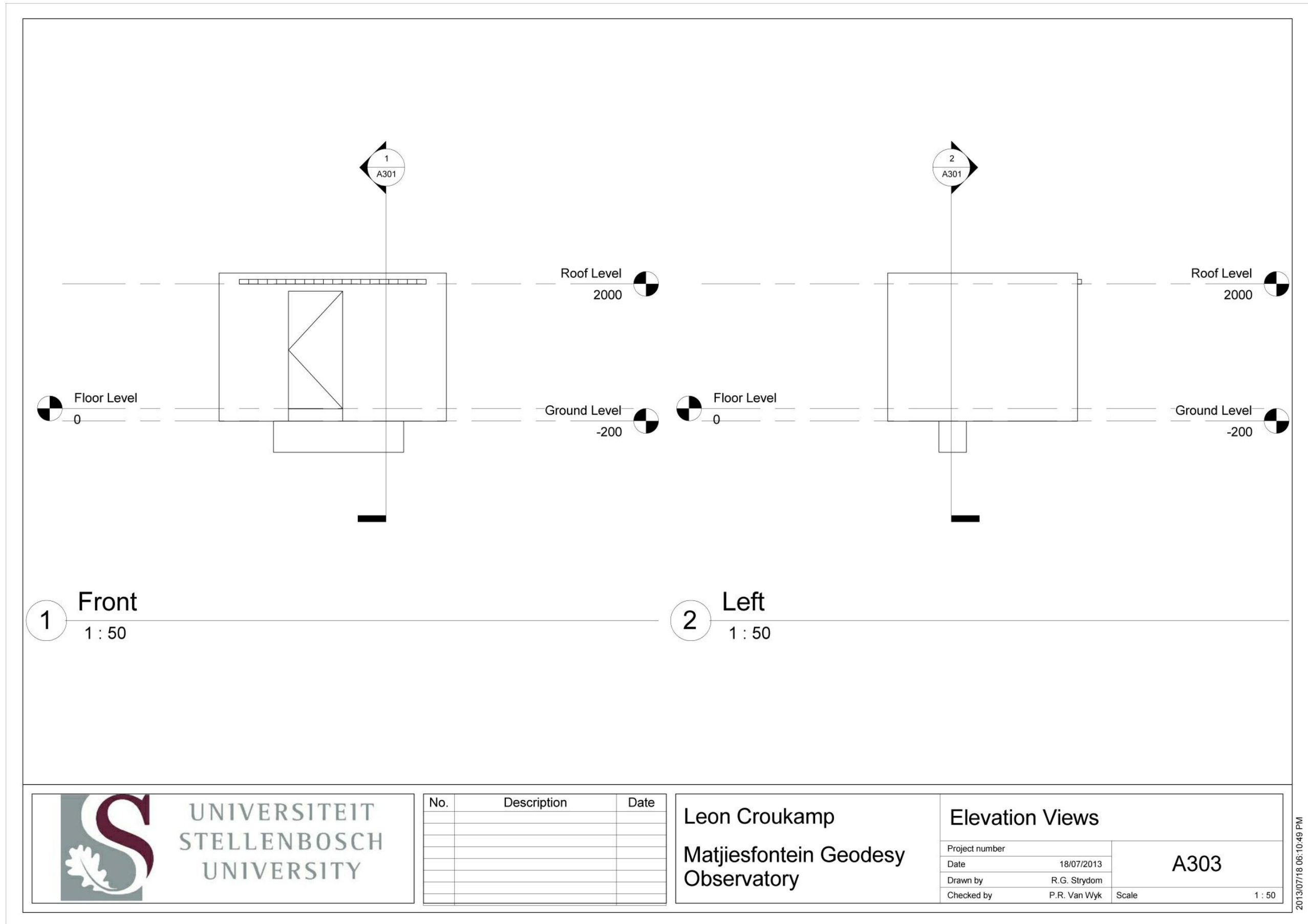


Figure 3.10: Gravimeter vault design. Front and left hand side view.

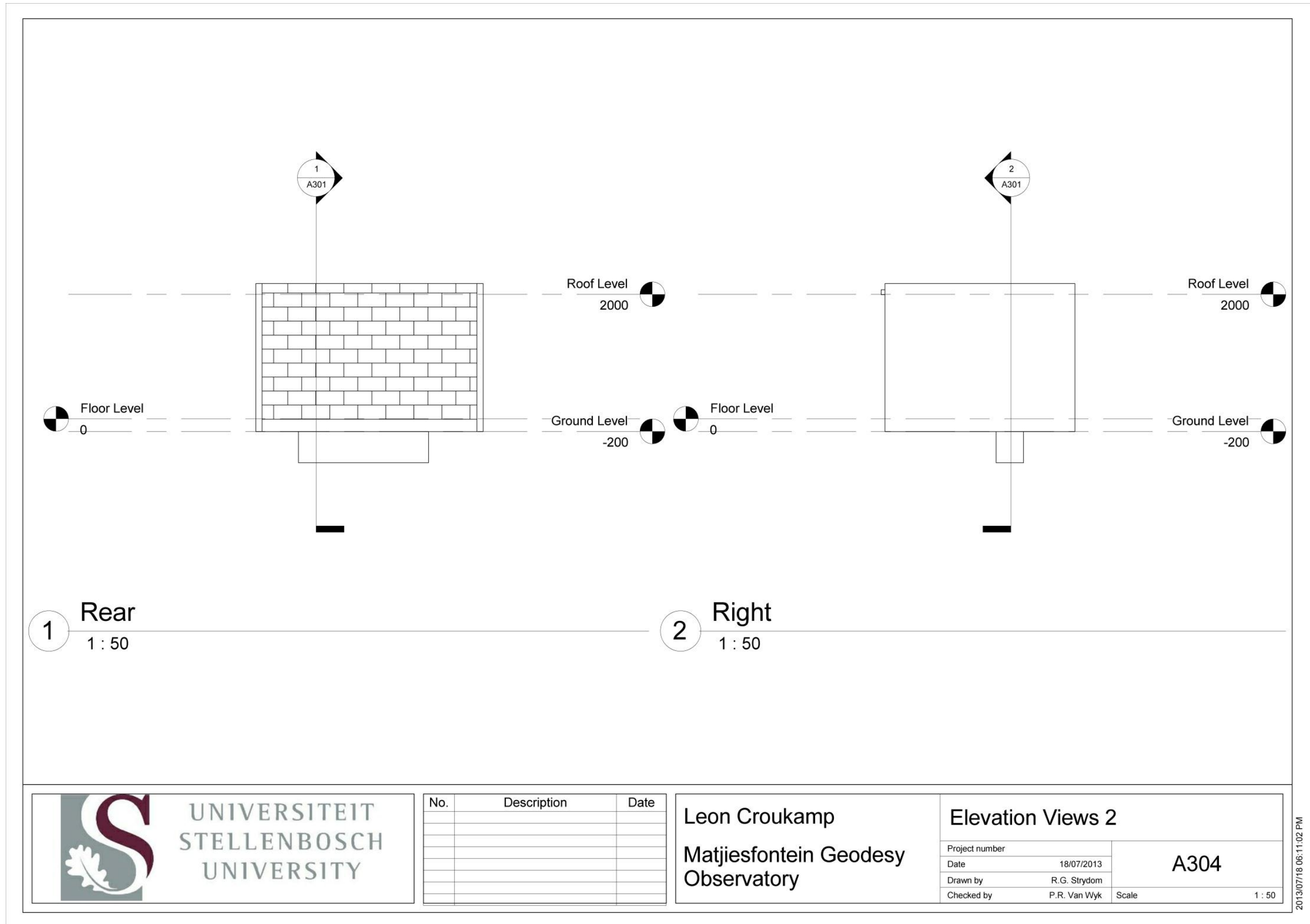


Figure 3.11: Gravimeter vault design. Rear and right hand side view.

3.3. Petrographic analysis

3.3.1. PXRD analysis

PXRD analysis was conducted on four samples of each rock type (quartzitic/hard sandstone, shale and tillite) as well as on one sample of river sand; i.e., thirteen samples altogether. Only one sample of river sand was tested because the river sand in the area is a relatively homogeneous mixture of weathered material from the area.

Samples were crushed into a fine powder (particle size $< 70 \mu\text{m}$) with a jaw-crusher and milled in a tungsten-carbide Zibb mill (figure 3.12) prior to the preparation of a pellet. The jaw crusher and mill were cleaned with clean uncontaminated quartz between consecutive samples to avoid cross contamination.



Figure 3.12: Left: Tungsten-carbide Zibb mill use to mill material into a fine powder. Right: Milling bowl, in which material is placed to be milled into a fine powder.

The phases present within the aggregate samples were determined through quantitative and qualitative analysis. The data from the analysis was processed using X'Pert Highscore plus software. The relative phase amounts (weight percentages) were estimated using the Rietveld method. A PANalytical X'Pert Pro (figure 3.13) XRD machine was used for the analysis. All sample preparation and analysis was conducted at the Central Analytical Facility (CAF) at the University of Stellenbosch (South Africa).



Figure 3.13: PANalytical X'Pert Pro machine used for XRD analysis.

Experimental conditions

The following experimental set-up conditions were applied during testing:

- Goniometer: PW3050/60 (Theta/Theta)
- Sample stage: Reflection- transmission spinner PW3064/60
- Diffractometer system: XPert-PRO
- Anode material: Cu
- K-Alpha1 wavelength: 1.5405980 Å
- K-Alpha2 wavelength: 1.5444260 Å
- Ratio K-Alpha2/K-Alpha: 1: 0.50
- Divergence slit (fixed): 0.19 mm
- Monochromator used: No
- Generator voltage: 45 V
- Tube current: 40 A
- Scan range: 2.998000003° - 85.000197307°
- Scan step size: 0.0083556°
- No. of points: 9814
- Scan type: Continuous
- Time per step: 11.430 s

3.3.2. XRF analysis

Samples were crushed into a fine powder as explained for the PXRD analysis prior to the preparation of a fused disc for major elements analysis. Glass disks were prepared for XRF analysis using ten grams of high purity trace element and Rare Earth Element-free flux ($\text{LiBO}_2 = 32.83\%$, $\text{Li}_2\text{B}_4\text{O}_7 =$

66.67%, LiI = 0.50%) mixed with 1g of the powdered sample, which had been dried. To form the glass discs, the samples were heated to 1000°C (figure 3.14), poured into molds and then left to cool and solidify.

Whole-rock major element compositions were determined by XRFS on a PANalytical Axios Wavelength Dispersive spectrometer. The spectrometer is fitted with a rhodium (Rh) tube and the following analyzing crystals: LIF200, LIF220, PE 002, Ge 111 and PX1. The instrument is fitted with a gas-flow proportional counter and a scintillation detector using a 90% argon-10% methane mixture of gas. Major elements were analyzed at 50 kV and 50 mA tube operating conditions. Matrix effects in the samples were corrected by applying theoretical alpha factors and measured line overlap factors to the raw intensities measured using SuperQ PANalytical software. The concentration of the control standards that were used in the calibration procedures for major element analyses fit the range of concentration of the samples. Amongst these standards were NIM-G (Granite from the Council for Mineral Technology, South Africa) and BE-N (Basalt from the International Working Group).

Like the PXRD analysis, the XRF analysis was conducted at the University of Stellenbosch as part of CAF.



Figure 3.14: Melting of the samples, which are then cooled to make fusion discs.

3.3.3. SEM analysis

In the SEM analysis samples of quartzite, quartzitic sandstone, tillite and shale were analysed using a Zeiss EVO® MA15 Scanning Electron Microscope in figure 3.15 at the University of Stellenbosch (CAF). The SEM analysis was used as an alternative means to determine the petrography of the different rock types from Matjiesfontein and to see if strained quartz could be identified using SEM. Flat samples of rock were polished and qualitative analysis and backscatter imaging (mapping) were conducted. Samples were identified with backscattered electron (BSE) images, and phase

compositions were quantified by Energy-dispersive X-ray spectroscopy (EDX) analysis using an Oxford Instruments® X-Max 20 mm² detector and Oxford INCA software. EDX was only suitable for determining major elements of minerals at concentrations over 0.1 wt% for major elements.



Figure 3.15: SEM machine and computer used in the SEM analysis.

Experimental conditions

- Sample coating: gold (15 µm thickness)
- Beam conditions
 - 20 kV
 - Working distance: 8.5 mm
 - Approximate beam current: 20 nA
 - Counting time: 10 s
- Standardization and verification of analyses: scientific mineral standards used
- Pure Cobalt (Co) used periodically to correct for detector drift

Limitations

The polishing of the samples proved a longer process than anticipated and upon inspection many of the samples were not polished to a high enough standard. This created some difficulty in identifying strained quartz within the samples but valuable petrographic characteristics could be established, which other tests could not.

3.3.4. Petrographic microscope – strained quartz

A petrographic microscope was used to determine if strained quartz exists within the samples. Thin-sections of tillite, shale, sandstone/quartzitic sandstone and quartzite were inspected under polarized light. Grains of quartz can clearly be seen as different shades of grey. As mentioned before, when rotating the thin-section, strained quartz will appear to be darker (or lighter) in extinction bands within

the same quartz grain known as undulatory extinction, hence indicating a strain/deformation in the quartz lattice. Photo-micrographs of different quartz crystals were taken to enable the identification of strained quartz. The thin-sections were prepared at the University of Cape Town (Geology Faculty) and inspection for strained quartz at the University of Stellenbosch (Geology Faculty).

Chapter 4. Results

4.1. Test results and interpretation

4.1.1. Slake durability results

The slake durability test revealed that quartzite and tillite were the most durable materials, losing only 10.5% and 16.5% of their initial sample mass respectively. As illustrated in figure 4.1, sandstone and shale proved drastically less durable than quartzite and tillite, losing over half their initial mass during five wet/dry cycles.

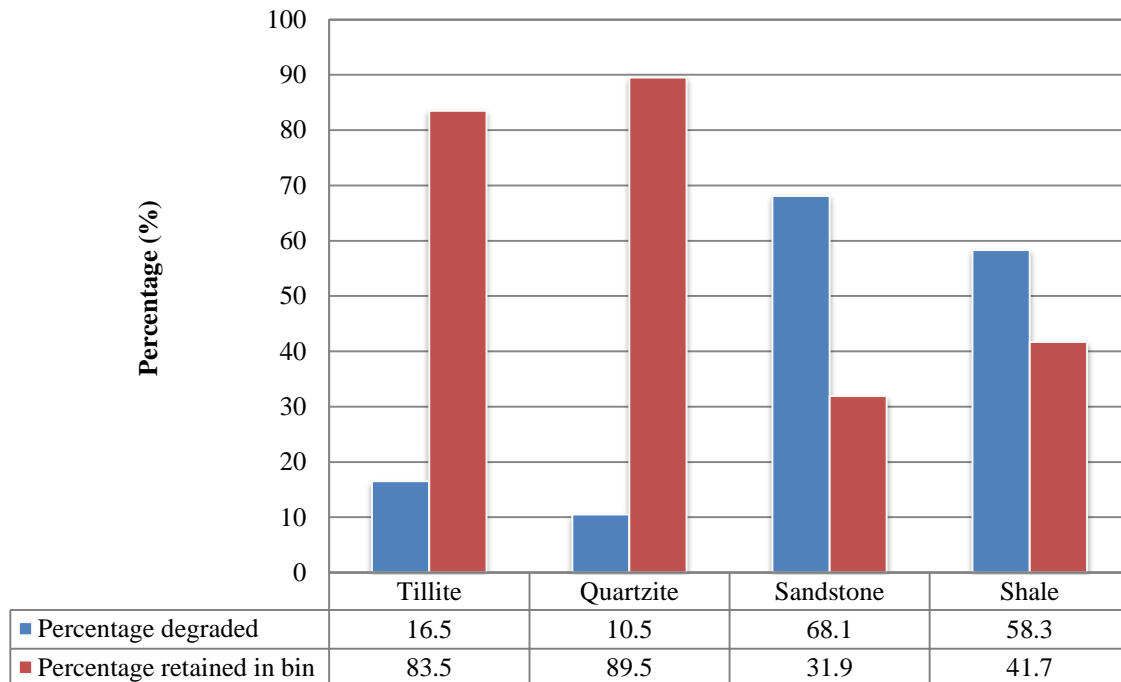


Figure 4.1: Slake durability test results of the percentage, which the different rock types degraded and the percentage of the initial mass remained in the bins after test completion.

Figure 4.2 below shows photographs of the samples taken before and after the test. Quartzite showed little breakdown and weathering and much of the material that was collected in the container underneath the basket throughout the test was in the form of silt size particles similar to dust that had, through mechanical interaction with the surfaces of the apparatus and other lumps of rock, degraded. The quartzite lumps generally remained in an angular form but rounded at the edges.

Like quartzite, tillite had shown little breakdown and the material recovered in the container under the tillite bin consisted of tiny flaky pieces of rock material and a “powderish” appearance. The tillite lumps also remained angular with rounded edges.

Sandstone showed the most weathering and the material collected in the container was in the form of sand particles. The shapes of the sandstone lumps changed from angular in appearance to rounded small to medium size lumps, many of which were small enough to fall out of the bin into the container and are; therefore, < 20 mm in diameter.

Shale, as was expected, broke down in different shapes and sizes although with the tumbling action of the wheel they were rounded at the edges. In nature this would not necessarily be the case and the slaked off fragments would be angular and sharp but the test does reveal the extent to which typical shale rocks degrade. Far less silt size particles and flaky pieces of material were found in the container than that of the other rock types.

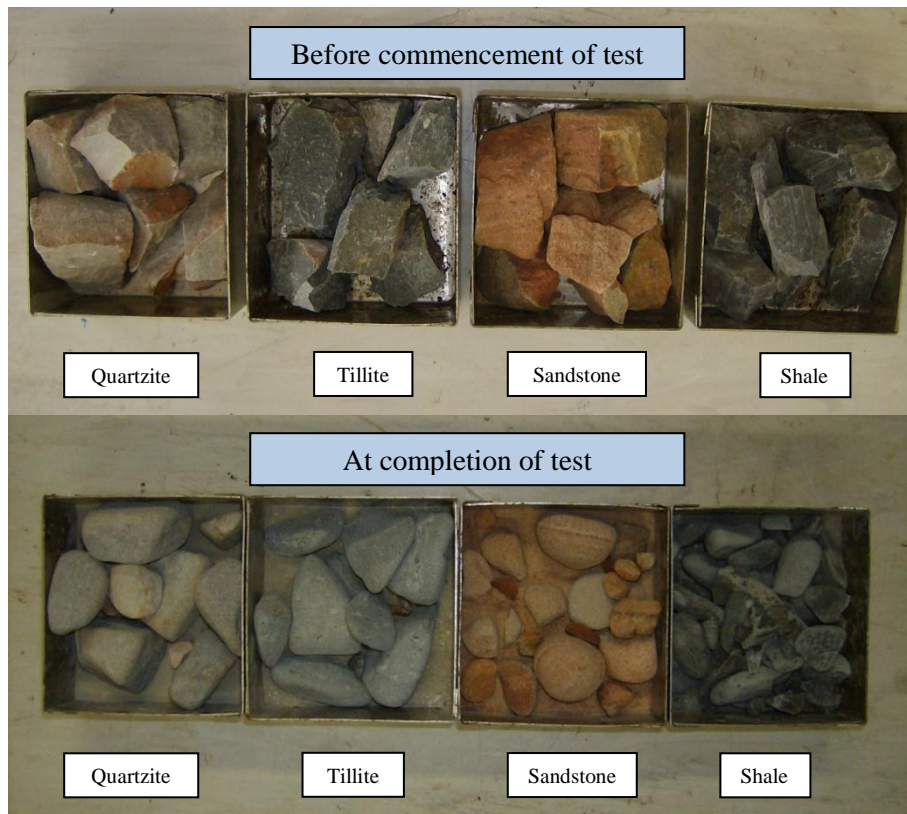


Figure 4.2: Images of the different rock types prior to the slake durability test and after.

4.1.2. 10%FACT results

Figure 4.3 and table 4.1 below summarizes the 10%FACT results for the rock types in the wet and dry conditions. As mentioned previously, the 10%FACT value in the dry condition should be more than 210 kN and the wet-to-dry ratio greater than 75% in order for the aggregate to be deemed fit for road construction. Tillite and shale both satisfied these prerequisites whereas sandstone and quartzite did not. This is probably because sandstone and quartzite generally break down into smaller (finer) particles instead of fragmenting like tillite and shale before getting crushed enough in the crushing mechanism to yield 10% fines, thus requiring a larger force.

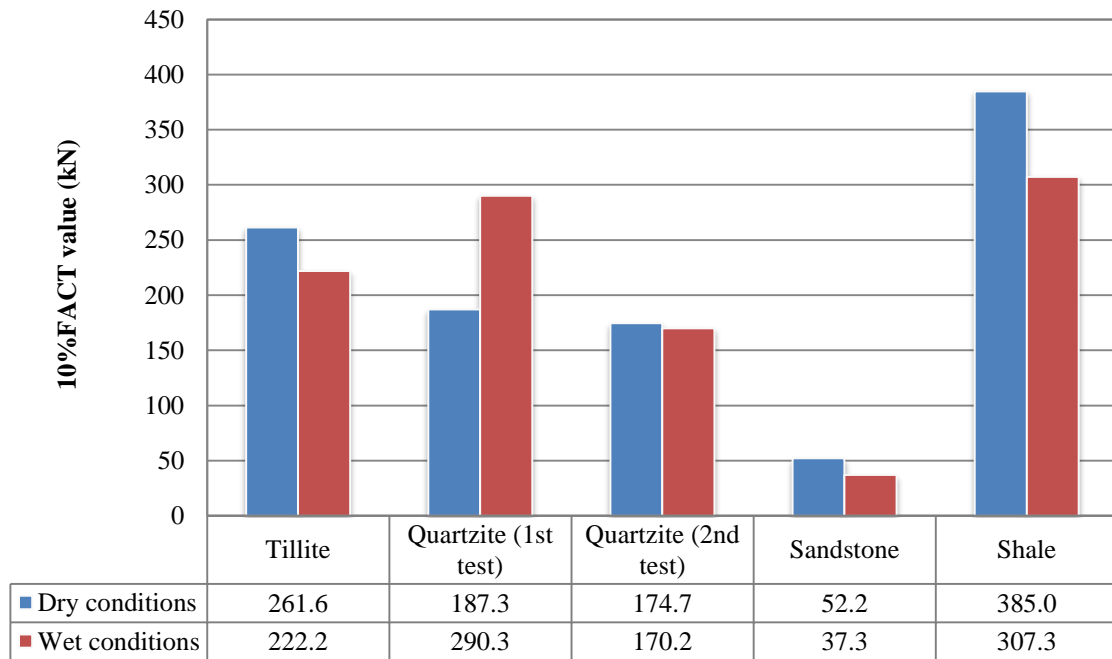


Figure 4.3: 10%FACT results showing the 10%FACT value for each rock type in the wet and dry condition.

Although sandstone showed a wet-to-dry ratio of less than 75%, recent studies in South Africa have suggested relaxing the specification (Thothela *et al.*, 2011). The 10%FACT value for the wet condition for the first quartzite test was significantly higher than that of dry condition, resulting in a 155% wet-to-dry 10%FACT ratio.

Table 4.1: Wet-to-dry 10%FACT ratio results.

Rock type		Wet-to-dry 10%FACT ratio
Tillite		84.9%
Quartzite	1 st test	155.0%
	2 nd test	97.4%
Sandstone		71.5%
Shale		79.8%

4.1.3. UCS results

Two samples of tillite were tested but the one (tillite 2 in table 4.2) was not completely intact (crack, which can be seen in figure 4.4); therefore, the sample broke under a low axial load. A rating system for tillite, published in Brink (1983:38) classifies 122 – 298 MPa as unweathered, 80 – 130 MPa as slightly weathered, 10 – 40 MPa as moderately weathered, 5 – 22 MPa as highly weathered and < 1 MPa as completely weathered. The tested tillite would be classified closer to moderately weathered with 41.92 MPa. This is an accurate indication of the sampled tillite, because during site visits it was noted that the collected tillite had protruded from the ground and had been subject to initial weathering.

As can be seen in table 4.2, quartzite yielded very high stress results in comparison to the tillite specimens, which is attributed to its closely compacted structure and hardness. It is classified as unweathered.

In comparison to the Matjiesfontein samples tested by Rossouw (2010) in table 2.3, the quartzite sample yielded high stress results similar to the dolerite samples from the SAAO and the tillite samples similar to the quartzitic sandstone sample from the original site of the gravimeter vault.

Table 4.2: UCS test results.

Rock sample	Cross-sectional area (m ²)	Volume (m ³)	Unit weight (kg/m ³)	Stress (MPa)	Rating
Tillite 1	0.01	0.001	2643.3	41.92	± Moderately weathered
Tillite 2	0.01	0.001	2428.4	15.27	Moderately weathered
Quartzite	0.01	0.001	2590.6	154.67	Unweathered

Figure 4.4 shows the core specimens after testing. Quartzite exhibits vertical cracks with splinters breaking off, whereas tillite has cracks more diagonally through the specimens.



Figure 4.4: Test specimens after testing. Left to right: quartzite, tillite 2 and tillite 1.

4.1.4. Grading analysis

Fine aggregate: River sand

As mentioned previously, the first grading analysis was conducted on a large sample of roughly 3 kg mass, from which the larger material was not sieved. This was to determine the most natural sieve analysis curve of the sand shown in figure 4.5. Complete sieve analysis results can be found in Appendix A, table A.1. The sieve analysis showed that only 84% of the material passed the 4.75 mm sieve and were retained on the 0.075 mm sieve. Therefore, the river sand in its natural form is not classified as a fine aggregate according to SANS 1083 (2006). Hence, the larger material (> 4.75 mm) was sieved out and the second sieve analysis (Appendix A, table A.2) was conducted according to SANS 201 (2008).

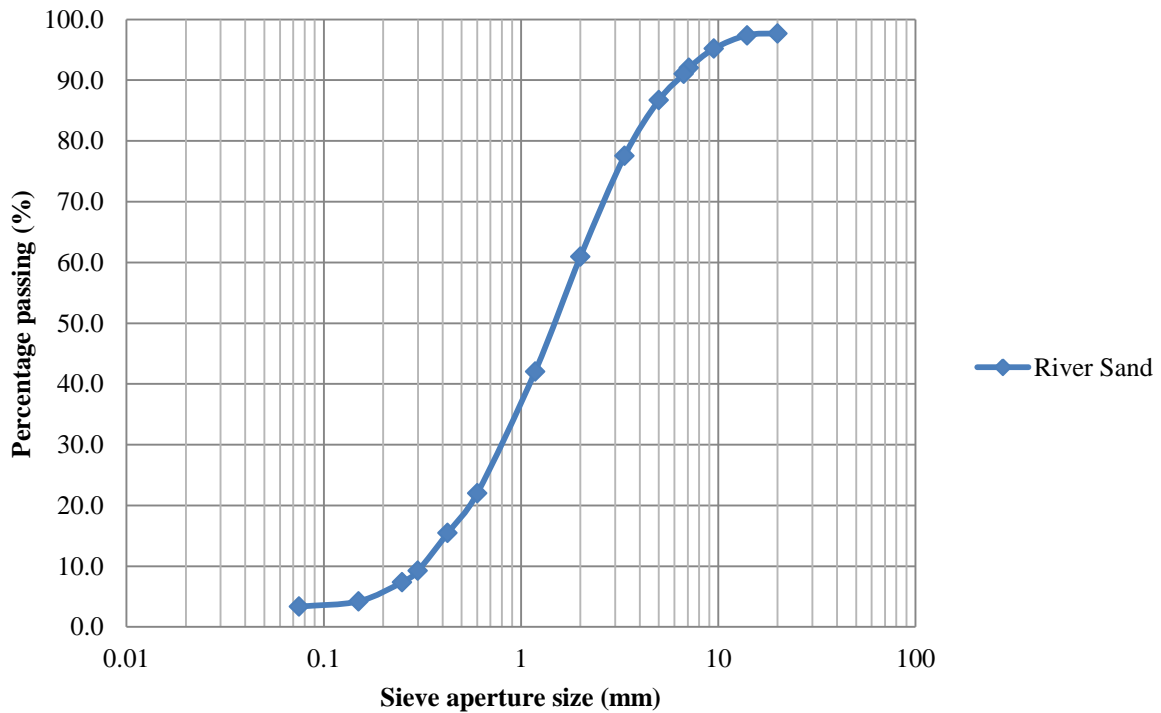


Figure 4.5: First natural sieve analysis curve of river sand (without sieving out the larger material > 4.75 mm) as found in a river at Matjiesfontein close to the MGO site.

From the sieve analysis the dust content was found to be 3.7 % and the FM was 3.2. According to SANS 1083 (2006), the limit for dust content for a blend of fine aggregate is 5% and a FM between 1.2 and 3.5. Therefore, the river sand with 3.7% dust satisfies this limit. The FM also falls within the FM limit of 1.2 to 3.5.

The graph in figure 4.6 shows the grading of the natural sand from Matjiesfontein where the larger material greater than 4.75 mm has been removed. This graph also shows the fine/coarse limits as mentioned previously. As can be seen the river sand from Matjiesfontein transgresses the coarse limit, which explains the unworkable nature of the concrete mixtures, in which the river sand was used as fine aggregate.

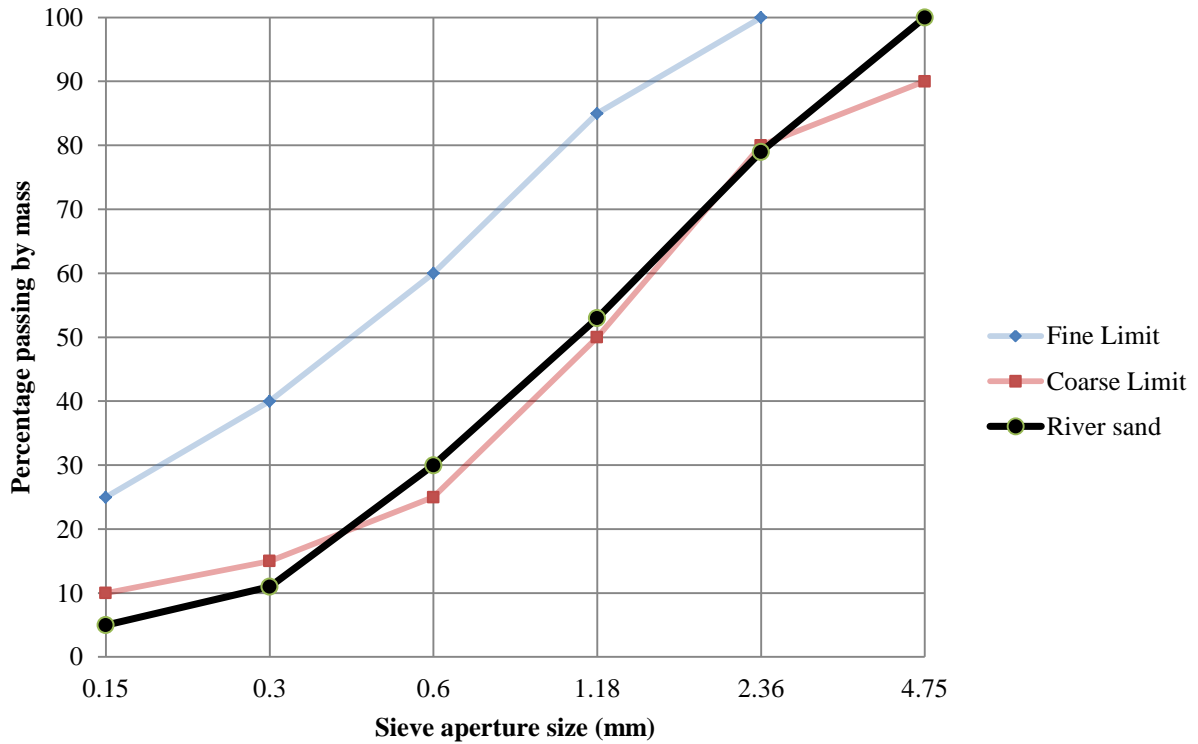


Figure 4.6: Grading of natural river sand from Matjiesfontein showing the fine/coarse limits according to Addis (1998: 88).

Coarse aggregate

The sieve analysis for coarse aggregate can be seen in figure 4.7. The tillite and quartzite curves are very similar. Tabular results and calculations of the sieve analysis can be found in Appendix A.

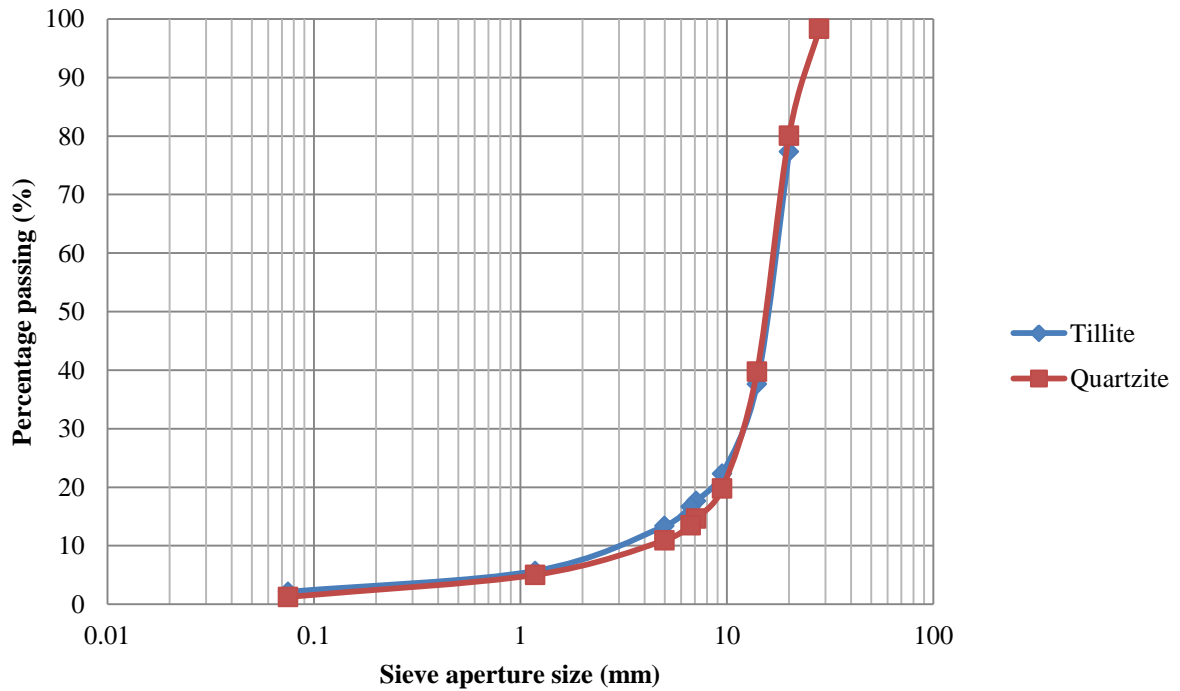


Figure 4.7: Sieve analysis of crushed tillite and quartzite from the MGO site for the use of coarse aggregate.

The dust contents for tillite and quartzite aggregate were found to be 2% and 1%, respectively. According to SANS 1083 (2006), the limit for dust content is 2%. If the dust content was greater than 2%, it may result in a concrete mixture that is less workable.

The coefficient of uniformity (U_a) for tillite and quartzite aggregate are 1.5 and 1.4 respectively. Typically, a project plan would include a contractual specification of a coefficient of uniformity in terms of a specific nominal aperture size to be maintained during delivery. This nominal aperture is the size of aggregate to be used in the concrete mix design. Earlier, in the mix design, 19 mm rock was screened out and used as the ‘nominal’ aperture size.

4.1.5. RD results

The average RD for quartzite, tillite and river sand from Matjiesfontein were found to be 2.61, 2.66 and 2.66 respectively. The complete results can be seen in Appendix B, table B.1. The average relative densities were used in determining mix designs in 3.2.1. The RD’s of other materials used in the concrete mix design, such as the Malmesbury sand and cement (2.62 and 3.14 respectively), were according to Ramat, pers. comm. (2012).

4.2. Cube strength

The desired 28-day cube strength of 40 MPa was achieved with all the mix designs that were tested as can be seen in table 4.3. Complete 7-day and 28-day results can be found in Appendix B, table B.2 and B.3.

Table 4.3: Average 28-day compression cube strength of mix designs.

Mix design number	Average 28-day compression strength (MPa)
1	44.53
2	43.72
3	45.35
4	48.57

The average cube strength for mix designs 1 and 2, where Malmesbury sand was used as fine aggregate, were slightly lower than mix design 3 and 4, where river sand from Matjiesfontein was used as fine aggregate.



Figure 4.8: Cube strength testing of mix design 1.

4.3. Vault Construction

4.3.1. Difficulties experienced during construction

Difficulties experienced during construction were mainly as a result of the location's remoteness. The access road to the site consists of a dirt track that had been eroded over years creating ditches and exposing sharp rocks. Therefore, delivery of material using larger vehicles was not possible and most material had to be transported using a 4×4 pick-up truck. During construction care had to be taken to minimize the impact on the environment.

Weather conditions also affected productivity as day temperatures ranged from 10-30°C over the construction period with occasional rainfall. Photographs taken during construction in chronological order are shown in Appendix C.



Figure 4.9: MGO gravimeter vault at completion.

4.3.2. Costs

A prerequisite of the project was to make use of local labour and procure building materials locally as much as possible in order to bring financial benefit and involvement for the local community. Most building materials were resourced locally from Laingsburg and surrounds. Although some of the materials were expensive in comparison to materials resourced from further away, transportation costs were less. The costs of the construction in 2013 of the gravimeter vault at Matjiesfontein are summarized in table 4.4.

Table 4.4: Costs involved with building the gravimeter vault at the MGO.

	Item	Price	Amount	Cost
Excavation	Drilling and blasting	R 400 /m ²	18 m ²	R 7200
	Delivery of explosives	R 2850 /delivery	1 delivery	R 2850
Building Materials	Bricks (220×105×73 mm)	R 1.60 /brick	2800 bricks	R 4480
	Delivery of bricks	R 600 /delivery	3 deliveries	R 2800
	Stone aggregate	R 170 /ton	5 tons	R 850
	Sand aggregate	R 750 /m ²	6.5 m ²	R 4875
	Delivery of sand	R 350 /delivery	2 deliveries	R 700
	Reinforcement rebar	R 9000 /ton	0.093 tons	R 840
	Mesh reinforcement (6×2.4 m)	R 300 /sheet	1 sheet	R300
	Brick force	R 120 /roll	1 roll	R 120
	Cement	R 70 /bag	50 bags	R 3500
	Wire	R 810 /roll	1 roll	R 810
	Building foam	R 500 /canister	2 canisters	R 1000
	Steel door with frame	R 500 /door	1 door	R500
	Plastic sheet (4×4 m)	R 45 /sheet	1 sheet	R 50
	Damp course (25 m roll)	R 90 /roll	1 roll	R 90
	Creststone	R 236.25 /bag	3 bags	R 710
Machinery	Drive unit	R 100 /day	20 days	R 2000
	Generator	R 200 /day	20 days	R 4000
	Poker unit	R 100 /day	20 days	R 2000
	Concrete mixer	R 180 /day	20 days	R 3600
	Fuel for machinery	R 13 /L	20 L	R 260
	Builder's tools and scaffolding	R 150 /day	20 days	R 3000
Vehicles	4×4 pick-up truck rental	R 700 /day	31 days	R 21700
	Fuel	R 13 /L	692 L	R 9000

Table 4.4 cont.: Costs involved with building the gravimeter vault at the MGO.

Item		Price	Amount	Cost
Vehicles cont.	Trailer rental	R 150 /day	20 days	R 3000
	Toll (other occasional vehicles to site incl.)	R 29 /payment	17 payments	R 490
Labour	Foreman	R 350 /day	20 days	R 7000
	Mason	R 200 /day	20 days	R 4000
	Labourers	R 150 /day	20 days	R 3000
Accommodation	Project coordinators	R 400 /day	20 days	R 8000
Subsistence	Project coordinators	R 180 /day	25 days	R 4600
	Cell phones	R 500 /phone /month	2 phone for 1 month	R 1000
Unforeseen expenses	Tube replacement in tyre	R 90 /tube	1 tube	R 90
	Burst trailer tyre	R 780 /tyre	1 tyre	R 780
	Building expenses (tools)	vary	n/a	R 1000
	Electrical supplies (cabling)	R 80 /roll	1 roll	R 80
			Total	R 110275

4.4. Petrography

4.4.1. PXRD results

The average weight percentages of four samples for each of the main phases identified in the analysis are summarized in table 4.5. The complete PXRD results are in Appendix C. The chemical compositions for the different phases are as follows and give an idea of what elements/minerals may exist in the different material types:

- Chlorite – $(\text{Mg, Fe})_3(\text{Si, Al})_4\text{O}_{10}(\text{OH})_2 \cdot (\text{Mg, Fe})_3(\text{OH})_6$
- Microcline – KAlSi_3O_8
- Muscovite – $\text{KAl}_2(\text{AlSi}_3\text{O}_{10})(\text{F, OH})_2$ or $(\text{KF})_2(\text{Al}_2\text{O}_3)_3(\text{SiO}_2)_6(\text{H}_2\text{O})$
- Plagioclase – $\text{NaAlSi}_3\text{O}_8$ to $\text{CaAl}_2\text{Si}_2\text{O}_8$
- Quartz – SiO_2

PXRD, XRF and SEM analyses are combined to identify the different materials.

Table 4.5: Average relative phase amounts (weight %) of materials from Matjiesfontein.

Material type	Average relative phase amounts by wt %				
	Chlorite	Microcline	Muscovite	Plagioclase	Quartz
Tillite	13.59 ± 0.96%	11.09 ± 1.02%	5.45 ± 0.56%	27.19 ± 1.12%	42.69 ± 1.02%
Shale	11.76 ± 1.11%	2.78 ± 0.77%	13.82 ± 1.01%	15.28 ± 1.36%	56.36 ± 1.45%
Sandstone (quartzitic)	2.05 ± 0.53%	0.71 ± 0.37%	1.66 ± 0.33%	0.51 ± 0.28%	95.08 ± 0.70%
River sand	11.48 ± 1.53%	1.81 ± 0.84%	12.08 ± 1.17%	15.32 ± 1.35%	59.30 ± 1.74%

4.4.2. XRF results

The major elements identified in the samples in different quantities as illustrated in figure 4.10 are:

- Aluminium (Al)
- Calcium (Ca)
- Chromium (Cr)
- Iron (Fe)
- Potassium (K)
- Magnesium (Mg)
- Manganese (Mn)
- Sodium (Na)
- Phosphorus (P)
- Silicon (Si)
- Titanium (Ti)

The Loss on Ignition (LOI) represents the loss in weight when the samples are heated to 1000°C, caused by volatiles that exist in the minerals being released during melting.

All the elements identified correspond with the PXRD and SEM analyses except for chromium. In figure 4.10, chromium is in such small quantity that it may be ignored. Most of the mineral phases in all the rock types (shown in 4.4.1) contain silicon in some form and quantity except for quartzite, where the majority of the silicon is contained in the quartz minerals.

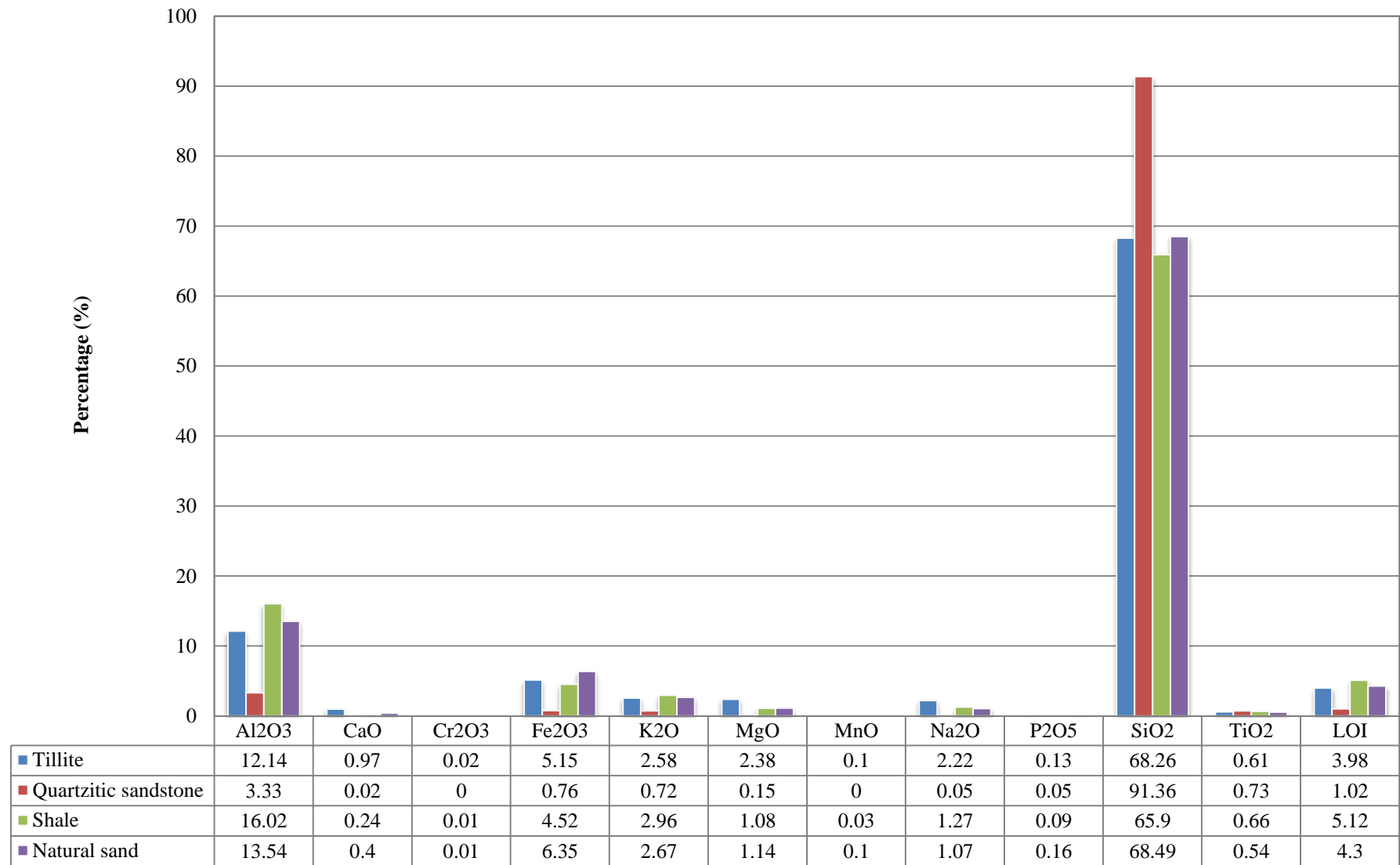


Figure 4.10: XRF results.

4.4.3. SEM results

Strained quartz

From the SEM analysis strained quartz could not easily be identified. Separate quartz crystals could also not easily be seen as other minerals seem to be embedded in a matrix of quartz. Only one area on the quartzite sample looked like strained quartz in the form of microscopic cracks as can be seen in figure 4.11. Although this may indicate the presence of strained quartz, it was concluded that the images do not comprehensively or conclusively indicate the presence of strained quartz. Therefore, examinations of thin-sections under a petrographic microscope were conducted.

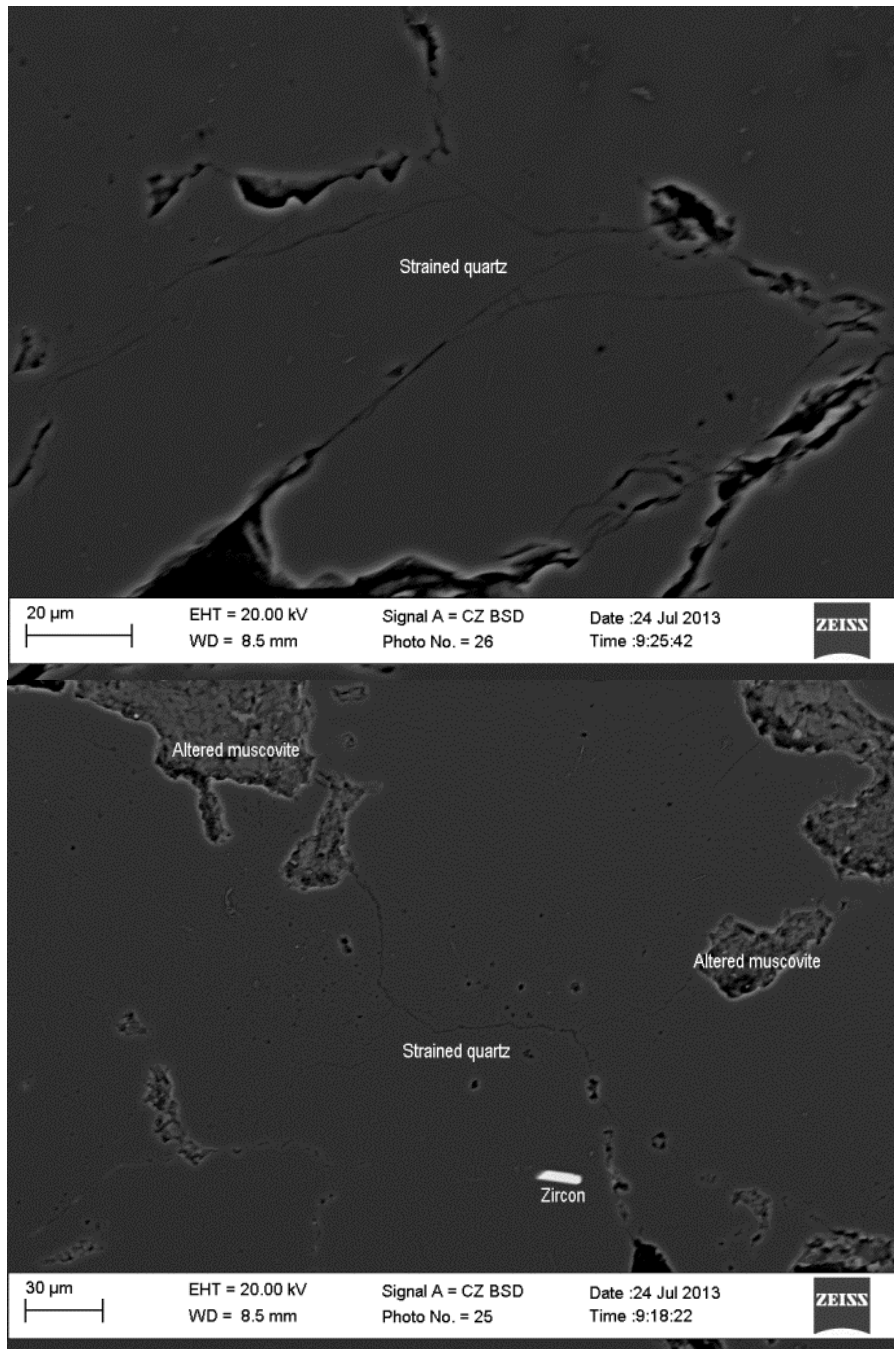


Figure 4.11: SEM images indicating what may be strained quartz in a quartzite sample.

Mineralogy

The main minerals (with general chemical composition) that could easily be identified are as follows:

- Quartzite
 - Quartz – SiO_2
 - Rutile – TiO_2
 - Muscovite – $\text{KAl}_2(\text{AlSi}_3\text{O}_{10})(\text{F}, \text{OH})_2$ or $(\text{KF})_2(\text{Al}_2\text{O}_3)_3(\text{SiO}_2)_6(\text{H}_2\text{O})$
 - Hematite – Fe_2O_3
 - Monazite – $(\text{Ce}, \text{La})\text{PO}_4$
- Tillite
 - Quartz – SiO_2
 - Rutile – TiO_2
 - Albite (plagioclase feldspar mineral) – $\text{NaAlSi}_3\text{O}_8$
 - Biotite (mica group) – $\text{K}(\text{Mg}, \text{Fe})_3\text{AlSi}_3\text{O}_{10}(\text{F}, \text{OH})$
 - Monazite – $(\text{Ce}, \text{La})\text{PO}_4$
- Shale
 - Same as tillite

One interesting mineral that was found in relatively large abundance in all the samples was zircon (ZrSiO_4). According to Ramphaka, pers. comm. (2013), zircon can be used for dating rocks; i.e., determining the age of the rock mass through isolating and dating the zircon within the rock mass.

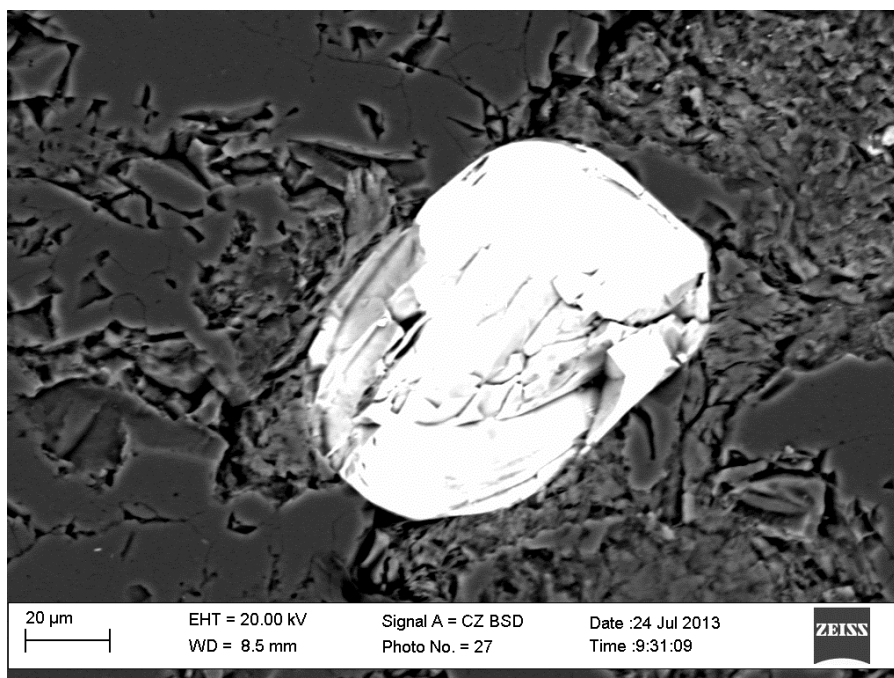


Figure 4.12: Zircon mineral in quartzite sample.

Elemental Mapping

As can be seen in figure 4.13, different minerals and shapes can be distinguished. The silicon indicates the quartz minerals; aluminium and potassium the muscovite minerals; and titanium the rutile minerals. The relevant minerals are indicated by the white/bright shades in the images. See Appendix D for complete mapping images for the different rock types.

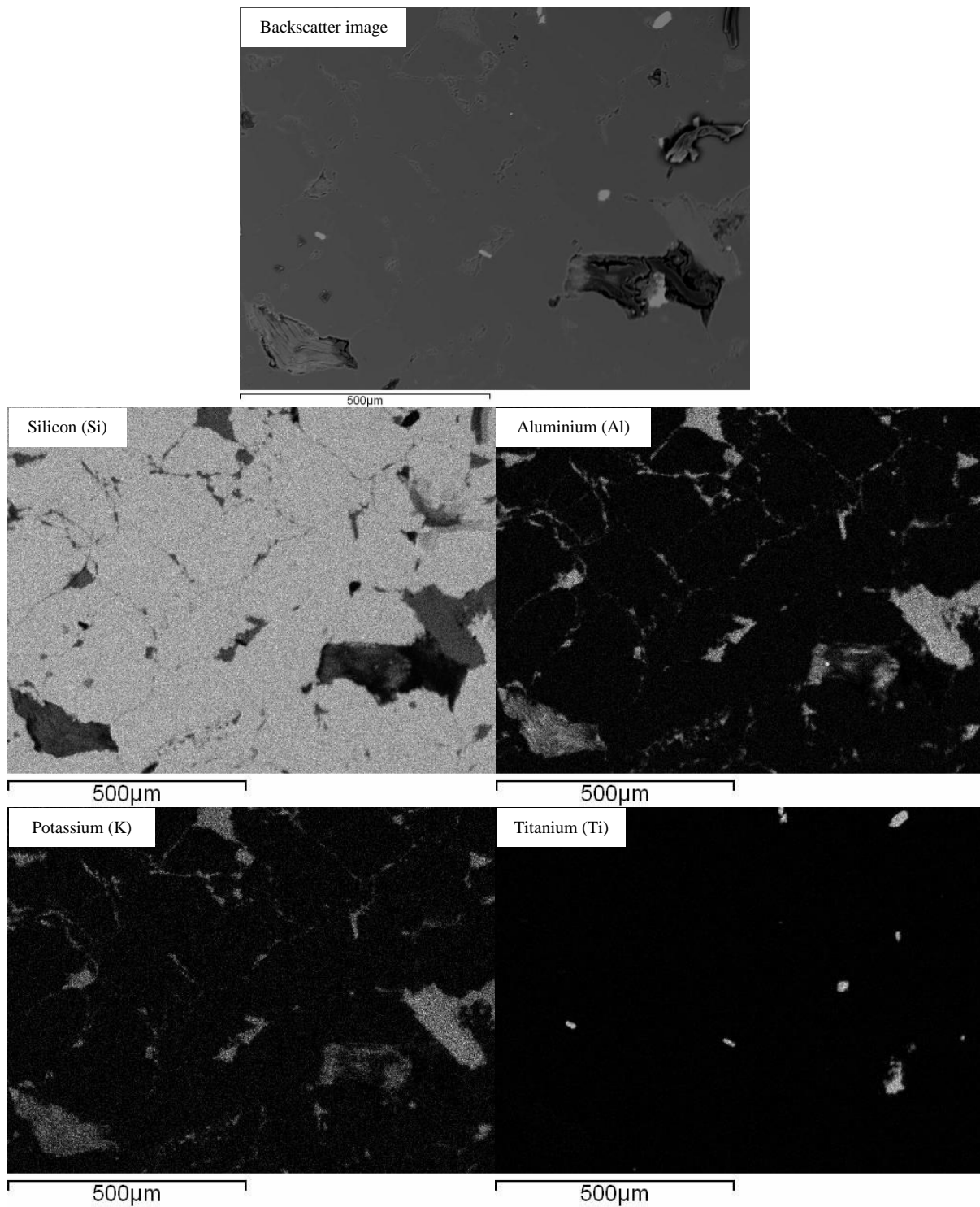


Figure 4.13: Elemental mapping indicating some prominent elements (silicon, aluminium, potassium and titanium) by the brighter shades in quartzite sample.

4.4.4. Petrographic microscope examination – strained quartz

Strained quartz was identified in the quartzite and quartzitic sandstone samples. As can be seen in figure 4.14, several quartz crystals have discolourations (undulatory extinction) within the grains, which indicate strained quartz. According to Miller, pers. comm. (2013), the samples show partial straining as not every quartz crystal within the samples are strained. Although the quartz is partially strained it was concluded that the evidence is sufficiently comprehensive and conclusively indicates the presence of strained quartz. Further tests are recommended, such as the mortar-bar test.

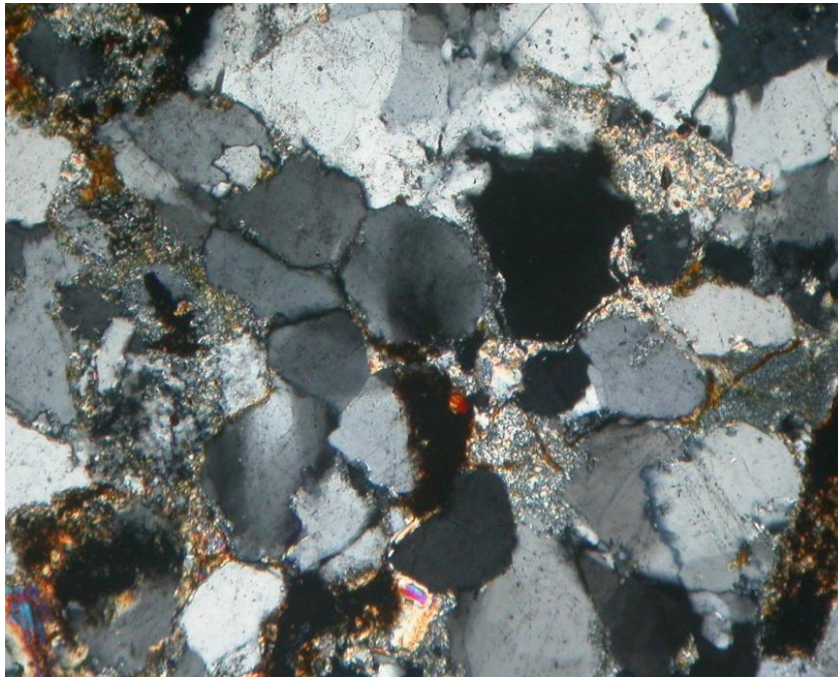


Figure 4.14: Strained quartz in the quartzitic sandstone identified by undulatory extinction in the quartz grains.

The tillite and shale samples showed minimal strained quartz and consists of much smaller particles. In figure 4.15, the microscope was focused on a single quartz particle. As the stage was rotated slightly, the colour changed homogeneously over the whole crystal indicating that the quartz crystal is not strained.

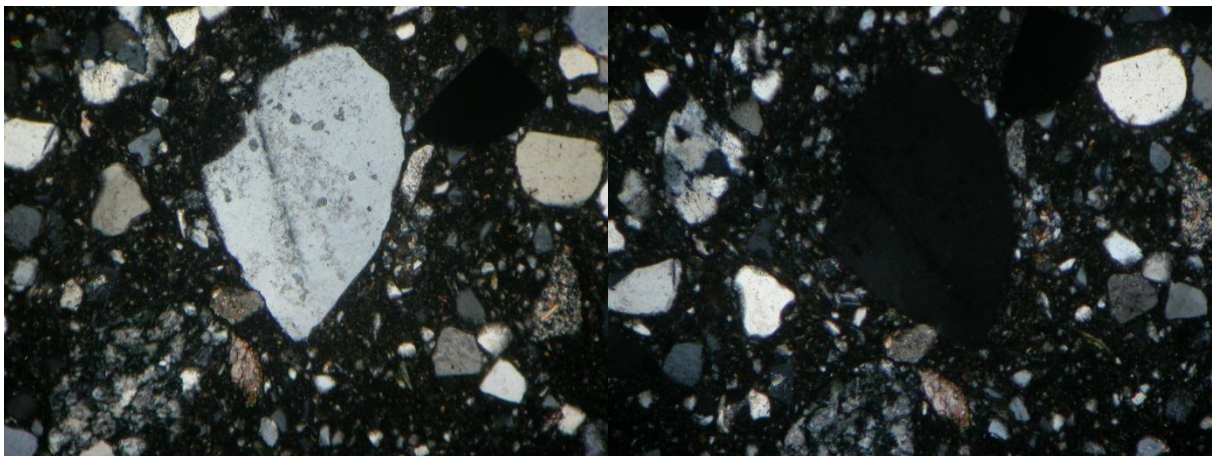


Figure 4.15: Quartz crystal in tillite sample.

Chapter 5. Conclusions and recommendations

5.1. Slake durability

The findings for tillite from an arid region (Matjiesfontein) indicate that, despite continual wetting, drying and tumbling, tillite is nearly as durable as quartzite, which is considered the most durable rock from Matjiesfontein. This can be seen in figure 4.1 and 4.2; where, more than 80% of the original tillite and quartzite masses were retained in the respective bins, after the wet/dry five cycles. According to Brink (1983:35), tillite consists mainly of primary minerals; therefore, are more susceptible to decomposition in humid regions. Since humidity in the Karoo is generally low, it can be concluded that tillite at Matjiesfontein is not susceptible to slaking. The manner in which shale slaked into fragments of different shapes and not into silt sizes indicated that, although shale is impermeable to water; water can penetrate along bedding planes causing the lumps to slake. Shale disintegrated less than sandstone, probably because the tested sandstone lumps were weathered to a larger extent and much softer than the shale. Sandstone is more porous; therefore, water is absorbed more readily causing the lumps to disintegrate into sand size particles.

5.2. 10%FACT

The result of the wet 10%FACT test for quartzite was higher than the 10%FACT value for the dry test (figure 4.3). This was unexpected because, according to Thothela *et al.* (2011), only pre-coated materials have shown results greater than 120%. This is due to the ability of pre-coated materials to reel water or decrease the ability of water to be absorbed into the aggregate. It is understandable that the quartzite can repel moisture due to the closely compacted particles and hardness. Based on the high 10%FACT wet-to-dry ratio (155%), observed for quartzite, it is concluded that water acts as an adhesive agent similar to a pre-coated aggregate, which is impossible. It was recommended that the result be considered inconclusive (Thothela, pers. comm., 2011) and the 10%FACT test for quartzite was redone (second quartzite test in figure 4.3 and table 4.1). The wet-to-dry ratio was found to be 97.4% (figure 4.3). According to Thothela, pers. comm. (2011), this is more realistic because quartzite is a very hard rock and the 10%FACT should be close to 100%.

Amongst the local construction materials, tillite and shale satisfy the specifications according to the 10%FACT test. Karoo sandstone of the Laingsburg formation, which is not far from Matjiesfontein, has an average dry 10%FACT value of 282 kN (Brink, 1983), much higher than the results obtained at Matjiesfontein. Therefore, it is recommended that the 10%FACT test should be conducted on less weathered sandstone from Matjiesfontein. Opening a quarry on site is a possibility, but it would negatively influence the aesthetic value, which the local Matjiesfontein community wish to uphold.

5.3. Rock strength

All rock types on the MGO site have varying degrees of initial weathering; therefore, the strengths may vary from one test to another but these results do give an indication of which rock types are stronger. The strength of the rock is closely related to porosity, the rate at which the different rock types weather and if the rock type is prone to slaking. Figure 5.1 below indicates a general hierarchy in terms of strength (UCS) of the different rock types tested in this thesis and in work conducted at Matjiesfontein prior to this thesis.

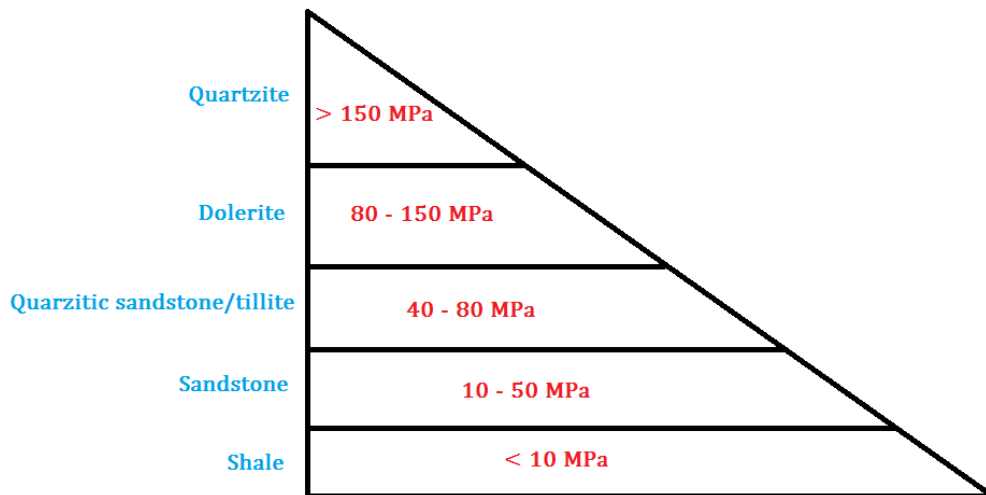


Figure 5.1: Hierarchy of rock types in terms of strength.

5.4. Mix design

As mentioned before, problems occurred in the workability of the mixtures for mix design 3 and 4, in which river sand from Matjiesfontein was used. According to Addis (1998:86-87), river sands on the banks of rivers, such as at Matjiesfontein, often contain particles of roughly the same size. This is not conducive to workability because of a large deficiency or excess of a certain size fraction. A possibility to remedy the situation is mixing the river sand with another type to compensate for the deficiency/excess. Another possibility is to use a superplastizer or other admixture to increase the fluidity of the mixture.

According to Croukamp, pers. comm. (2012), 40 MPa concrete may be unnecessary as the concrete will not be subjected to high loading and a strength of 25-30 MPa may well be sufficient. In order to decrease the overall concrete strength, the W:C ratio may be decreased and a cheaper design can be achieved. The strength of the concrete cubes containing river sand from Matjiesfontein as fine aggregate was generally higher than that of cubes containing Malmesbury sand. This could be because the cement content was higher for mix design 3 and 4 than mix design 1 and 2. It is recommended that more comprehensive analyses such as chloride content, organic impurities and clay content be conducted in accordance with SANS 1083 (2006). Another recommendation, is to determine the

Oxygen Permeability Index, absorptivity and chloride conductivity on the concrete cubes when the cube strength is determined.

5.5. Vault construction

Relative humidity inside the vault remained high (98%) for several weeks after construction. This may be because of the thick walls and the fact that no ventilation had yet been installed. Fortunately, the temperature inside the vault has remained relatively stable around 5°C; which, according to Combrinck, pers. comm. (2012), is good for the instrumentation as large temperature fluctuations may influence data accuracy. However, installation of ventilation is recommended to overcome the excess of moisture, which may result in greater temperature fluctuations. Other alternative means can also be implemented to regulate moisture and temperature fluctuations by installing a de-humidifier or/and an air-conditioner.

5.6. Cost comparison to using local materials for construction

In South Africa, crushed aggregate is usually sourced from large quarries and the use of local material on site is often overlooked, especially for projects in isolated areas. Recycled concrete may also be crushed and used as aggregate for construction in larger municipal areas where demolished concrete buildings are readily available. Small-scale crushers, such as the Red Rhino Series 5000 mini crusher in figure 5.2, are relatively new to South Africa and may be used on site to crush excavated rock or recycled concrete to form high quality aggregate. The use of such a crusher can save on procurement and transportation costs. However, other costs are incurred if one had to use such a crusher such as fuel, hire, labour, maintenance and transportation of the crusher to the site. According to Morris, pers. comm. (2013), if one were to invest in a Series 5000 machine for R650 000 and hire it out at R2500 per day (accurate market related estimate including operator), the return on investment (ROI) would be less than two years based on 60% utilization (less than 3000 hours over two years). During that time, based on a conservative approach, 50 tons of aggregate can be produced per day totaling 13 000 tons in a year. At R70 per ton (recycled concrete), this would represent a monetary value of approximately R900 000 per year. Disposing of a demolished building instead of utilizing it as recycled concrete would cost around R1000 for every 10 tons of debris disposed. Therefore, for the same amount of material (13 000 tons) it would cost R1.3 million to dispose the demolished concrete, R400 000 more than utilizing the debris for recycled aggregate.

From a client's perspective at Matjiesfontein, purchasing a mini-crusher is not feasible. The amount of aggregate needed for the construction of the gravimeter vault is minimal in comparison to what the mini-crusher can deliver in one day. In table 4.4, only 5 tons of concrete was needed for construction of the gravimeter vault as opposed to 50 tons that the mini-crusher can deliver. Therefore, the decision to procure the material from Laingsburg is justified. However, if all the construction for the other outbuildings and LLR station were to take place over the same period; hiring a mini-crusher may make financial sense because a greater volume of aggregate is needed. About 250 tons of stone aggregate

would be needed to complete construction for the Matjiesfontein project including culverts and foundations.

With delivery from the closest source (Worcester), stone aggregate costs around R450 per ton; therefore, totaling over R100 000 for stone aggregate to complete all construction at Matjiesfontein. This amount is more than what it would cost to hire a small scale crusher to deliver the same amount of aggregate as well as the running costs and other vehicles needed on site such as an excavator. Costs that may influence the decision to use local materials are environmental impacts but this may be overcome through including it in initial impact studies, as excavation is regarded as a listed activity.



Figure 5.2: Red Rhino Series 5000 mini crusher.

5.7. Final remarks

Amongst the rock types at Matjiesfontein, tillite satisfies all pre-requisites for construction investigated in this thesis and would be recommended for construction purposes above the other rock types. The slake durability results indicated that tillite is nearly as durable as quartzite, which is considered the most durable rock at Matjiesfontein. Although quartzite is durable, it would not be recommended as concrete aggregate due to the high quartz/silica content (> 90 weight % indicated by the PXRD and XRF analyses) and the presence of strained quartz indicated by inspection under the petrographic microscope. Unlike areas with high humidity and moisture, the Karoo is dry, hence the slaking properties of tillite is far less than in areas closer to the sea such as in KZN. Shale however, slakes easily when exposed to the atmosphere; therefore, immediate covering is necessary when excavated, by either a cement or asphalt layer. The 10%FACT value of tillite is 261.6 kN, which is above the required 210 kN. The wet-to-dry ratio of tillite is 84.9%, which is above 75%, indicating the suitability of tillite as a road building aggregate. The strength in terms of UCS indicated that the tested tillite was moderately weathered. Tillite, indicated by the PXRD analysis (table 4.5), has ± 43 weight

% quartz within the rock, which is far less than the other rock types. This, and the identification of minimal strained quartz under a petrographic microscope, indicates that concrete containing tillite would not be at risk of ASR's.

All the concrete cubes from the respective mix designs achieved the desired 40 MPa. However, despite river sand falling within the boundaries of the South African standards for FM and dust content, problems occurred with the workability of mixtures containing river sand from Matjiesfontein. This was because the sand is too coarse and has a deficiency or excess in certain aperture sizes, which is common amongst natural river sands. It was concluded that river sand would need to be mixed with other sands to compensate for deficiencies or admixtures such as superplasticizers should be used to increase the fluidity of the mixtures. This would result in more expensive mixtures. Removing certain size fractions to increase workability would also be impractical and time-consuming. 40 MPa design strength for the concrete may be unnecessary for the gravimeter vault because applied loads on the structure would be small. It is; therefore, recommended to lower the design strength to 25 or 30 MPa, hence requiring less cement in the mix designs and lowering the cost of design. It is recommended that further tests be conducted in accordance with SANS 1083 such as clay content, organic impurities and chloride content. It is also recommended that concrete cubes containing natural aggregates sourced from Matjiesfontein be analyzed for oxygen permeability, absorptivity and chloride conductivity.

The gravimeter vault was constructed using materials mainly sourced from the local municipal area, Laingsburg. The cost of the vault was approximately R110 000. Upon completion, the decision to procure the materials was positively justified as only a small volume of stone aggregate was required to build the vault. Hiring a small-scale crusher only for the construction of the gravimeter vault would have been costly. The use of local materials for the rest of the construction would however be financially beneficial if all construction would take place over the same period. Enough local material may be crushed to sustain the construction phase, hence avoiding aggregate procurement and transportation costs.

A risk of alkali-silica reactivity in concrete exists when using sandstone, quartzitic sandstone or quartzite as aggregate. This is because strained quartz was noted in these high quartz-bearing samples. In order to harness excavated material for construction; especially quartzite/quartzitic sandstone and sandstone material from along the same ridge and south of the ridge it is recommended to conduct the mortar-bar test. SEM analyses of the samples could not clearly indicate the presence of strained quartz because samples were not polished enough. In future SEM analyses, for identification of strained quartz, samples must be polished to a high enough standard in order to identify the miniscule strain cracks. Zircon, was found in abundance in the all the rock types. In future, if dating of rocks from the Matjiesfontein area is necessary, this mineral can be used to determine the age of the rock mass.

References

- A'Bear, T. 2012A. Percussion Chip Logging. Course notes. (SAIMM 00470 Geotechnical Core Logging, Soil Profiling and Chip Logging Course). 16-18 May 2012. Midrand: SAIEG.
- A'Bear, T. 2012. Personal interview. 18 May, Midrand.
- A'Bear, T. 2012B. Soil Profiling. Course notes. (SAIMM 00470 Geotechnical Core Logging, Soil Profiling and Chip Logging Course). 16-18 May 2012. Midrand: SAIEG.
- Addis, B. 1998. *Fundamentals of Concrete*. Midrand: Cement and Concrete Institute.
- American Society for Testing and Materials C295. 1998. *Standard Guide for Petrographic Examination of Aggregates for Concrete*. West Conshohocken: ASTM.
- Association of Engineering Geologists. 1976. A guide to core logging for rock engineering. Proceedings of a symposium on Exploration for Rock Engineering. Johannesburg: South African Section of The Association of Engineering Geologists. November: 71-86
- Bieniawski, Z.T. 1989. *Engineering rock mass classifications*. New York: Wiley.
- Bragg's law*. 2013. [Online]. Available: http://en.wikipedia.org/wiki/Bragg's_law [2013, June 25].
- Brink, A.B.A. 1983. *Engineering Geology of Southern Africa*. Pretoria: Building Publications. 3: 89-90
- Cilliers, P., & Opperman, B. 2009. *Report on attendance of 3rd Matjiesfontein Space Geodesy Station Technical Workshop*. Matjiesfontein. 16-20 March 2009.
- Cole, D. 2011. *Report on Economically-Viable Mineral Resources in the City of Cape Town's Administrative Area*. Cape Town: Council for Geoscience. June.
- Combrinck, L. 2012. Personal interview, 18 April, Matjiesfontein.
- Concrete Society. 1987. Alkali-silica reaction: minimising the damage to concrete. *Technical report*. No. 30. London: Concrete Society.
- Croukamp, L. 2011. Personal interview. 12 August, Stellenbosch.
- Croukamp, L. 2012. Personal interview. 4 December. Stellenbosch.
- Croukamp, L. 2013. Personal interview. 10 February, Stellenbosch.
- Croukamp, L., Rossouw, J.J., Fourie, C.J., & Combrinck, L. 2011. Geotechnical Investigation for the Construction of a Vault in a Rockface for the Placement of a Gravimeter and a Long Period

- Seismograph at Matiesfontein, South Africa. *South African Journal of Geology*, 114.3-4: 561-572.
- Davis, G. 2012. Geotechnical core logging. Course notes. (SAIMM 00470 Geotechnical Core Logging, Soil Profiling and Chip Logging Course). 16-18 May 2012. Midrand: SAIEG.
- Deere, D.U. 1989. *Rock quality designation (RQD) after 20 years: Final report*. U.S. Army Corps of Engineers Contract Report GL-89-1. Vicksburg: US Army Engineer Waterways Experiment Station.
- Deere, D.U. & Deere, D.W. 1988. The Rock Quality Designation (RQD) Index in Practise, in L. Kirkaldie (ed.). *Rock Classification Systems for Engineering Purposes, ASTM STP 984*, Philadelphia: American Society for Testing and Materials. 91-101.
- Earth and air tides*. n.d. [Online]. Available: <http://covenk.tripod.com/index-5.html> [2012, April 23].
- Frazenburg, M. 2013. Personal interview. 4 June, Stellenbosch.
- Fourie, C. 2012. Personal interview. 17 April, Matjiesfontein.
- Geology of KwaZulu-Natal*. (2007). [Online]. Available: <http://www.geology.ukzn.ac.za/GEM/kzngeol/ecca.html> [2011, July 29].
- Handy, R., & Spangler, M. (2007). *Geotechnical Engineering: Soil and Foundation Principles and Practise, Fifth Edition*. New York, Chicago, San Francisco, Lisbon, Madrid, Mexico City, Milan, New Delhi, San Juan, Seoul, Singapore, Sydney and Toronto: The McGraw-Hill Companies.
- Hime, W. G., & Erlin, B. 2013. *Alkali-silica reaction*. [Online]. Available: <http://www.concreteconstruction.net/concrete-masonry/alkali-silica-reaction.aspx> [2013, May 9].
- Hoek, E. 2007. *Rock mass classification*, in Practical Rock Engineering. [Online]. Available: http://www.roscience.com/hoek/corner/Practical_Rock_Engineering.pdf [2012, May 24].
- Janse van Rensburg, F. 2012. Determination of the Suitability of Local Materials to be used in Road Construction and a Preliminary Design of the Access Road to the Matjiesfontein Geodesy Observatory site. Unpublished bachelor's project report. Stellenbosch: University of Stellenbosch.
- Jennings, J.E., Brink, A.B.A, & Williams, A.A.B. 1973. Revised Guide to Soil Profiling for Civil Engineering Purposes in Southern Africa. *Die Siviele Ingenieur in Suid-Afrika*, January: 3-13.

- Kosmatka, S.H., Kerkhoff, B., & Panarese, W.C. 2003. *Design and Control of Concrete Mixtures*, EB001, 14th Edition, Skokie (Illinois, USA): Portland Cement Association.
- Map of the Region*. 2008. [Online]. Available: <http://www.mmilotours.com/index.php?id=24> [2013, May 21].
- McHone, J.G. 2013. *Polarizing, Petrographic, Geological Microscopes*. [Online]. Available <http://earth2geologists.net/Microscopes> [2013, June 24].
- Method for Determining the Unconfined Compressive Strength of Intact Rock Specimens*. n.d. [Online]. Available: <http://www.scdot.org/doing/technicalPDFs/materialsResearch/testProcedure/soils/SCT39.pdf> [2011, October 5].
- Miller, J. 2013. Personal interview. 25 July. Stellenbosch.
- Milne, D., Hadjigeorgiou, J., & Pakalnis, R. (1998). Rock Mass Characterization for Underground Hard Rock Mines. *Tunnelling and Underground Space Technology*, 13(4), October-December: 383-391.
- Moorhouse, W.W. 1959. *The Study of Rocks in Thin Section*. New York and Evanston: Harper & Row.
- Morris, A. 2013. Small-scale crushers, E-mail to P.R. van Wyk [Online], 6 August. Available E-mail: andrew@i-world.co.za.
- Oberholster, B. 2001. Alkali-silica reaction, in B. Addis, & G. Owens (eds.). *Fulton's Concrete Technology*. Midrand: Cement & Concrete Institute. 8: 163-185.
- Paige-Green, P. 1980. Durability testing and specifications for degrading Dwyka tillite in southern Africa, in M.D. Gidigas, A.A. Hammond & J.O. Gogo (eds.). *Proceedings of the Seventh Regional Conference for Africa on Soil Mechanics and Foundation Engineering*, June: 1: 209-214.
- Properties of water*. 2012. [Online]. Available: http://en.m.wikipedia.org/wiki/Properties_of_water [2012, May 3].
- Pycnometer Top and Jar*. 2013. [Online]. Available: http://www.hoskin.ca/catalog/index.php?main_page=product_info&products_id=1757 [2013, July 24].
- Ramat, C. 2012. Personal interview, 19 September, Stellenbosch.
- Ramphaka, P.L. 2013. Personal interview. 26 June, Stellenbosch.
- Reactive Solutions. 2012. *An FHWA Technical Update on Alkali-Silica Reactivity*. 5(4): 3, Fall.

- Rossouw, J.J. 2010. Research the design of a vault for the placement of LaCoste/Rohmberg gravimeter at Matjiesfontein. Unpublished bachelor's project report. Stellenbosch: Stellenbosch University.
- Sanchez-Garrido, C. 2013. Personal interview. 12 August, Stellenbosch.
- Sanchez-Garrido, C. 2013. XRF Spectrometry: Principles, instrumentation, data and sample preparation. Guest presentation (356/2013 Soil Behaviour short course). 4 June 2013. Stellenbosch.
- Seigel, H.O. 1995. *A Guide to High Precision Land Gravimeter Surveys*. Concord (Ontario): Scintrex Ltd.
- Smith, V. 2013. Powder X-ray Diffraction (PXRD). Guest presentation (356/2013 Soil Behaviour short course). 4 June 2013. Stellenbosch.
- South African Bureau of Standards 842. 1994. *The determination of the 10 per cent fines aggregate crushing value*. Pretoria: Standard Test Methods.
- South African National Standard 1083. 2006. *Aggregates from natural sources - Aggregates for concrete*. Pretoria: Standards South Africa.
- South African National Standard 201. 2008. *Sieve analysis fines, content and dust content*. Pretoria: Standards South Africa.
- South African National Standard 5841. 2008. *Aggregate crushing value of coarse aggregates*. Pretoria: SABS Standards Division.
- South African National Standard 5842. 2006. *FACT value (10 % fines aggregate crushing value) of coarse aggregates*. Pretoria: Standards South Africa.
- South African National Standard 5844. 2006. *Particle and relative densities of aggregates*. Pretoria: Standards South Africa.
- South African National Standard 5845. 2006. *Bulk densities and voids content of aggregates*. Pretoria: Standards South Africa.
- Swapp, S. 2013. *Scanning Electron Microscopy (SEM)*. [Online]. Available: http://serc.carleton.edu/research_education/geochemsheets/techniques/SEM.html [2013, July 9].
- Table Mountain Sandstone (Geological Formation)*. 2011. [Online]. Available: [http://en.wikipedia.org/wiki/Table_Mountain_Sandstone_\(Geological_Formation\)](http://en.wikipedia.org/wiki/Table_Mountain_Sandstone_(Geological_Formation)) [2011, July 29].

- Technical Methods for Highways 1, 1986. Method B1. *The determination of the aggregate crushing value*. Edition 2 ed. Pretoria: Department of Transport.
- Terzaghi, K. 1946. Rock defects and loads on tunnel supports. In R.V. Proctor & T.L. White (eds.), *Rock tunnelling with steel supports*. Youngstown: Commercial Shearing and Stamping Company. 17-99.
- Thothela, T. 2011. Correspondence, 4 October, Cape Town.
- Thothela, T., Robertson, G., & Jenkins, K. 2011. Improving the Durability of Seal aggregate by Precoating. *The 10th Conference on Asphalt Pavements for Southern Africa (CAPSA 2011)*. KwaZulu-Natal [S.n.:s.l.] [Electronic] Available: <http://www.capsa11.co.za/paperdir/approved/78-1032.pdf> [2011, Sep].
- West, G. 1996. *Alkali-aggregate reaction in concrete roads and bridges*. London: Thomas Telford Publications.
- Wikimedia Commons. 2012. [Online]. Available: http://upload.wikimedia.org/wikipedia/commons/1/10/Calcareous_Soil_Profile,_Seven_Sisters_Country_Park_-_geograph.org.uk_-_1280181.jpg [2013, May 21].
- Will, G. 2006. *Powder Diffraction: The Rietveld Method and the Two-Stage Method*. Berlin: Springer.

Appendix A

Slake durability results

Table A.1: Slake durability results.

Rock Sample	Initial mass (g)	Mass retained in bin (g)	Percentage retained (%)	Percentage degraded (%)
Tillite	454.8	379.7	83.5	16.5
Quartzite	539.0	482.3	89.5	10.5
Sandstone	529.6	169.0	31.9	68.1
Shale	440.4	183.7	41.7	58.3

10%FACT results

Table A.2: Dry 10%FACT results.

Rock sample	Applied force (kN)	Initial mass (g)	Fines mass (g)	Percentage fines (%)	10%FACT value (kN)
Tillite	300	2500.4	301.4	12.05	261.6
Quartzite	200	2529.4	277.0	10.95	187.3
Sandstone	50	2550.4	240.2	9.42	52.2
shale	350	2541.8	221.8	8.73	385.0

Table A.3: Wet 10%FACT results.

Rock sample	Applied force (kN)	Initial mass (g)	Fines mass (g)	Percentage fines (%)	10%FACT value (kN)
Tillite	200	2430.0	209.0	8.60	222.2
Quartzite	250	2490.5	200.6	8.05	290.3
Sandstone	30	2669.8	193.9	7.26	37.3
shale	350	2449.9	292.6	11.94	307.3

Grading analysis results

Fine aggregate**Table A.4: First sieve analysis of a large sample (± 3 kg) of natural river sand from a river close the MGO site without sieving out the larger material > 4.75 mm.**

Sample No. Monster Nr.	River sand (without sieving large material out - natural)	Date Datum	06/08/2012
Dry Mass Droë Massa		3240.6 g	
Sieve Aperture Sifopening (mm)	Mass Retained Massa wat agterbly (g)	Percentage retained Persentasie wat agterbly (%)	Percentage passing Persentasie wat deurgaan (%)
20.0	74.1	2	98
14.0	10.2	0.3	97
9.5	71.5	2	95
7.1	101.9	3	92
6.7	33.1	1	91
5.0	139.5	4	87
3.35	297.6	9	78
2.0	537.7	17	61
1.18	611.6	19	42
0.6	650.3	20	22
0.425	211.8	7	15
0.3	201.6	6	9
0.25	60.5	2	7
0.15	102.5	3	4
0.075	28.1	1	3.4
Receiver	108.6	3.4	
Total/Totaal	3240.6	100.0	

Table A.5: Second sieve analysis of 500 g natural sand sample from a river close to the MGO site done according to SANS 201 (2008). The larger material (> 4.75 mm) has been sieved out prior to this analysis.

Sample No.	4) River sand (≤ 4.75 mm)		Date:	29/10/2012	
Dry Mass			a = 500.1 g		
Sieve Aperture (mm)	Individual mass retained (g)	Individual percentage retained (%)	Cumulative percentage (5 to 0.15mm sieves) (%)	Percentage of material that passed (%)	Percentage of material that passed (rounded off)
5	2.2	0.4	0.4	99.6	100
2.36	101.1	20.1	20.5	79.5	79
1.18	131.6	26.4	46.9	53.1	53
0.6	117.3	23.5	70.4	29.6	30
0.3	93.3	18.7	89.1	10.9	11
0.15	32	6.4	95.5	4.5	5
Subtotal 1	476.5	95.5	322.8	-	-
0.075	4.1	0.8	-	3.7	4
Pan	Mass c	0.5	0.1	-	-
	Mass a - b	17.9	3.6	-	-
Subtotal 2	18.4	3.7	-	-	-
Total M	499.0	100.0	-	-	-

$$\text{Dust content} = \frac{(500.1 - 482.2) + 0.5}{499.0} \times 100 = 3.7 \%$$

$$FM = \frac{322.8}{100} = 3.2$$

Coarse aggregate

Table A.6: Results for the tillite coarse aggregate sieve analysis.

Sample No. Monster Nr.	tillite	Date Datum	06/08/2012
Dry Mass Droë Massa		d = 3434.5 g	
Sieve Aperture Sifopening (mm)	Mass Retained Massa wat agterbly (g)	Percentage retained Persentasie wat agterbly (%)	Percentage passing Persentasie wat deurgaans (%)
20.0	779.0	22.7	77.3
14.0	1362.2	39.7	37.6
9.5	525.3	15.3	22.3
7.1	160.4	4.7	17.7
6.7	33.5	1.0	16.7
5	113.4	3.3	13.4
1.18	263.4	7.7	5.7
0.075	122.6	3.6	2.1
Pan	0.1	0.003	
d-g	72.9	2.1	
Total	3432.8	100.0	

$$\text{Dust content (tillite aggregate)} = \frac{3434.5 - 3361.6}{3432.8} \times 100 = 2 \%$$

$$D_{60}(\text{tillite aggregate}) = 14 + (20 - 14) \times \frac{60 - 37.6}{77.3 - 37.6} = 17.4 \text{ mm}$$

$$D_{30}(\text{tillite aggregate}) = 9.5 + (14 - 9.5) \times \frac{30 - 22.3}{37.6 - 22.3} = 11.8 \text{ mm}$$

$$U_a(\text{tillite aggregate}) = \frac{17.4}{11.8} = 1.5$$

Table A.7: Results for the quartzite coarse aggregate sieve analysis.

Sample No. Monster Nr.	Quartzite	Date Datum	06/08/2012
Dry Mass Droë Massa		d = 3183.5 g	
Sieve Aperture Sifopening (mm)	Mass Retained Massa wat agterbly (g)	Percentage retained Persentasie wat agterbly (%)	Percentage passing Persentasie wat deurgaans (%)
28.0	53.2	1.7	98.3
20.0	581.3	18.3	80.1
14.0	1282.4	40.3	39.8
9.5	636.3	20.0	19.8
7.1	164.0	5.2	14.6
6.7	36.0	1.1	13.5
5	82.0	2.6	10.9
1.18	187.4	5.9	5.0
0.075	120.2	3.8	1.3
Pan	0.5	0.02	
d-g	39.3	1.2	
Total	3182.6	100.0	

$$Dust\ content\ (quartzite\ aggregate) = \frac{3183.5 - 3144.2}{3182.6} \times 100 = 1\%$$

$$D_{60}(quartzite\ aggregate) = 14 + (20 - 14) \times \frac{60 - 39.8}{80.1 - 39.8} = 17.0\ mm$$

$$D_{30}(quartzite\ aggregate) = 9.5 + (14 - 9.5) \times \frac{30 - 19.8}{39.8 - 19.8} = 11.8\ mm$$

$$U_a(quartzite\ aggregate) = \frac{17.0}{11.8} = 1.4$$

Appendix B

Concrete mix design parameters and cube strength results

RD results**Table B.1: RD results from using the pycnometer method.**

Aggregate type	Test	M _w (g)	M _s (g)	M _T (g)	RD	Average RD
Quartzite	1	1298.0	520.5	1620.8	2.63	2.61
	2	1299.0	560.6	1644.5	2.61	
	3	1300.2	569.0	1649.3	2.59	
Tillite	1	1296.7	558.0	1643.2	2.64	2.66
	2	1294.5	581.8	1659.5	2.68	
	3	1295.0	586.8	1661.9	2.67	
River sand	1	1297.9	752.7	1767.8	2.66	2.66
	2	1297.9	740.5	1760.7	2.67	
	3	1297.9	724.4	1749.9	2.66	

7 day cube strength results**Table B.2: cube strength after 7 days of curing.**

Mix design number	Aggregate type	No.	Mass (g)	Area (mm × mm)	Force (kN)	Compression Strength (MPa)	Average compression strength (MPa)
1	Quartzite + Malmesbury sand	1	2352.3	100 × 100	394.2	39.42	38.36
		2	2342.4	100 × 100	387.4	38.74	
		3	2362.1	99 × 100	365.4	36.91	
2	Tillite + Malmesbury sand	1	2364.2	100 × 100	351.1	35.11	35.98
		2	2388.1	99 × 100	380.1	38.39	
		3	2351.3	100 × 100	344.3	34.43	
3	Quartzite + Matjiesfontein river sand	1	2355.3	100 × 100	355.0	35.50	35.50
		2	2334.9	100 × 100	359.8	35.98	
		3	2338.5	100 × 100	350.2	35.02	
4	Tillite + Matjiesfontein river sand	1	2366.0	100 × 101	367.6	36.40	37.00
		2	2386.0	100 × 100	372.6	37.26	
		3	2389.7	100 × 100	373.3	37.33	

28 cube strength results**Table B.3: cube strength after 28 days of curing.**

Mix design number	Aggregate type	No.	Mass (g)	Area (mm × mm)	Force (kN)	Compression Strength (MPa)	Average compression strength (MPa)
1	Quartzite + Malmesbury sand	1	2392.0	99 × 99	425.6	43.42	44.53
		2	2348.4	99 × 100	446.4	45.09	
		3	2401.1	100 × 100	450.9	45.09	
2	Tillite + Malmesbury sand	1	2361.9	99 × 100	448.5	45.30	43.72
		2	2380.6	99 × 100	418.0	42.22	
		3	2339.8	100 × 100	436.4	43.64	
3	Quartzite + Matjiesfontein river sand	1	2325.3	100 × 100	452.8	45.28	45.35
		2	2322.7	100 × 100	446.7	44.67	
		3	2340.9	100 × 100	461.1	46.11	
4	Tillite + Matjiesfontein river sand	1	2385.7	100 × 100	502.2	50.22	48.57
		2	2362.1	101 × 101	473.0	46.37	
		3	2322.7	100 × 101	496.0	49.11	

Appendix C

Calculations for vault design

Reinforcement calculations for plinth

Tension reinforcement:

$$\frac{100A_{s_{min}}}{A_c} = 0.13 \quad (\text{SABS 0100 – 1: 2000, p. 95})$$

$$A_{s_{min}} = 0.0013 \times A_c = 0.0013 \times 1200 \times 440 = 686.4 \text{ mm}^2$$

Choose 4 Y16's, therefore $A_s = 804 \text{ mm}^2 > A_{s_{min}} = 686.4 \text{ mm}^2$ (satisfactory)

Links:

$$\frac{A_{sv_{min}}}{S_v} = 0.0012b_t \quad (\text{SABS 0100 – 1: 2000, p. 96})$$

$$A_{sv_{min}} = 0.0012 \times 440 \times 210 = 110.9 \text{ mm}^2$$

Choose 2 Y9's, therefore $A_s = 127 \text{ mm}^2 > A_{sv_{min}} = 110.9 \text{ mm}^2$ (satisfactory)

Side bars

$$\phi_{min} = \sqrt{\frac{S_b \times b}{f_y}} = \sqrt{\frac{220 \times 440}{450}} = 14.66 \text{ mm} \quad (\text{SABS 0100 – 1: 2000, p. 94})$$

Therefore, choose Y16's, $\phi = 16 \text{ mm} > \phi_{min} = 14.66 \text{ mm}$ (satisfactory)

Floor mesh reinforcement calculation

By considering the floor slab as a beam per meter width:

$$\frac{100A_{s_{min}}}{\text{depth per meter}} = 0.13 \quad (\text{SABS 0100 – 1: 2000, p. 95})$$

$$A_{s_{min}} = 0.0013 \times \text{depth} \times 1000 \text{ mm} = 0.0013 \times 200 \times 1000 = 260.0 \text{ mm}^2/\text{m}$$

Therefore, choose mesh reinforcement sheet, reference: 500 (SANS 1024:2006)

$$A_{500} = 318 \text{ mm}^2 > A_{s_{min}} = 260.0 \text{ mm}^2 \quad (\text{satisfactory})$$

Vault construction photographs in chronological order



Figure C.1: Blasting into the hillside for vault location.



Figure C.2: Foundation with mesh reinforcement.



Figure C.3: Foundation at completion.



Figure C.4: Walls of the vault strengthened with 'brick force' wire.



Figure C.5: Walls with installation of the steel door and wire on the outside, which holds the stone cladding to the sides.



Figure C.6: Stone cladding on the sides of the walls.



Figure C.7: Installation of plinth reinforcement.



Figure C.8: Roof of lintels stacked next to each other.



Figure C.9: Concrete slab on the top of the roof with plastic to prevent seepage.



Figure C.10: Inside walls and ceiling plastered with cretstone.



Figure C.11: Bracket for the communications pole/antenna.



Figure C.12: Plinth finishes. Building foam separating plinth from the rest of the structure.

Appendix D

Petrographic results

PXRD results

Table D.1: Relative phase amounts for tillite.

Rock Type	Sample Number	Relative phase amounts										
		Chlorite		Microcline		Muscovite		Plagioclase		Quartz		
		Weight %	Ave. weight %	Weight %	Ave. weight %	Weight %	Ave. weight %	Weight %	Ave. weight %	Weight %	Ave. weight %	
Tillite	1	13.27	13.59	11.70	11.09	7.31	5.45	24.30	27.19	43.43	42.69	
	2	15.22		10.16		5.04		27.11		42.46		
	3	10.98		12.42		4.12		29.42		43.05		
	4	14.88		10.07		5.33		27.91		41.83		
			Error (3 sigma level) (weight %) – std. dev.									
			Chlorite		Microcline		Muscovite		Plagioclase		Quartz	
			Weight %	Ave. weight %	Weight %	Ave. weight %	Weight %	Ave. weight %	Weight %	Ave. weight %	Weight %	Ave. weight %
		1	1.53	0.96	1.83	1.02	0.96	0.56	1.8	1.12	1.74	1.02
		2	0.78		0.75		0.45		0.9		0.81	
		3	0.75		0.75		0.42		0.9		0.78	
		4	0.78		0.75		0.42		0.87		0.75	

Table D.2: Relative phase amounts for shale.

Rock Type	Sample Number	Relative phase amounts										
		Chlorite		Microcline		Muscovite		Plagioclase		Quartz		
		Weight %	Ave. weight %	Weight %	Ave. weight %	Weight %	Ave. weight %	Weight %	Ave. weight %	Weight %	Ave. weight %	
Shale	1	10.88	11.76	1.36	2.78	16.71	13.82	14.95	15.28	56.11	56.36	
	2	12.19		3.62		13.68		14.15		56.35		
	3	11.16		2.57		13.20		17.71		55.37		
	4	12.80		3.58		11.70		14.30		57.62		
			Error (3 sigma level) (weight %) – std. dev.									
			Chlorite		Microcline		Muscovite		Plagioclase		Quartz	
			Weight %	Ave. weight %	Weight %	Ave. weight %	Weight %	Ave. weight %	Weight %	Ave. weight %	Weight %	Ave. weight %
		1	1.71	1.11	0.69	0.77	1.47	1.01	2.04	1.36	2.16	1.45
		2	0.93		0.90		0.72		1.17		1.26	
		3	0.87		0.63		1.11		1.05		1.14	
		4	0.93		0.87		0.72		1.17		1.23	

Table D.3: Relative phase amounts for quartzitic sandstone.

Rock Type	Sample Number	Relative phase amounts										
		Chlorite		Microcline		Muscovite		Plagioclase		Quartz		
		Weight %	Ave. weight %	Weight %	Ave. weight %	Weight %	Ave. weight %	Weight %	Ave. weight %	Weight %	Ave. weight %	
Sandstone (quartzitic)	1	1.68	2.05	0.81	0.71	2.83	1.66	0.27	0.51	94.41	95.08	
	2	2.02		0.55		1.47		0.50		95.46		
	3	2.31		0.92		1.42		0.68		94.67		
	4	2.17		0.55		0.92		0.60		95.76		
	Error (3 sigma level) (weight %) – std. dev.											
			Chlorite		Microcline		Muscovite		Plagioclase		Quartz	
			Weight %	Ave. weight %	Weight %	Ave. weight %	Weight %	Ave. weight %	Weight %	Ave. weight %	Weight %	Ave. weight %
		1	0.69	0.53	0.51	0.37	0.54	0.33	0.36	0.28	0.99	0.70
		2	0.45		0.29		0.26		0.26		0.57	
		3	0.48		0.39		0.24		0.24		0.63	
		4	0.48		0.28		0.26		0.25		0.60	

Table D.4: Relative phase amounts for river sand.

Rock Type	Sample Number	Relative phase amounts					
		Chlorite	Microcline	Muscovite	Plagioclase	Quartz	
River sand		weight %	weight %	weight %	weight %	weight %	
	1	11.48	1.81	12.08	15.32	59.30	
		Error (3 sigma level) (weight %) – std. dev.					
		Sample Number	Chlorite	Microcline	Muscovite	Plagioclase	Quartz
			weight %	weight %	weight %	weight %	weight %
		1	1.53	0.84	1.17	1.35	1.74

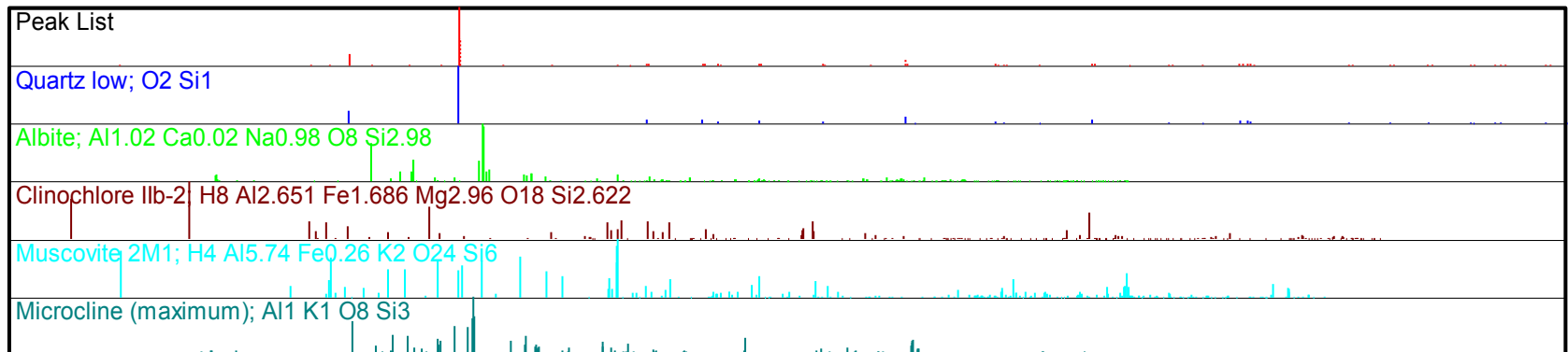
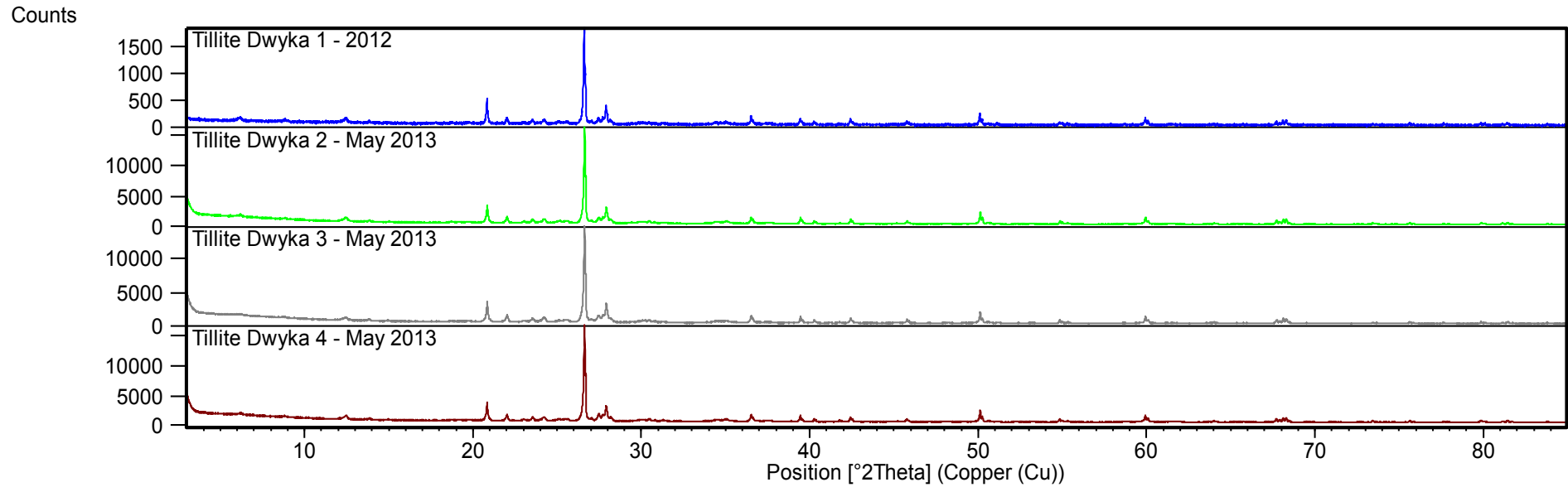


Figure D.1: PXRD peak list for tillite.

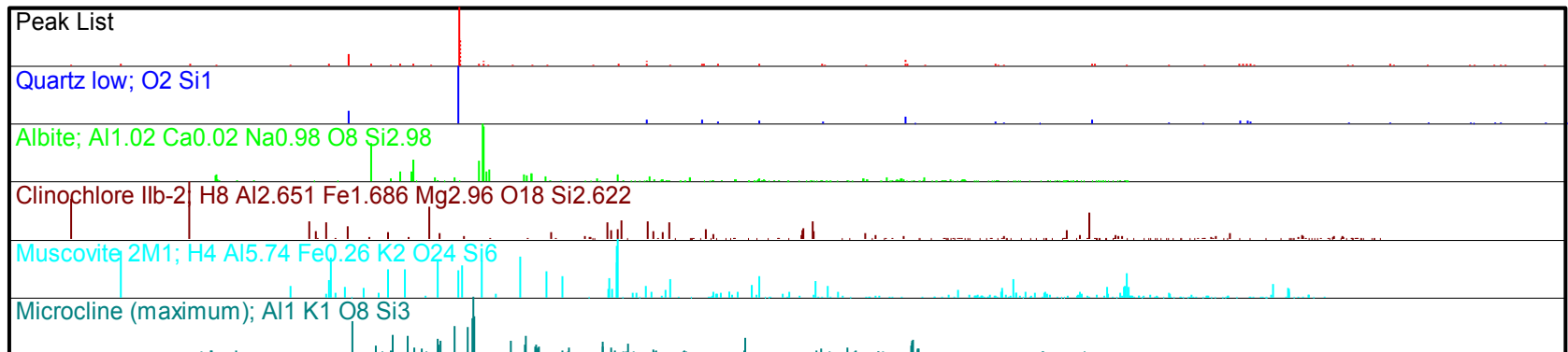
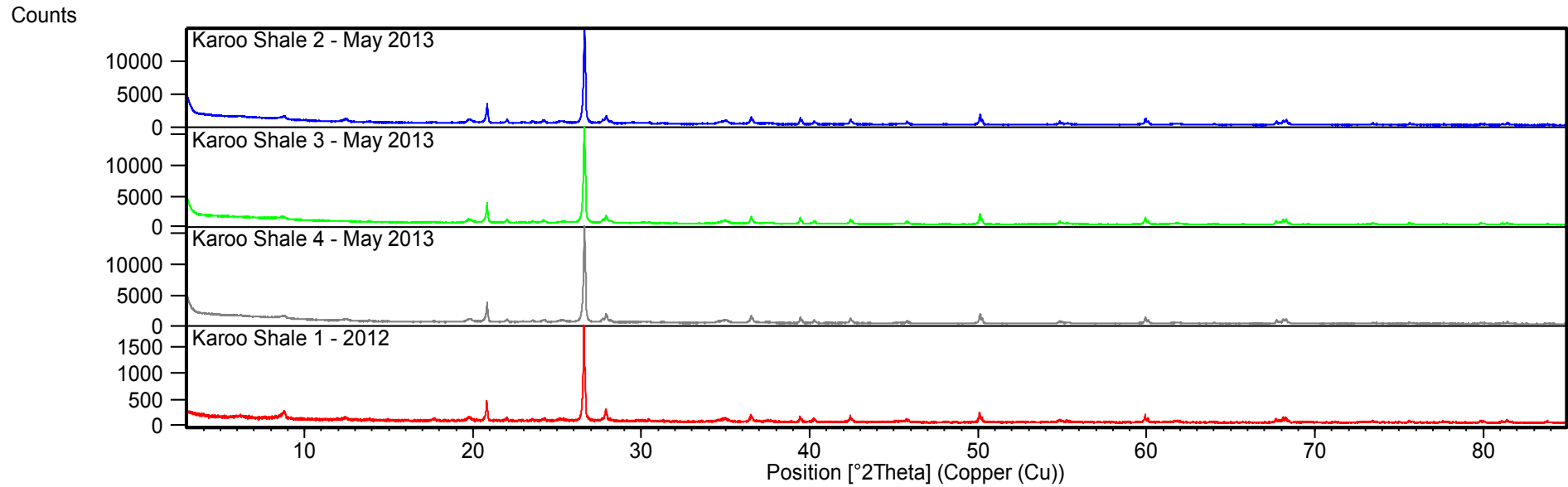


Figure D.2: PXRD peak list for shale.

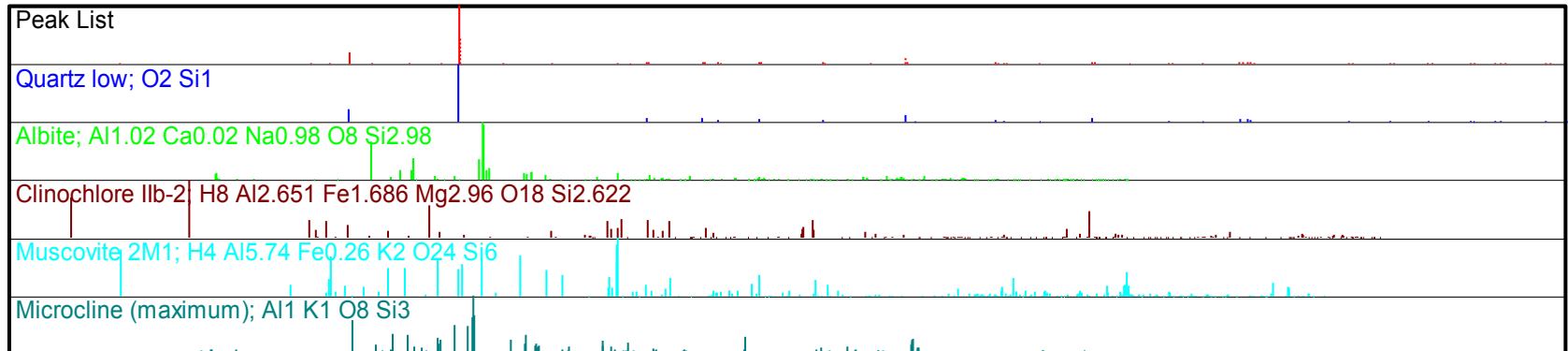
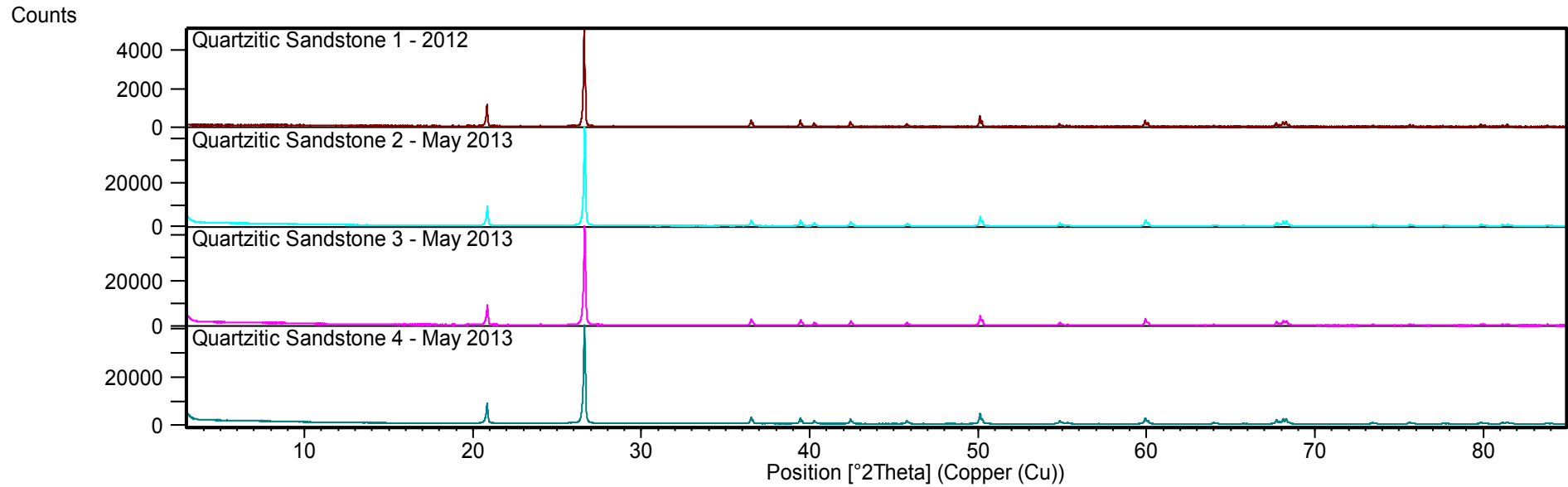


Figure D.3: PXRD peak list for quartzitic sandstone.

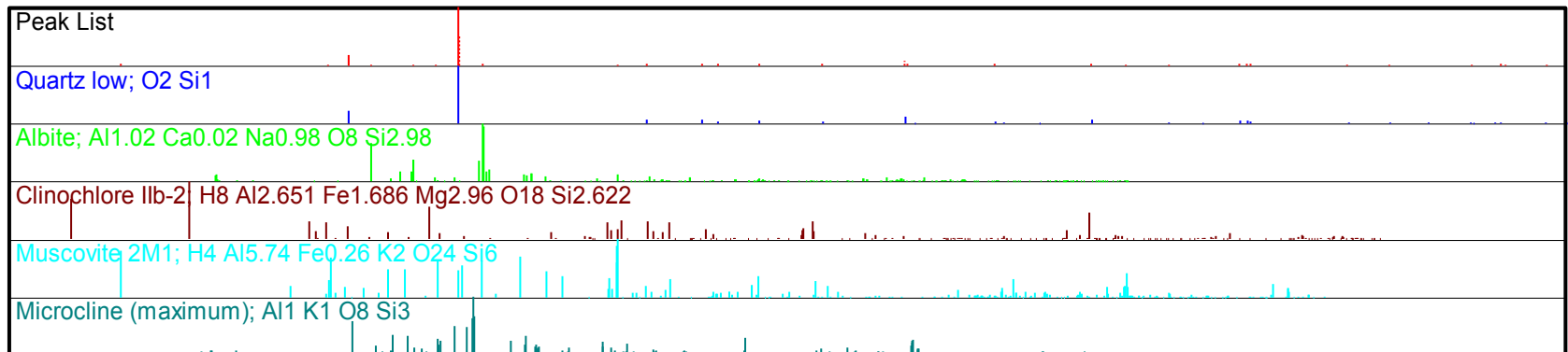
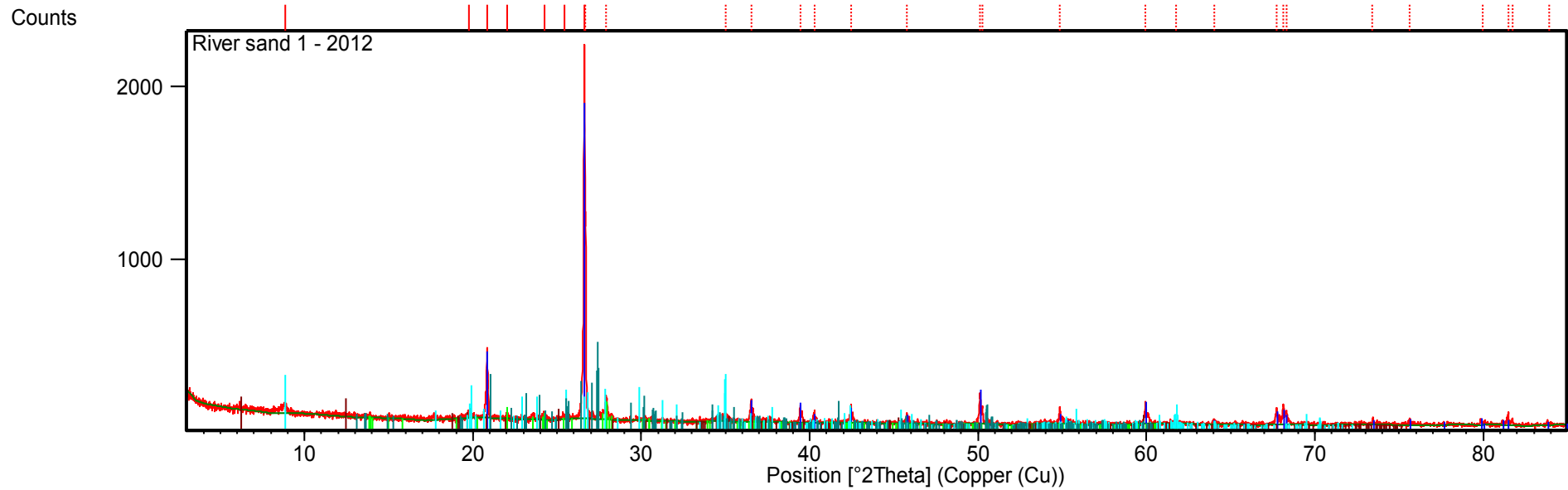


Figure D.4: PXRD peak list for river sand.

XRF results**Table D.5: XRF results of material from Matjiesfontein.**

Sample name	Meas. Date/time	Al ₂ O ₃ (%)	CaO (%)	Cr ₂ O ₃ (%)	Fe ₂ O ₃ (%)	K ₂ O (%)	MgO (%)	MnO (%)	Na ₂ O (%)	P ₂ O ₅ (%)	SiO ₂ (%)	TiO ₂ (%)	LOI (%)	Sum of conc. (%)
Tillite	2012/11/21 08:17	12.14	0.97	0.02	5.15	2.58	2.38	0.10	2.22	0.13	68.26	0.61	3.98	98.54
Shale	2012/11/21 08:10	16.02	0.24	0.01	4.52	2.96	1.08	0.03	1.27	0.09	65.90	0.66	5.12	97.89
Quartzitic sandstone	2012/11/21 08:02	3.33	0.02	0.00	0.76	0.72	0.15	0.00	0.05	0.05	91.36	0.73	1.02	98.19
Natural river sand	2012/11/20 18:34	13.54	0.40	0.01	6.35	2.67	1.14	0.10	1.07	0.16	68.49	0.54	4.30	98.77

Standards used with analyzing data**Table D.6: Quality control standard for 2010-2011.**

Sample name	Meas. Date/time	Al ₂ O ₃ (%)	CaO (%)	Cr ₂ O ₃ (%)	Fe ₂ O ₃ (%)	K ₂ O (%)	MgO (%)	MnO (%)	Na ₂ O (%)	P ₂ O ₅ (%)	SiO ₂ (%)	TiO ₂ (%)	LOI (%)	Sum of conc. (%)
Average HUSG		13.75	1.52	0.00	3.78	4.66	1.04	0.06	2.57	0.21	69.77	0.54	0.73	98.65
STDEV		0.20	0.04	0.00	0.14	0.06	0.04	0.01	0.18	0.01	0.54	0.02	0.05	0.71
MIN		13.04	1.48	0.00	3.64	4.55	0.94	0.05	2.30	0.20	68.42	0.52	0.53	97.23
MAX		14.30	1.63	0.01	4.56	4.80	1.22	0.08	3.30	0.23	70.96	0.60	0.80	100.40
HUSG 24-10-12B	2012/11/04 21:30	12.84	1.45	0.01	3.69	4.58	0.84	0.06	1.98	0.18	69.35	0.52	1.00	96.50
HUSG 24-10-12B	2012/11/01 11:47	13.68	1.54	0.01	3.77	4.62	1.09	0.05	2.40	0.21	69.49	0.54	1.00	98.40
HUSG 24-10-12C	2012/11/05 11:51	13.71	1.55	0.01	3.73	4.60	0.91	0.05	2.19	0.21	69.75	0.53	1.00	98.24
HUSG 24-10-12C	2012/11/01 11:08	13.82	1.56	0.01	3.78	4.62	1.10	0.06	2.41	0.21	69.57	0.54	1.00	98.68

Table D.6 cont.: Quality control standard for 2010-2011.

Sample name	Meas. Date/time	Al ₂ O ₃ (%)	CaO (%)	Cr ₂ O ₃ (%)	Fe ₂ O ₃ (%)	K ₂ O (%)	MgO (%)	MnO (%)	Na ₂ O (%)	P ₂ O ₅ (%)	SiO ₂ (%)	TiO ₂ (%)	LOI (%)	Sum of conc. (%)
HUSG 24-10-12C	2012/11/01 10:49	13.77	1.55	0.01	3.76	4.59	1.07	0.06	2.41	0.21	69.78	0.54	0.00	97.75
HUSG 25.10.12C	2012/11/06 13:02	13.81	1.56	0.00	3.77	4.66	1.08	0.06	2.41	0.22	70.09	0.54	0.64	98.84
HUSG 25.10.12C	2012/11/06 12:56	13.86	1.56	0.01	3.77	4.64	1.08	0.06	2.45	0.21	69.92	0.55	0.64	98.75
HUSG 25.10.12C	2012/11/06 12:50	13.83	1.56	0.01	3.76	4.67	1.08	0.06	2.41	0.21	70.02	0.55	0.64	98.80
HUSG 25.10.12C	2012/11/05 21:29	13.81	1.55	0.01	3.78	4.64	1.09	0.06	2.41	0.21	70.13	0.54	0.64	98.87
HUSG 25.10.12C	2012/11/05 17:47	13.85	1.55	0.01	3.77	4.66	1.10	0.05	2.43	0.21	69.98	0.54	0.64	98.79
HUSG 25-10-12A	2012/11/06 09:19	13.89	1.55	0.00	3.74	4.65	1.00	0.06	2.26	0.22	70.17	0.54	0.64	98.72
HUSG 25-10-12A	2012/11/06 09:14	13.65	1.55	0.01	3.74	4.64	0.75	0.05	2.24	0.22	70.13	0.54	0.64	98.16
HUSG 25-10-12A	2012/11/06 09:08	13.60	1.56	0.01	3.74	4.64	0.84	0.06	2.26	0.21	70.13	0.54	0.64	98.23
HUSG 25-10-12A	2012/11/05 18:39	13.85	1.56	0.00	3.75	4.65	1.08	0.05	2.44	0.22	70.07	0.54	0.64	98.85
HUSG 25-10-12A	2012/11/05 14:10	13.87	1.56	0.00	3.76	4.64	1.09	0.06	2.44	0.21	69.99	0.54	0.64	98.80
HUSG 25-10-12B	2012/11/06 09:56	13.81	1.56	0.01	3.72	4.64	1.02	0.05	2.28	0.21	70.42	0.54	0.64	98.90
HUSG 25-10-12B	2012/11/06 09:50	13.93	1.57	0.00	3.72	4.66	1.03	0.06	2.29	0.21	70.71	0.53	0.64	99.35
HUSG 25-10-12B	2012/11/06 09:44	13.92	1.57	0.00	3.72	4.64	0.83	0.05	2.25	0.21	70.58	0.54	0.64	98.95
HUSG 25-10-12B	2012/11/05 18:46	13.97	1.56	0.00	3.71	4.65	1.08	0.05	2.47	0.21	70.27	0.53	0.64	99.14
HUSG 25-10-12B	2012/11/05 14:18	13.98	1.57	0.00	3.73	4.63	1.07	0.06	2.46	0.21	70.52	0.54	0.64	99.41

Table D.7: NIM-G standard.

Sample name	Meas. Date/time	Al ₂ O ₃ (%)	CaO (%)	Cr ₂ O ₃ (%)	Fe ₂ O ₃ (%)	K ₂ O (%)	MgO (%)	MnO (%)	Na ₂ O (%)	P ₂ O ₅ (%)	SiO ₂ (%)	TiO ₂ (%)	LOI (%)	Sum of conc. (%)
Granite Reference values		12.08	0.78	0.0012	2.02	4.99	0.06	0.02	3.36	0.01	75.7	0.09		99.11
NIM-G OLD STD	2012/11/06 11:26	12.15	0.77	0.00	2.05	4.97	0.06	0.02	3.02	0.00	75.65	0.09	0.78	99.56
NIM-G OLD STD	2012/11/06 11:21	12.21	0.78	0.00	2.03	4.96	0.01	0.02	2.93	0.00	75.65	0.09	0.78	99.46
NIM-G OLD STD	2012/11/06 11:15	12.16	0.78	0.00	2.04	4.96	0.05	0.02	2.96	0.00	75.42	0.09	0.78	99.26
NIM-G OLD STD	2012/11/05 19:07	12.19	0.79	0.00	2.04	4.99	0.05	0.02	3.10	0.00	75.68	0.09	0.78	99.73
NIM-G OLD STD	2012/11/05 14:52	12.16	0.78	0.00	2.03	4.97	0.06	0.02	3.11	0.00	75.41	0.09	0.78	99.41
NIM-G OLD STD	2012/11/05 12:21	12.19	0.78	0.00	2.05	4.96	0.07	0.02	3.00	0.00	75.57	0.09	0.78	99.51
NIM-G OLD STD	2012/11/05 09:19	12.11	0.78	0.00	2.05	4.96	0.05	0.02	2.98	0.00	75.44	0.09	0.78	99.26
NIM-G OLD STD	2012/11/01 11:31	12.18	0.77	0.00	2.11	4.97	0.06	0.02	3.11	0.00	75.52	0.09	1.00	99.83
NIM-G OLS STD	2012/11/02 16:22	12.17	0.78	0.00	2.03	4.96	0.06	0.02	2.99	0.00	75.55	0.09	0.78	99.43
NIM-G OLS STD	2012/11/01 17:10	12.19	0.78	0.00	2.04	4.96	0.06	0.02	2.97	0.00	75.42	0.09	0.78	99.31
NIM-G OLS STD	2012/11/01 15:54	12.10	0.77	0.00	2.03	4.99	0.05	0.02	3.02	0.00	75.67	0.09	0.78	99.52

Table D.8: BE-N standard.

Sample name	Meas. Date/time	Al ₂ O ₃ (%)	CaO (%)	Cr ₂ O ₃ (%)	Fe ₂ O ₃ (%)	K ₂ O (%)	MgO (%)	MnO (%)	Na ₂ O (%)	P ₂ O ₅ (%)	SiO ₂ (%)	TiO ₂ (%)	LOI (%)	Sum of conc. (%)
Basalt Reference values		10.05	14.03		12.61	1.40	12.95	0.19	3.18	1.06	38.38	2.59	2.45	98.90
BE-N OLD STD	2012/11/06 10:50	9.98	13.87	0.05	12.56	1.42	13.01	0.19	3.28	1.09	38.09	2.65	2.48	98.67
BE-N OLD STD	2012/11/06 10:44	9.97	13.92	0.05	12.56	1.43	13.03	0.19	3.32	1.09	38.06	2.67	2.48	98.77
BE-N OLD STD	2012/11/06 10:38	9.98	13.88	0.05	12.53	1.43	13.02	0.19	3.30	1.08	38.15	2.66	2.48	98.75
BE-N OLD STD	2012/11/05 14:39	9.93	13.87	0.05	12.58	1.42	13.02	0.20	3.27	1.09	38.18	2.67	2.48	98.76
BE-N OLD STD	2012/11/05 12:13	9.98	13.87	0.05	12.58	1.43	13.00	0.19	3.17	1.07	38.04	2.66	2.48	98.52
BE-N OLD STD	2012/11/05 09:06	9.94	13.86	0.05	12.56	1.42	12.95	0.19	3.22	1.08	37.99	2.67	2.48	98.41

SEM elemental mapping images

Quartzite

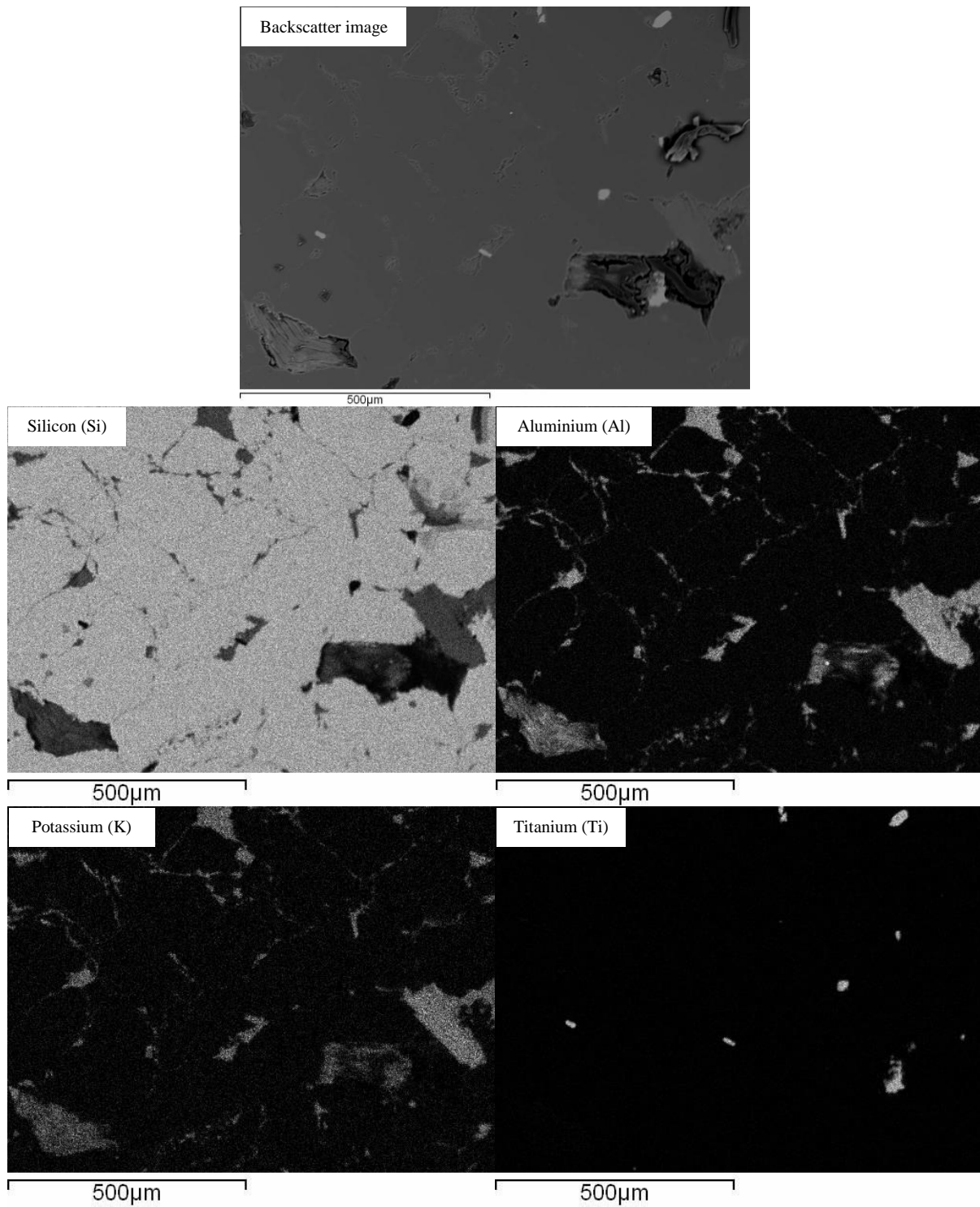


Figure D.5: Elemental mapping indicating the elements in quartzite sample.

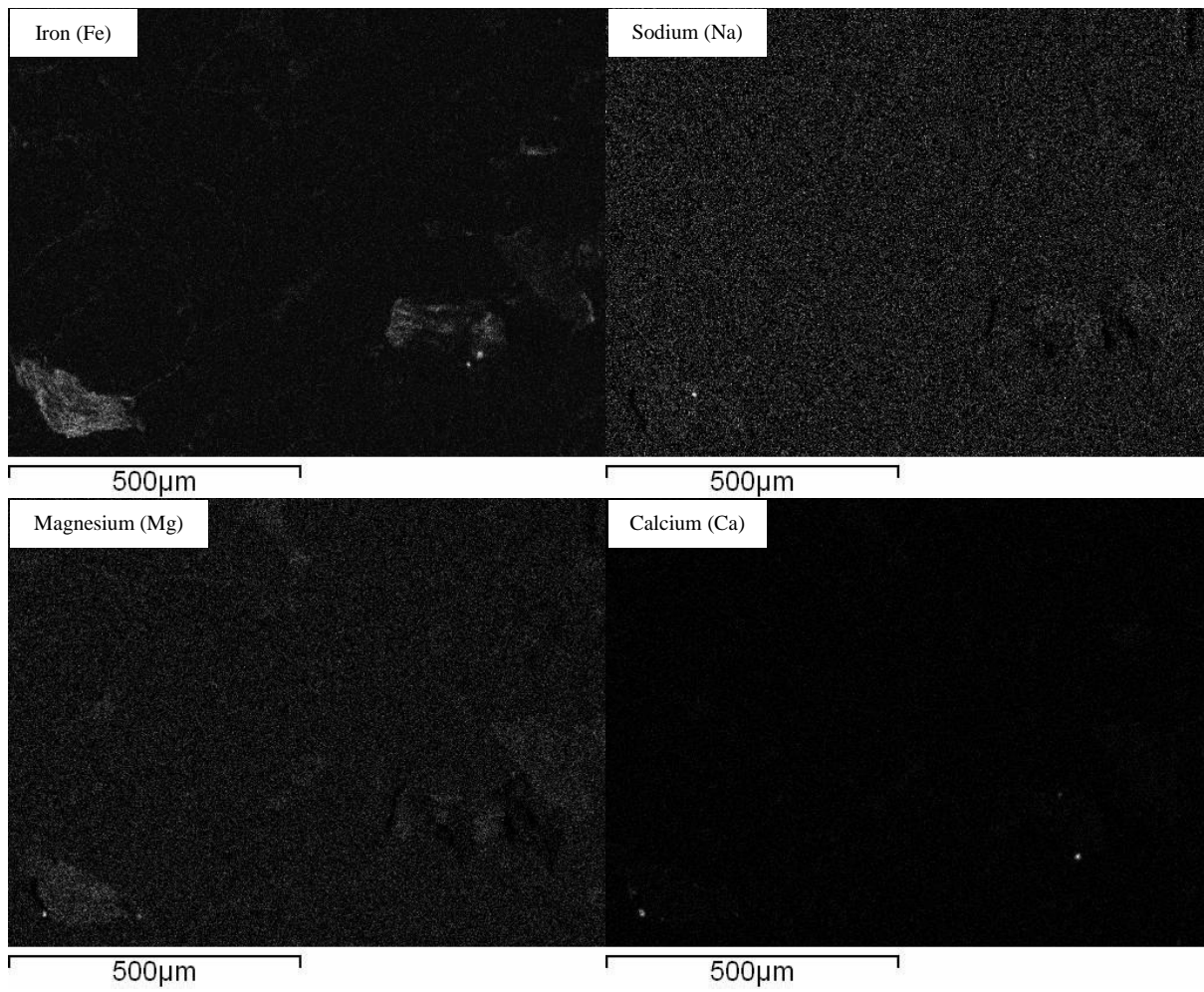


Figure D.5 cont.: Elemental mapping indicating the elements in quartzite sample.

Tillite

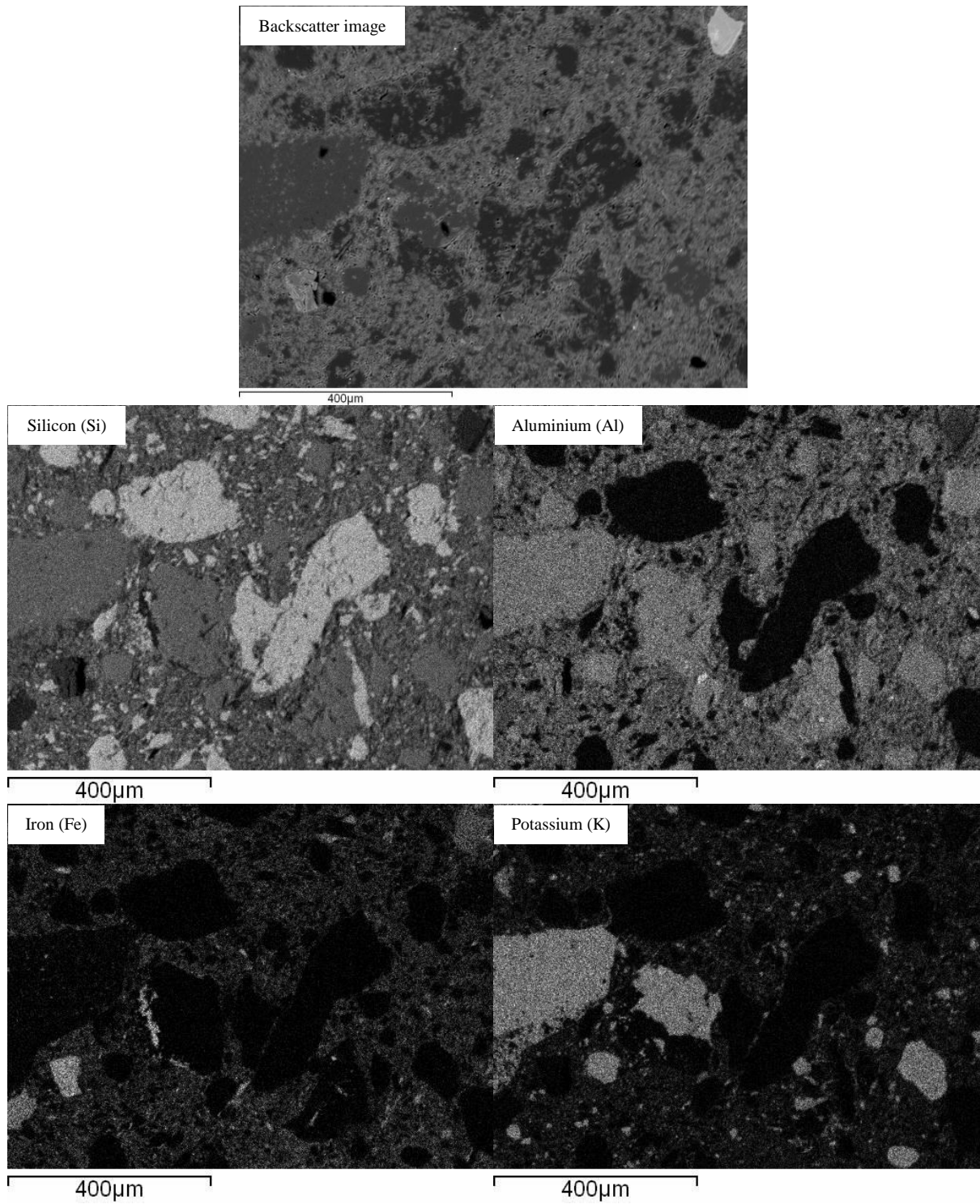


Figure D.6: Elemental mapping indicating the elements in tillite sample.

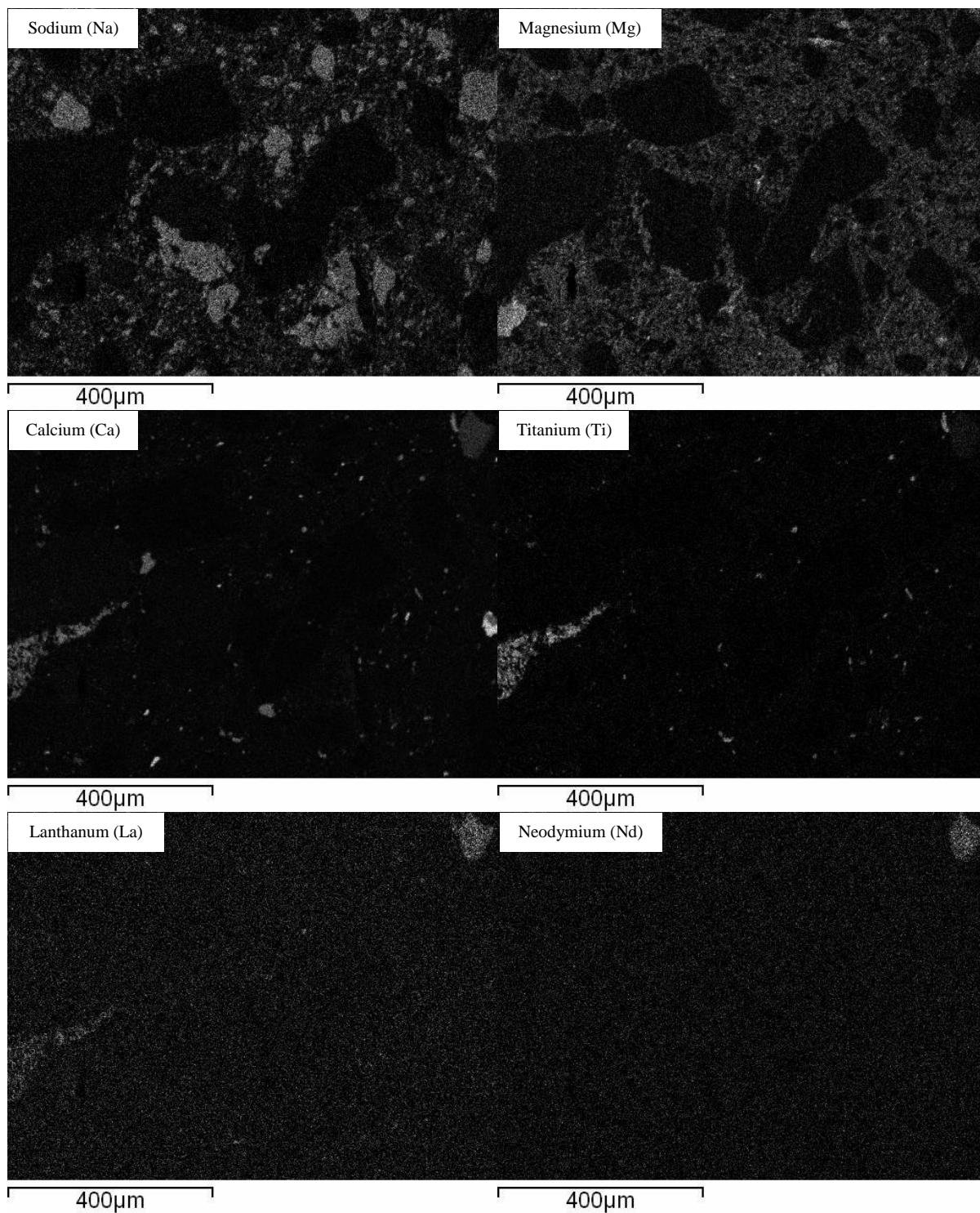


Figure D.6 cont.: Elemental mapping indicating the elements in tillite sample.

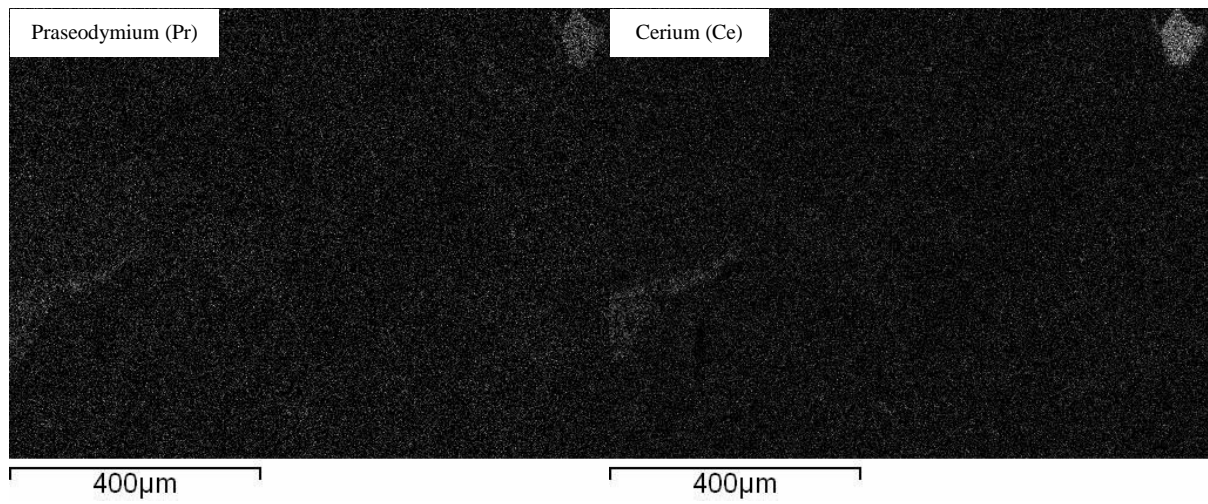


Figure D.6 cont.: Elemental mapping indicating the elements in tillite sample.

Shale

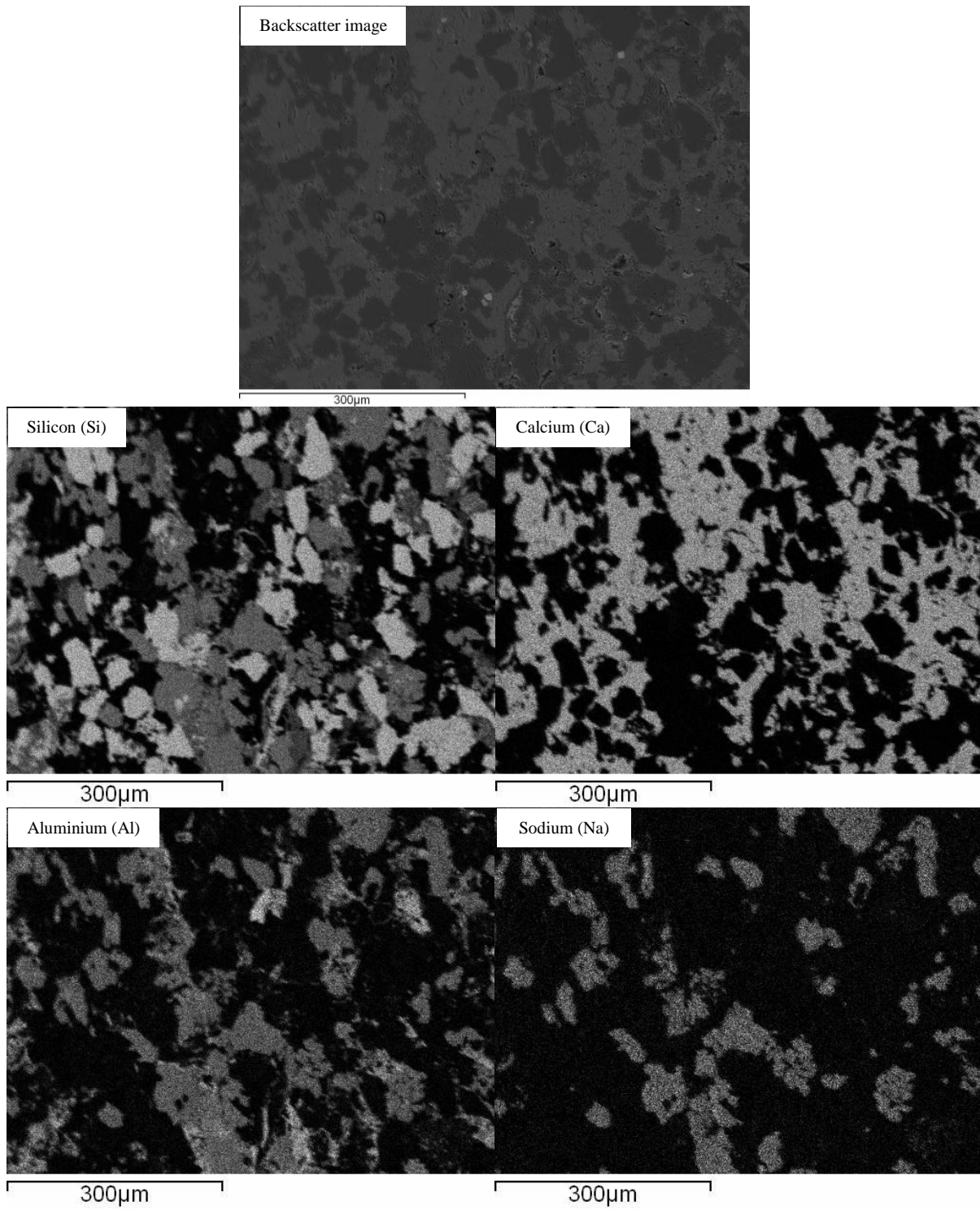


Figure D.7: Elemental mapping indicating the elements in shale sample.

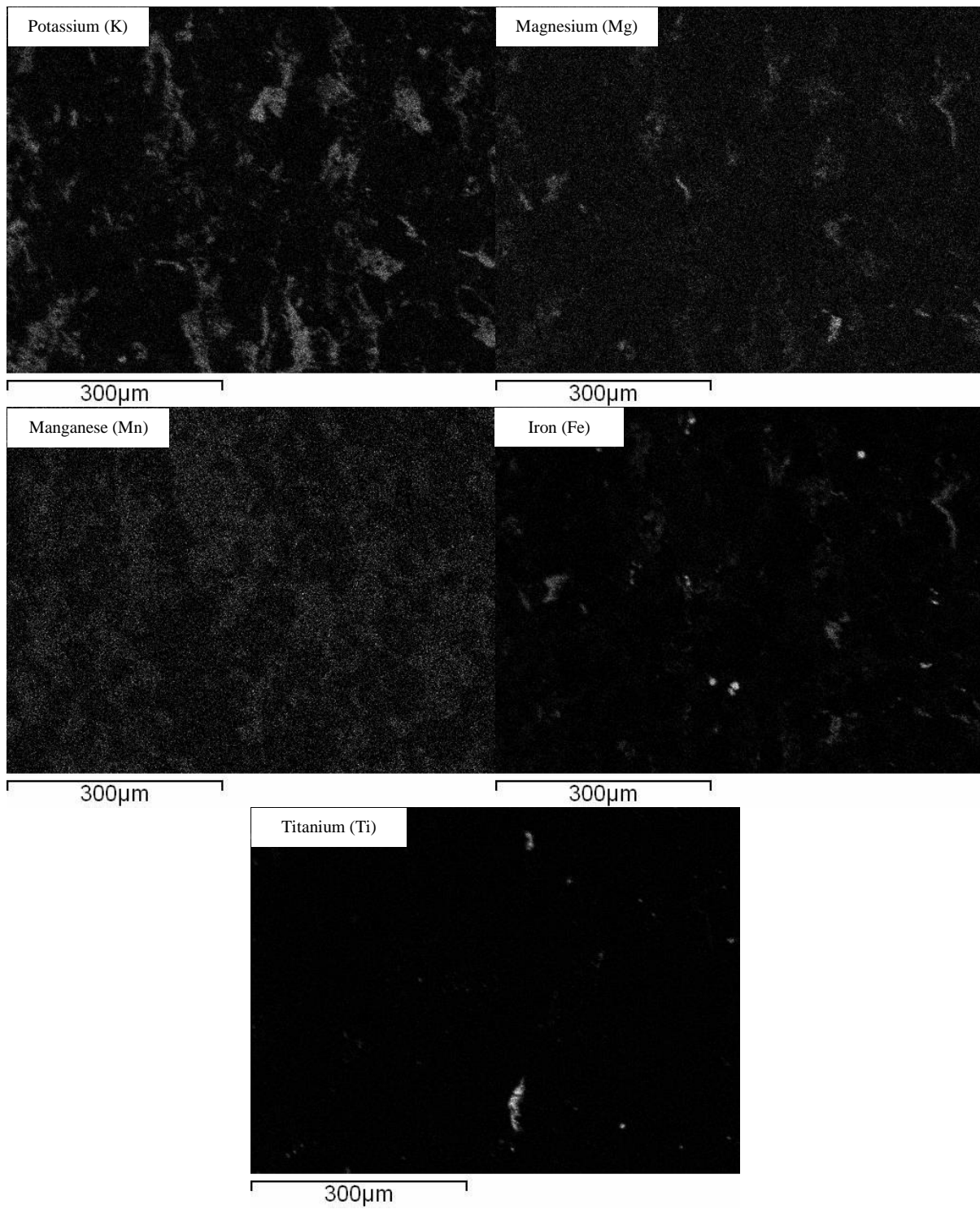


Figure D.7 cont.: Elemental mapping indicating the elements in shale sample.